

INFORMATION TO USERS

This material was produced from a microfilm copy of the original document. While the most advanced technological means to photograph and reproduce this document have been used, the quality is heavily dependent upon the quality of the original submitted.

The following explanation of techniques is provided to help you understand markings or patterns which may appear on this reproduction.

1. The sign or "target" for pages apparently lacking from the document photographed is "Missing Page(s)". If it was possible to obtain the missing page(s) or section, they are spliced into the film along with adjacent pages. This may have necessitated cutting thru an image and duplicating adjacent pages to insure you complete continuity.
2. When an image on the film is obliterated with a large round black mark, it is an indication that the photographer suspected that the copy may have moved during exposure and thus cause a blurred image. You will find a good image of the page in the adjacent frame.
3. When a map, drawing or chart, etc., was part of the material being photographed the photographer followed a definite method in "sectioning" the material. It is customary to begin photoing at the upper left hand corner of a large sheet and to continue photoing from left to right in equal sections with a small overlap. If necessary, sectioning is continued again — beginning below the first row and continuing on until complete.
4. The majority of users indicate that the textual content is of greatest value, however, a somewhat higher quality reproduction could be made from "photographs" if essential to the understanding of the dissertation. Silver prints of "photographs" may be ordered at additional charge by writing the Order Department, giving the catalog number, title, author and specific pages you wish reproduced.
5. PLEASE NOTE: Some pages may have indistinct print. Filmed as received.

University Microfilms International

300 North Zeeb Road

Ann Arbor, Michigan 48106 USA

St. John's Road, Tyler's Green

High Wycombe, Bucks, England HP10 8HR

7904004

MITA, KATSUNORI

PART I. BILOCAL FIELD THEORY AND A MODEL FOR
MESON SPECTROSCOPY. PART II. TRIDENT
PRODUCTION BY HIGH ENERGY CHARGED PARTICLES
ON NUCLEI.

IOWA STATE UNIVERSITY, PH.D., 1978

University
Microfilms
International

300 N. ZEEB ROAD, ANN ARBOR, MI 48106

Part I. Bilocal field theory and a model for meson
spectroscopy

Part II. Trident production by high energy charged particles
on nuclei

by

Katsunori Mita

A Dissertation Submitted to the
Graduate Faculty in Partial Fulfillment of
The Requirements for the Degree of
DOCTOR OF PHILOSOPHY

Department: Physics

Major: Elementary Particle Physics

Approved:

Signature was redacted for privacy.

In Charge of Major Work

Signature was redacted for privacy.

For the Major Department

Signature was redacted for privacy.

For the Graduate College

Iowa State University

Ames, Iowa

1978

TABLE OF CONTENTS

	Page
PART I. BILOCAL FIELD THEORY AND A MODEL FOR MESON SPECTROSCOPY	1
I. INTRODUCTION	2
II. BILOCAL FIELD AND ITS FIELD EQUATION	6
A. Definitions	6
B. Euler-Lagrange Equation	8
III. CONSERVATION LAWS	9
A. Translations	9
B. Homogeneous Lorentz Transformations	11
IV. MEANING OF THE RELATIVE TIME AND PROPERTIES OF THE CELL	14
A. Relative time	14
B. Spherical Cell	16
V. FIELD EQUATION FOR LAGRANGIAN DENSITY WITH INTERNAL DIRECT INTERACTION	19
A. Field Equation	19
B. Condition for Physical Mesons	21
VI. INTERNAL COVARIANT HARMONIC OSCILLATOR INTERACTION AND MESON SPECTROSCOPY	22
A. Covariant Harmonic Oscillator Interaction	22
B. Solutions	23
C. Chew-Frautschi Plots for Mesons	24
D. Spherical Cells and Radii of Mesons	26
E. Charmed Mesons	34
VII. CONCLUSION	37

VIII. BIBLIOGRAPHY	39
IX. ACKNOWLEDGEMENT	42
PART II. TRIDENT PRODUCTION BY HIGH ENERGY CHARGED PARTICLES ON NUCLEI	43
I. INTRODUCTION	44
II. SECOND-ORDER PROCESSES	50
A. Notations	51
B. Differential Cross Section	51
C. Integrations Over Kinematic Variables	56
D. Cross Section Formula	66
E. Proton Case	68
III. FIRST-ORDER PROCESSES	69
A. Differential Cross Section	70
B. Bremsstrahlung Part	71
C. Primary Part	74
D. Cross Section Formula	82
E. Proton Case	83
F. Interference Term	84
IV. RADIATIVE CORRECTIONS	86
A. Virtual Photon Radiative Corrections	88
B. Real Photon Radiative Corrections	91
C. Cancellation of Infrared Divergences	95
D. Matrix Elements for Radiative Corrections	97
V. NUMERICAL COMPUTATION OF CROSS SECTIONS	100
A. Formulae for the Pair Energy Distribution and the Pair Energy Partition Distribution	100
B. Atomic Form Factors	102

C. Examples	103
VI. CONCLUSION	109
VII. BIBLIOGRAPHY	111
VIII. ACKNOWLEDGEMENT	114
IX. APPENDIX A: LIST OF PAIR PRODUCTION EXPERIMENTS	115
X. APPENDIX B	119
A. Evaluation of $g_{\alpha\beta}^B u^\mu u^\nu$	119
B. Evaluation of $u_\alpha u_\beta B^{\alpha\beta} u^\mu u^\nu$	120
XI. APPENDIX C	122
XII. APPENDIX D	123
XIII. APPENDIX E	124
XIV. APPENDIX F	125
XV. APPENDIX G	127

PART I. BILOCAL FIELD THEORY AND A
MODEL FOR MESON SPECTROSCOPY

I. INTRODUCTION

It has been over twenty-five years since Yukawa's initial proposal of non-local field theory(1). The intention of the author was "to describe relativistically a system which was elementary in the sense that it could no longer be decomposed into more elementary constituents, but was so substantial, nevertheless, as to be able to contain implicitly a great variety of particles with different masses, spins and other intrinsic properties"(2).

The essential idea in Yukawa's theory is to introduce a finite extension of elementary particles through the postulate of reciprocity suggested by Born (3). This postulate states that the laws of physics should be symmetric in space-time x_μ and energy-momentum p_μ ($\mu = 0, 1, 2, 3$). Inspired by Born's idea, Yukawa assumed that for non-local fields the position operator x_μ does not commute with the field ϕ but satisfies the following commutation relationship.

$$[x_\mu, [x^\mu, \phi]] = -\lambda^2 \phi \quad (1.1)$$

with an auxiliary condition

$$[x_\mu, [p^\mu, \phi]] = 0 \quad (1.2)$$

to restrict the possible form of ϕ . Replacing x_μ by p_μ and λ by m in accordance with the postulate of reciprocity, we see that Eq. (1.1) has the same form as the Klein-Gordon equation expressed as

$$[p_\mu, [p^\mu, \phi]] = m^2 \phi \quad (1.3)$$

The non-local field ϕ can be represented by a matrix

$$\langle x_1 | \phi | x_2 \rangle \equiv \phi(x_1, x_2) \equiv \phi(X, x) \quad (1.4)$$

where

$$X = \frac{1}{2} (x_1 + x_2), \quad x = x_1 - x_2 \quad (1.5)$$

Note we use the same symbol ϕ to denote the field after the change of variables. In this representation Eqs. (1.1), (1.2), and (1.3) are rewritten as

$$(x_\mu x^\mu + \lambda^2) \phi(X, x) = 0 \quad (1.6)$$

$$\left(\frac{\partial^2}{\partial x_\mu \partial x^\mu} + m^2 \right) \phi(X, x) = 0 \quad (1.7)$$

$$x_\mu \frac{\partial}{\partial X_\mu} \phi(X, x) = 0 \quad (1.8)$$

Here X_μ are interpreted as the conventional space and time coordinates of the elementary particle and x_μ as the internal variables describing the internal motion of the particle. λ is identified as the radius of the particle.

As a direct generalization of local theory, Yukawa formulated an S-matrix theory for the non-local field. However, as pointed out by Yennie (4), Yukawa's S-matrix theory has a crucial difficulty in that, for higher order of interactions, the formalism does not reduce to the local theory. Investigating this point further, Rayski concluded that Yukawa's type of theory is consistent with either the postulate of reciprocity or local field theory but not with both simultaneously (5). Another well-known difficulty of introducing the extension of elementary particles was the non-commutability of physical quantities on space-like hypersurfaces in conflict with special relativity.

Despite these difficulties, Yukawa's bilocal field theory had the attention of several authors who extended the idea and amended its difficulties. Rayski suggested the idea of space-time quantization (6). Markov introduced "dynamically deformable form factors" to avoid the conflict with special relativity in the extended particle models (7). Pócsik gave a modified method of the second quantization of the bilocal scalar field (8). Also an intriguing variant of bilocal field theory was proposed by Takabayashi who used bilocal wave equations to describe baryons (9).

The works mentioned above were intended to provide a proper theoretical framework for physics of hadrons. However, the workers of bilocal field theory did not have in mind a composite model of hadrons (10). They did not identify x_1 and x_2 as the space-time coordinate of the constituents.

Recently, as an approach to the problem of quark confinement, Preparata and Craigie proposed the massive quark model wherein the fields which depend on two space-time coordinates of quarks were used (11). As pointed out by Chiang, this model possesses features equivalent to Yukawa's bilocal field theory (12). In an attempt to give a more precise mathematical framework to the approach of Preparata and Craigie, Capri and Chiang suggested a different model of the extended meson fields (13). Still another version of bilocal field theory was given by Karr (14) who combined bilocal field theory with the covariant harmonic oscillator quark model.

This is the intention of the present work though the details of approach differ significantly from Karr's. The formalism can be viewed as a direct generalization of local Lagrangian field theory. Following the usual local theory, we shall use the variational principle to find the Euler-Lagrange equation for the bilocal field. For a special class of Lagrangian densities satisfying a boundary condition on the hypersurface of the internal domain which we shall call as the cell, the Euler-Lagrange equation appears to be a simple generalization of the local equation. For such Lagrangian densities there exist proper conservation laws of energy-momentum and angular momentum. The Lagrangian density with an internal covariant harmonic oscillator interaction will then be introduced to describe the static properties of the mesons.

The organization of this article is as follows. In Sec. II the definitions and assumptions are introduced and the Euler-Lagrange equation and an additional boundary condition on the cell are given. The conservation laws for the bilocal field under translations and homogeneous Lorentz transformations are described in Sec. III. An interpretation of the relative time and some properties of the cell are discussed in Sec. IV. Sec. V gives the model Lagrangian densities with internal interactions and their equations of motion. In Sec. VI the covariant harmonic oscillator interaction is chosen as a model for the meson spectroscopy. This gives the linear Chew-Frautschi plots for the mesons with the proper quark masses. The charmed mesons are also considered.

II. BILOCAL FIELD AND ITS FIELD EQUATION

A. Definitions

Consider a scalar field ϕ depending on two points x_1 and x_2 in Minkowski space. We will regard these points as the space-time coordinates of the constituents (quark and anti-quark pair) of the mesons. The Lagrangian density in general may be written as

$$\mathcal{L} = \mathcal{L}[x_1, x_2; \phi(x_1, x_2), \frac{\partial}{\partial x_1^\mu} \phi(x_1, x_2), \frac{\partial}{\partial x_2^\mu} \phi(x_1, x_2)]. \quad (2.1)$$

The action is defined by the integral

$$S = \iint d^4x_1 d^4x_2 \mathcal{L}. \quad (2.2)$$

To treat the bilocal field properly, we introduce the center of mass (external) coordinate X and the relative (internal) coordinate x .

$$\begin{aligned} X &= \alpha_1 x_1 + \alpha_2 x_2, & \alpha_1 + \alpha_2 &= 1 \\ x &= x_1 - x_2. \end{aligned} \quad (2.3)$$

The field is now denoted as $\phi(X, x)$ and the Lagrangian density may be rewritten as

$$\mathcal{L} = \mathcal{L}[x; \phi(X, x), D_\mu \phi(X, x), d_\mu \phi(X, x)] \quad (2.4)$$

where $D_\mu = \partial/\partial X^\mu$ and $d_\mu = \partial/\partial x^\mu$. Note that there is no explicit dependence on X in the Lagrangian density thereby ensuring translational invariance.

The infinitesimal volume element is unchanged by the redefinition of the coordinates and the action is given by

$$S = \int_{\Omega} d^4X \int_{\omega} d^4x \mathcal{L} . \quad (2.5)$$

Here the external integration domain Ω may be considered to be the same as that of the usual local field theory. Assume that the dominant contribution to the action integral comes from a bounded internal integration domain ω . There is no a priori reason that any relative coordinate x should be finite. However, since it gives a measure of the "extension" of the particles, let us assume that every x in ω is finite. In this context one may wonder about the meaning of the finite relative time. As we shall see in Sec. IV, the relative time is directly related to the spatial distance between the constituents. According to our interpretation, the finite spatial distance implies the finite relative time. (See Eq. (4.6)) With this ansatz of bounded ω it may be said that the "confinement" of the quarks is built into the theory at the outset. For simplicity we will refer to the hypersurface enclosing ω as the "cell" and denote it by C .

In the present discussion the quark and anti-quark are not associated with separate fields. Their presence is represented by the space-time coordinates of the bilocal field. A question may arise as to what binds the quarks and causes the relative coordinate x to be always finite. In this model, use is not made of a mediating field between the constituents. Instead the interaction between the constituents is directly expressed in terms of the internal coordinate x (15). The explicit dependence on x appearing in the Lagrangian density represents this direct interaction.

B. Euler-Lagrange Equation

Let us now find the appropriate bilocal field equation from the action principle. As in the usual local theory, the field variation $\delta\phi$ is assumed to vanish on the boundary surface of Ω . The change of the action integral S due to the variation with respect to the field ϕ is given by

$$\begin{aligned} \delta S = & \int_{\Omega} d^4x \int_{\omega} d^4x \left[\frac{\delta \mathcal{L}}{\delta \phi} - D_{\mu} \frac{\delta \mathcal{L}}{\delta (D_{\mu} \phi)} - d_{\mu} \frac{\delta \mathcal{L}}{\delta (d_{\mu} \phi)} \right] \delta \phi \\ & + \int_{\omega} d^4x \int_{\text{surface of } \Omega} ds_{\mu} \frac{\delta \mathcal{L}}{\delta (D_{\mu} \phi)} \delta \phi + \int_{\Omega} d^4x \int_c d\sigma n_{\mu} \frac{\delta \mathcal{L}}{\delta (d_{\mu} \phi)} \delta \phi \end{aligned} \quad (2.6)$$

where n_{μ} is the unit four-vector normal to the cell c . The second term in Eq. (2.6) vanishes since $\delta\phi = 0$ on the boundary surface of Ω . For a special class of Lagrangian densities for which

$$n_{\mu} \frac{\delta \mathcal{L}}{\delta (d_{\mu} \phi)} = 0 \quad \text{on } c, \quad (2.7)$$

the third term in Eq. (2.6) also vanishes. For such Lagrangian densities the principle of stationary action $\delta S = 0$ demands

$$\frac{\delta \mathcal{L}}{\delta \phi} - D_{\mu} \frac{\delta \mathcal{L}}{\delta (D_{\mu} \phi)} - d_{\mu} \frac{\delta \mathcal{L}}{\delta (d_{\mu} \phi)} = 0 \quad (2.8)$$

for arbitrary $\delta\phi$. This is the Euler-Lagrange equation of motion for the bilocal field. The boundary condition on the cell must be satisfied in order for Eq. (2.8) to be valid. Otherwise the combination of the first and the third term of Eq. (2.6) should be vanishing.

III. CONSERVATION LAWS

It is not readily apparent that the conservation laws are valid for bilocal fields. In this section it is shown that the conservation of energy-momentum and angular momentum for the bilocal field hold true for the Lagrangian densities which satisfy the boundary condition on the cell.

Let us define the Lagrange functional (16)

$$\mathcal{K} = \int_{\omega} d^4x \mathcal{L} \quad (3.1)$$

This is an implicit function of X and a functional of ϕ , $D_{\mu}\phi$ and $d_{\mu}\phi$.

Thus we may write

$$\mathcal{K} = \mathcal{K}[\phi(X), D_{\mu}\phi(X), d_{\mu}\phi(X)] \quad (3.2)$$

The functional \mathcal{K} will replace the Lagrangian density \mathcal{L} in considerations of the conservation laws of the bilocal field.

A. Translations

Perform the simultaneous, infinitesimal displacements of x_1 and x_2

$$x_{r\mu} \rightarrow x'_{r\mu} = x_{r\mu} + \epsilon_{\mu} \quad r = 1, 2 \quad (3.3)$$

Then

$$X_{\mu} \rightarrow X'_{\mu} = X_{\mu} + \epsilon_{\mu} \quad (3.4)$$

Under Eq. (3.4) the field transforms as

$$\phi(X, x) \rightarrow \phi(X + \epsilon, x) = \phi(X, x) + \delta\phi(X, x) \quad (3.5)$$

and the variation of the field is given by

$$\delta\phi(X, x) = D_{\nu}\phi(X, x)\epsilon^{\nu} \quad (3.6)$$

The translationally invariant Lagrange functional does not have explicit dependence on X . To first order in ϵ_μ , the change in \mathcal{K} is given by

$$\begin{aligned}\delta\mathcal{K} &= D_\nu \mathcal{K} \epsilon^\nu \\ &= \{D_\mu \left[\frac{\delta\mathcal{K}}{\delta(D_\mu\phi)} \cdot D_\nu\phi \right] + \int_c d\sigma n_\mu \frac{\delta\mathcal{L}}{\delta(d_\mu\phi)} \cdot D_\nu\phi\} \epsilon^\nu.\end{aligned}\quad (3.7)$$

The second line is due to the variation of the field and the Euler-Lagrange equation is used to obtain this. The dot denotes the implicit integration process

$$\frac{\delta\mathcal{K}}{\delta\varphi} \cdot \delta\varphi = \iint d^3Y d^3y \frac{\delta\mathcal{K}[\varphi]}{\delta\varphi(Y,y)} \delta\varphi(Y,y) \quad (3.8)$$

for an arbitrary function φ . For the Lagrangian densities satisfying Eq. (2.7), the surface integral over the cell vanishes and Eq. (3.7) can be rearranged and put into the form

$$D^\mu T_{\mu\nu} = 0 \quad (3.9)$$

with the energy-momentum stress tensor $T_{\mu\nu}$ defined by

$$T_{\mu\nu} = \frac{\delta\mathcal{K}}{\delta(D^\mu\phi)} \cdot D_\nu\phi - g_{\mu\nu} \mathcal{K}. \quad (3.10)$$

The above two equations express the differential conservation law of energy-momentum. The quantities given by

$$P_\nu = \int d^3X T_{0\nu} \quad (3.11)$$

are constants of motion. This may be regarded as the energy-momentum four-vector associated with the bilocal field.

B. Homogeneous Lorentz Transformations

Consider the simultaneous, infinitesimal Lorentz transformations of x_1 and x_2

$$x_{r\mu} \rightarrow x'_{r\mu} = \Lambda_{\mu\nu} x_r^\nu, \quad r = 1, 2 \quad (3.12)$$

where

$$\Lambda_{\mu\nu} = g_{\mu\nu} + \varepsilon_{\mu\nu}, \quad \varepsilon_{\mu\nu} = -\varepsilon_{\nu\mu}. \quad (3.13)$$

Then both the external and the internal coordinates are transformed as in Eq. (3.12).

$$\begin{aligned} X_\mu &\rightarrow X'_\mu = \Lambda_{\mu\nu} X^\nu \\ x_\mu &\rightarrow x'_\mu = \Lambda_{\mu\nu} x^\nu \end{aligned} \quad (3.14)$$

For the scalar field the transformation matrix is unit and

$$\phi'(X', x') = \phi(X, x) \quad (3.15)$$

When the Lorentz invariance of the Lagrangian density is assumed, the Lagrange functional defined by Eq. (3.1) is also Lorentz invariant.

A convenient test of the Lorentz invariance is to rewrite Eq. (3.15) as

$$\phi'(X, x) = \phi(X', x') \quad (3.16)$$

and require

$$\mathcal{K}[\phi'(X), D_\mu \phi'(X), d_\mu \phi'(x)] = \mathcal{K}[\phi(X'), D'_\mu \phi(X'), d'_\mu \phi(X')] \quad (3.17)$$

To first order in $\varepsilon_{\mu\nu}$, the right hand side of the above equation can be expanded as

$$\mathcal{K}[\phi(X'), D'_\mu \phi(X'), d'_\mu \phi(X')] = \mathcal{K} + D_\nu \mathcal{K} \varepsilon^{\nu\lambda} X_\lambda \quad (3.18)$$

and the left hand side as

$$\begin{aligned}
 & \mathcal{K} [\phi'(X), D_\mu \phi'(X), d_\mu \phi'(x)] \\
 &= \mathcal{K} + \frac{\delta \mathcal{K}}{\delta \phi} \cdot \delta \phi + \frac{\delta \mathcal{K}}{\delta (D_\mu \phi)} \cdot \delta (D_\mu \phi) + \frac{\delta \mathcal{K}}{\delta (d_\mu \phi)} \cdot \delta (d_\mu \phi) \\
 &= \mathcal{K} + D_\mu \left[\frac{\delta \mathcal{K}}{\delta (D_\mu \phi)} \cdot \delta \phi \right] + \int_c d\sigma n_\mu \frac{\delta \mathcal{K}}{\delta (d_\mu \phi)} \cdot \delta \phi
 \end{aligned} \tag{3.19}$$

where the variation of the field is given by

$$\delta \phi(X, x) = D_\nu \phi(X, x) \epsilon^{\nu\lambda} X_\lambda + d_\nu \phi(X, x) \epsilon^{\nu\lambda} x_\lambda \quad . \tag{3.20}$$

For the Lagrangian densities satisfying Eq. (2.7), the surface integral over the cell in Eq. (3.19) vanishes. In such a case we can equate Eqs. (3.18) and (3.19) and rearrange the terms to obtain

$$D^\mu m_{\mu\nu\lambda} = 0 \tag{3.21}$$

where the tensor $m_{\mu\nu\lambda}$ is given by

$$m_{\mu\nu\lambda} = (X_\nu T_{\mu\lambda} - X_\lambda T_{\mu\nu}) + \frac{\delta \mathcal{K}}{\delta (D^\mu \phi)} \cdot \Sigma_{\nu\lambda} \phi \tag{3.22}$$

and

$$i\Sigma_{\nu\lambda} = x_\nu p_\lambda - x_\lambda p_\nu \quad . \tag{3.23}$$

Here $p_\mu = id_\mu$ and the energy-momentum stress tensor has been previously defined by Eq. (3.10). The first term in Eq. (3.22) expresses the orbital angular momentum of the overall motion. The second term is due to the relative motion of the constituents and we may regard $i\Sigma_{\nu\lambda}$ as the "spin tensor" of the mesons. In this model the spin of the constituents is not taken into consideration. The conserved angular momentum is given by

$$M_{\nu\lambda} = \int d^3X \, m_{0\nu\lambda} \quad . \quad (3.24)$$

To conclude this section let us emphasize that the above conservation laws are valid for a special class of Lagrangian densities which satisfy the boundary condition on the cell. An example of such a Lagrangian density will be given in Sec. VI. For the Lagrangian density with the internal covariant harmonic oscillator interaction, both the field ϕ and $\delta\mathcal{L}/\delta(d_\mu\phi) = d_\mu\phi$ vanish beyond finite boundaries.

IV. MEANING OF THE RELATIVE TIME AND PROPERTIES OF THE CELL

In their discussion of the covariant harmonic oscillators, Kim and Noz pointed out the difficulty of giving a proper interpretation to the relative time (17). A similar situation is found in the analyses of the Bethe-Salpeter equation (18). In this section an attempt is made to provide a meaning to the relative time in the context of the present discussion. Some properties of the cell are then considered.

A. Relative Time

Suppose in a Lorentz frame L the space-time coordinates of the constituents are specified as x_1 and x_2 and the corresponding center of mass and relative coordinates are given by

$$\begin{aligned} X &= (T, \vec{R}) \\ x &= (t, \vec{r}) \end{aligned} \quad (4.1)$$

In another inertial frame L' these coordinates may be observed as

$$\begin{aligned} X'_\mu &= a_{\mu\nu} X^\nu = (T', \vec{R}') \\ x'_\mu &= a_{\mu\nu} x^\nu = (t', \vec{r}') \end{aligned} \quad (4.2)$$

where $a_{\mu\nu}$ are orthogonal. For the sake of concreteness we will consider the Lorentz boosts given by

$$\begin{aligned} a_{00} &= \gamma, \quad a_{0i} = v_i \\ a_{i0} &= -\gamma v_i, \quad a_{ij} = -\delta_{ij} - (\gamma - 1) \frac{v_i v_j}{v^2} \end{aligned} \quad (4.3)$$

where $\gamma = 1/\sqrt{1-v^2}$ and \vec{v} is the relative velocity from the inertial frame L to L' .

Now we take a particular frame in which

$$x_{10} = x_{20} = T \quad (4.4)$$

Call this frame the equal time frame L_0 . We can always choose L_0 to be the rest frame of the meson and \vec{R} to be zero. Let the frame L be the equal time frame L_0 . Then $t = 0$ and $R = 0$ in L_0 and Eqs. (4.1), (4.2), and (4.3) imply

$$T' = \gamma T$$

$$\vec{R}' = -\gamma \vec{v} T \quad (4.5)$$

and

$$t' = -\gamma \vec{v} \cdot \vec{r}$$

$$\vec{r}' = \vec{r} + (\gamma - 1) \frac{\vec{v}}{v} \vec{v} \cdot \vec{r} \quad (4.6)$$

From Eq. (4.5) it immediately follows that

$$\vec{R}' = -\vec{v} T' \quad (4.7)$$

and from Eq. (4.6)

$$t' = -\vec{v} \cdot \vec{r}' \quad (4.8)$$

Eq. (4.7) is a trivial result of the transformation indicating that the center of mass moves with the velocity $-\vec{v}$ in the frame L' . However, Eq. (4.8) is a non-trivial consequence giving a meaning to the relative time. Once the relative velocity is chosen, the frame L' is fixed and in this frame the change in \vec{r}' induces a change in t' according to

$$\Delta t' = -\vec{v} \cdot \Delta \vec{r}' \quad (4.9)$$

In the equal time frame L_0 the relative time is identically zero and the motion of the two body system takes place as the center of mass time T evolves. On the other hand, in another Lorentz frame L'

boosted by the relative velocity \vec{v} , the same motion occurs with the fluctuation of the relative time obeying Eq. (4.9). In this frame the time that measures the development of the motion is given by $T' = \gamma T$.

An implicit assumption in the above discussion is that the relative coordinate x is space-like. For this reason we may regard the space-like region of ω as physical and the rest as unphysical. We need not remove the unphysical region from the internal domain in the definition of the action S or the Lagrange functional \mathcal{K} . Instead we require that the expectation value of x must be space-like for physical particles.

B. Spherical Cell

Let us now turn our attention to a particular kind of cell which will play an important role in Sec. VI. When the bilocal field possesses internal spherical symmetry, one may parametrize ω in terms of t and r only. The shaded area in figure 1 shows the domain ω on the $r - t$ plane.

Suppose that the cell along $a - b$ is given by

$$f(t, r) = 0 \quad . \quad (4.10)$$

Since at each t , ω is a three-dimensional sphere with the radius r

$$\vec{\nabla} f = \vec{r} \quad . \quad (4.11)$$

Also for the maximum r

$$\frac{\partial f}{\partial t} = 0 \quad . \quad (4.12)$$

Thus the unit four-vector normal to the cell for the maximum r is given by

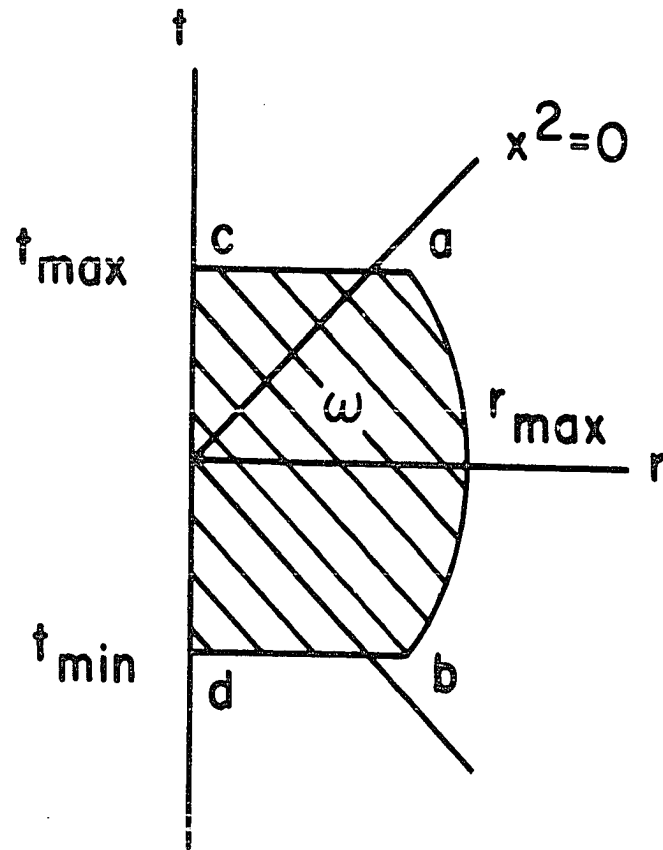


Figure 1. Spherically symmetric internal domain ω .

$$n_\mu = (0, \hat{r}) \quad . \quad (4.13)$$

At the time boundaries the cell is space-like with the null time component. Hence

$$n_\mu = (\pm 1, 0, 0, 0) \quad (4.14)$$

The positive sign should be taken for the upper time boundary a - c and the negative sign for the lower time boundary b - d.

V. FIELD EQUATION FOR LAGRANGIAN DENSITY WITH INTERNAL DIRECT INTERACTION

A. Field Equation

Consider a Lagrangian density of the form

$$\mathcal{L} = \frac{1}{2} [D_\mu \phi D^\mu \phi + d_\mu \phi d^\mu \phi + \Gamma(x^2) \phi^2 - \chi^2 \phi^2] \quad (5.1)$$

The first and second term of the above Lagrangian density are the kinetic terms respectively for the external and the internal motion. The third term represents the internal direct interaction. For a given function $\Gamma(x^2)$, the internal equation of motion and its mass eigenvalue spectrum are completely specified. The dependence on x^2 makes it explicit that $\Gamma(x^2)$ is manifestly Lorentz invariant. The last term may be referred as the mass term. The physical meaning of the constant χ^2 will be given explicitly in terms of the quark masses. The Euler-Lagrange equation for the above Lagrangian density is given by

$$[D_\mu D^\mu + d_\mu d^\mu - \Gamma(x^2) + \chi^2] \phi = 0 \quad (5.2)$$

To find the physical content of the constant χ^2 , consider two free particles of mass m_1 and m_2 with respective four-momentum p_1 and p_2 . Define the center of mass momentum P and the relative momentum p as

$$P = p_1 + p_2 \quad , \quad p = p_1 - p_2 \quad (5.3)$$

Then the equation of motion with the "free" quarks may be conjectured by squaring P and p and adding them together.

$$[D_\mu D^\mu + d_\mu d^\mu + 2(m_1^2 + m_2^2)] \phi = 0 \quad (5.4)$$

where the identifications $P_\mu = iD_\mu$ and $p_\mu = id_\mu$ are made. On the other hand when the interaction is turned off, Eq. (5.2) reduces to

$$(D_\mu D^\mu + d_\mu d^\mu + \chi^2)\phi = 0 \quad . \quad (5.5)$$

Comparison of Eqs. (5.4) and (5.5) suggests that we make the following identification

$$\chi^2 = 2(m_1^2 + m_2^2) \quad . \quad (5.6)$$

The solutions of Eq. (5.2) are separable and the field may be written as

$$\phi(X, x) = u(X)v(x) \quad . \quad (5.7)$$

Then we have a pair of equations for the external and the internal motion

$$(D_\mu D^\mu + \mu^2)u(X) = 0 \quad (5.8)$$

$$[d_\mu d^\mu - \Gamma(x^2) + \chi^2 - \mu^2]v(x) = 0 \quad (5.9)$$

μ^2 is a separation constant which can be identified as the square of the meson mass. These equations correspond to a particular case of Yukawa's bilocal field equations (2). With the above separation of variables the condition on the cell given by Eq. (2.7) becomes

$$n_\mu d^\mu v(x) = 0 \quad \text{on } C \quad (5.10)$$

for arbitrary $u(X)$.

B. Condition for Physical Mesons

For a bounded two body system, there usually exists a condition that the masses of the constituents and the mass of the total system must satisfy. In order to find this condition for our system, consider the following quantity

$$\begin{aligned}
 & \int_{\omega} d^4x p_{\mu} v^{*}(x) p^{\mu} v(x) \\
 &= \int_{\omega} d^4x v^{*}(x) d_{\mu}^{\mu} v(x) - \int_c d\sigma v^{*}(x) n_{\mu} d^{\mu} v(x) \\
 &= \mu^2 - \chi^2 + \int_{\omega} d^4x v^{*}(x) \Gamma(x^2) v(x)
 \end{aligned} \tag{5.11}$$

Here the second term of the second line vanishes due to the condition given by (5.10) and use has been made of Eq. (5.9) to obtain the third line. Also the internal field $v(x)$ is normalized as

$$\int_{\omega} d^4x v^{*}(x) v(x) = 1 \tag{5.12}$$

For the physical mesons $\mu^2 > 0$, and

$$m_1^2 + m_2^2 > \frac{1}{2} \left[\int_{\omega} d^4x v^{*}(x) \Gamma(x^2) v(x) - \int_{\omega} d^4x p_{\mu} v^{*}(x) p^{\mu} v(x) \right] \tag{5.13}$$

The above inequality may limit the form of the internal interaction $\Gamma(x^2)$ for a realistic meson mass spectrum.

VI. INTERNAL COVARIANT HARMONIC OSCILLATOR INTERACTION AND MESON SPECTROSCOPY

A. Covariant Harmonic Oscillator Interaction

It is a well-known fact that covariant harmonic oscillators give rise to linear Chew-Frautschi plots (19). Studies of hadron dynamics have been carried out using covariant harmonic oscillators (20). Also, covariant harmonic oscillators respect an invariance group $SU(3,1)$ which contains the homogeneous Lorentz group as a subgroup, and therefore the states belonging to the unitary representations of $SU(3,1)$ could be a possible basis for a relativistic system (21). From the view point of the interaction function, x^2 is the simplest Lorentz invariant interaction available.

For the above reasons consider the interaction function

$$\Gamma(x^2) = kx^2 \quad . \quad (6.1)$$

Then the internal equation of motion given by Eq. (5.9) becomes

$$(d_\mu d^\mu - kx^2 + \chi^2 - \mu^2)v(x) = 0 \quad . \quad (6.2)$$

The solutions of the above equation are separable and $v(x)$ may be written as

$$v(x) = y(t)Z(\vec{r}) \quad . \quad (6.3)$$

Eq. (6.2) separates into a pair of equations

$$\left(\frac{d^2}{dt^2} - kt^2 - \sigma\right)y(t) = 0 \quad (6.4)$$

$$[\nabla^2 - kr^2 - (\sigma - \mu^2 + \chi^2)]Z(\vec{r}) = 0 \quad (6.5)$$

where σ is a separation constant. Due to the separation of variables neither of the above equations maintains manifest Lorentz covariance separately.

B. Solutions

The solutions to the above equations are well-known from elementary quantum mechanics (22). For the time equation (6.4) the solutions are given in terms of Hermite polynomials H_p .

$$y_p(t) = N_p e^{-1/2 \eta^2 t^2} H_p(\eta t), \quad p = 0, 1, 2, \dots \quad (6.6)$$

where $\eta^4 = k$ and the normalization constants N_p are

$$N_p = \left(\frac{\eta}{\pi^{1/2} 2^p p!} \right)^{1/2} \quad (6.7)$$

The eigenvalue spectrum of σ is given by

$$\sigma = -(2p + 1)\eta^2 \quad (6.8)$$

For the space equation (6.5) the solutions are expressed in terms of the Laguerre polynomials $L_q^{s+1/2}$ and the spherical harmonics Y_{sm} .

$$Z_{qsm}(\vec{r}) = R_{qs}(r) Y_{sm}(\theta, \phi), \quad q, s = 0, 1, 2, \dots \quad (6.9)$$

where the radial solutions are given by

$$R_{qs}(r) = N_{qs} (\eta r)^s e^{-1/2 \eta^2 r^2} L_q^{s+1/2}(\eta^2 r^2) \quad (6.10)$$

and the normalization constants N_{qs} are

$$N_{qs} = \left(\frac{2\eta^3 q!}{[\Gamma(q + s + 3/2)]^3} \right)^{1/2} \quad (6.11)$$

The eigenvalue spectrum of $(\sigma - \mu^2 + \chi^2)$ is

$$\sigma - \mu^2 + \chi^2 = -(4q + 2s + 3)\eta^2 . \quad (6.12)$$

Comparison of Eqs. (6.8) and (6.12) yields the spectrum of the square of the meson masses as

$$\mu^2 = 2\eta^2(1 + s + 2q - p) + 2(m_1^2 + m_2^2) . \quad (6.13)$$

As pointed out earlier, separation of variables is not a Lorentz covariant process for the case under consideration. However, the above eigenvalue spectrum of μ^2 obtained thus should hold true in any Lorentz frame; particularly in the rest frame of the meson.

C. Chew-Frautschi Plots for Mesons

As shown in Sec. III the relative angular momentum of the constituents gives rise to the spin of the mesons in the present model. In terms of the spin s Eq. (6.13) is rewritten in the form of the Chew-Frautschi plots.

$$s = \alpha_0 + \alpha' \mu^2 \quad (6.14)$$

where

$$\alpha_0 = (p - 2q - 1) - \frac{1}{2} \frac{(m_1^2 + m_2^2)}{\eta} \quad (6.15)$$

$$\alpha' = \frac{1}{2\eta^2} \quad (6.16)$$

A look at Eq. (6.15) provides us with an idea of the physical significance of the quantum numbers p and q . The quantum number p fixes the maximum intercept for $q = 0$ and $m_1 = m_2 = 0$. As known from the Regge

pole picture and the experimental facts of meson spectroscopy, the possible maximum of α_0 is one corresponding to the Pomeranchuk trajectory. This suggests that we set an upper bound for p as

$$p_{\max} = 2 \quad (6.17)$$

The number q lowers the intercept with the spacing two. Since the spacing is two for the daughter trajectories with the same signature as the leading trajectory, it is appropriate to use q to label the even daughter trajectories. The odd daughters are absent in this model.

Evidently $q = 0$ corresponds to the leading trajectories.

The condition for $\mu^2 > 0$ is expressed as

$$m_1^2 + m_2^2 > (p - 2q - s - 1)\eta^2. \quad (6.18)$$

As we shall see shortly (See Eq. (6.22)), the minimum of the left hand side of the above inequality is 0.28 GeV^2 for the pair of u and d quarks. For this combination

$$s \geq 1 \quad (6.19)$$

with the assignment $p = 2$ and $q = 0$ corresponding to the ρ , K^* and φ trajectories. These leading trajectories are approximately parametrized as (23)

$$\begin{array}{ll} \alpha_\rho = 0.5 + 0.9\mu^2 & \rho, \omega, A_2, f, g, \omega^*, A_2^*, h \\ \alpha_{K^*} = 0.3 + 0.9\mu^2 & K^*, K^{**}, K^{***} \\ \alpha_\varphi = 0.1 + 0.9\mu^2 & \phi, f' \end{array} \quad (6.20)$$

Note that all of these mesons have the natural parity $P = (-1)^S$ consistent with the parity of the solution given by Eq. (6.9). The present model is not appropriate for treatment of the unnatural parity mesons such as π and K .

The quark masses appropriate for the above meson mass spectra can be evaluated from Eqs. (6.14), (6.15), (6.16), and (6.20). Since the quark contents of the mesons are given as

$$\rho^+ = u\bar{d}, \quad K^{*+} = u\bar{s}, \quad \varphi = s\bar{s}, \quad \text{etc.} \quad (6.21)$$

we obtain

$$m_u^2 + m_d^2 = 0.28, \quad m_u^2 + m_s^2 = 0.39, \quad 2m_s^2 = 0.51 \quad (6.22)$$

in GeV^2 . From this it follows

$$m_u = 0.37, \quad m_d = 0.38, \quad m_s = 0.5 \quad (6.23)$$

in GeV . These are in agreement with the usual phenomenological estimates (24).

D. Spherical Cells and Radii of Mesons

For the spherical cell the normal four-vectors are given by Eqs. (4.13) and (4.14). With these n_μ the condition on the cell given by Eq. (5.10) reduces to

$$\frac{d}{dt} y_p(t) = 0 \quad (6.24)$$

at the time boundaries for arbitrary values of $Z_{qsm}(\vec{r})$ and

$$\frac{d}{dr} R_{qs}(r) = 0 \quad (6.25)$$

for the maximum r for arbitrary values of $y_p(t)$. Note that all the functions $y_p(t)$, $dy_p(t)/dt$, $R_{qs}(r)$, and $dR_{qs}(r)/dr$ vanish beyond certain values of t and r . These values define the boundaries of the cell. In particular the eigenfunctions and their derivatives for $p = 2$ and $q = 0$ are shown in Fig. 2 ~ 6. As seen in these plots, the boundaries may be safely set as

$$|\eta t| < 5, \quad \eta r < 5 \quad \text{for } s = 1, 2, 3, 4 \quad (6.26)$$

In Sec. IV we made the requirement that the expectation value of x must be space-like for physical particles. To see if this requirement is satisfied for the present model, calculate the expectation value of t and r .

$$\bar{t}_p = N_p^2 \int_{-\infty}^{\infty} dt \, t \, e^{-\eta^2 t^2} H_p^2(\eta t) = 0 \quad (6.27)$$

$$\begin{aligned} \bar{r}_{qs} &= \frac{N_{qs}^2}{\eta^3} \int_0^{\infty} dr \, (\eta r)^{2s+3} e^{-\eta^2 r^2} [L_q^{s+1/2}(\eta^2 r^2)]^2 \\ &= \left[\frac{\Gamma(q + s + 2)}{\Gamma(q + s + 3/2)} \right]^3 \epsilon \end{aligned} \quad (6.28)$$

where $\epsilon = 1/\eta$ and the integration limits are extended to infinity for the sake of evaluation of the integrals. Since \bar{t}_p is zero for any p , the average distance between the constituents is purely space-like and \bar{r}_{qs} may be regarded as the radius of the meson. When s becomes large, Stirling's formula may be used to show that \bar{r}_{qs} approaches the limit

$$\bar{r}_{qs} \rightarrow s^{3/2} \epsilon, \quad s \rightarrow \infty \quad (6.29)$$

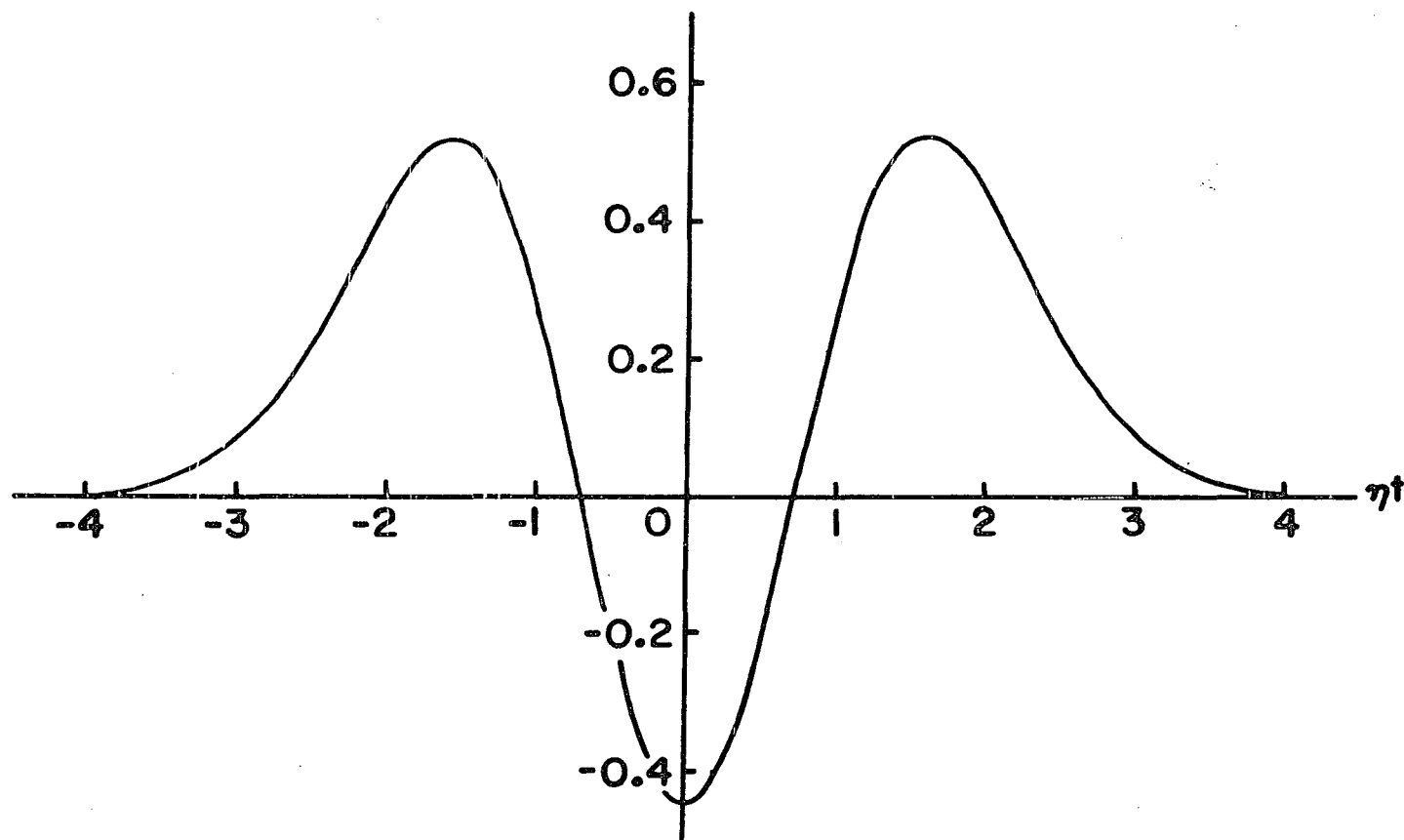


Figure 2a. $y_2(t)$

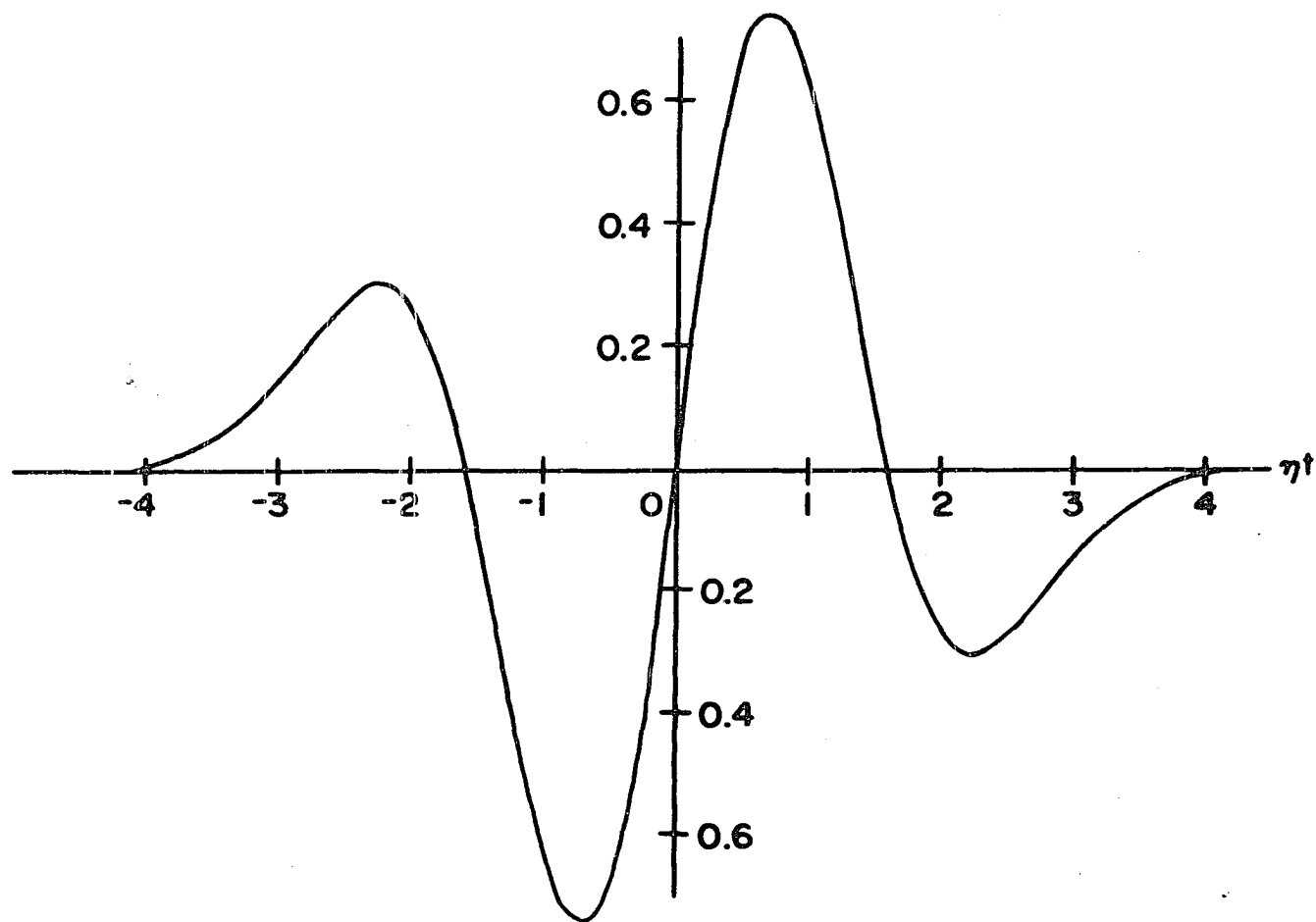


Figure 2b. $\frac{d}{dt} y_2(t)$

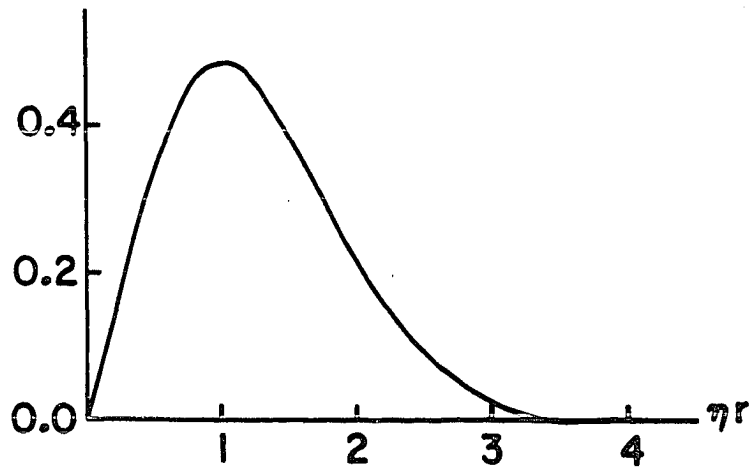


Figure 3a. $R_{01}(r)$

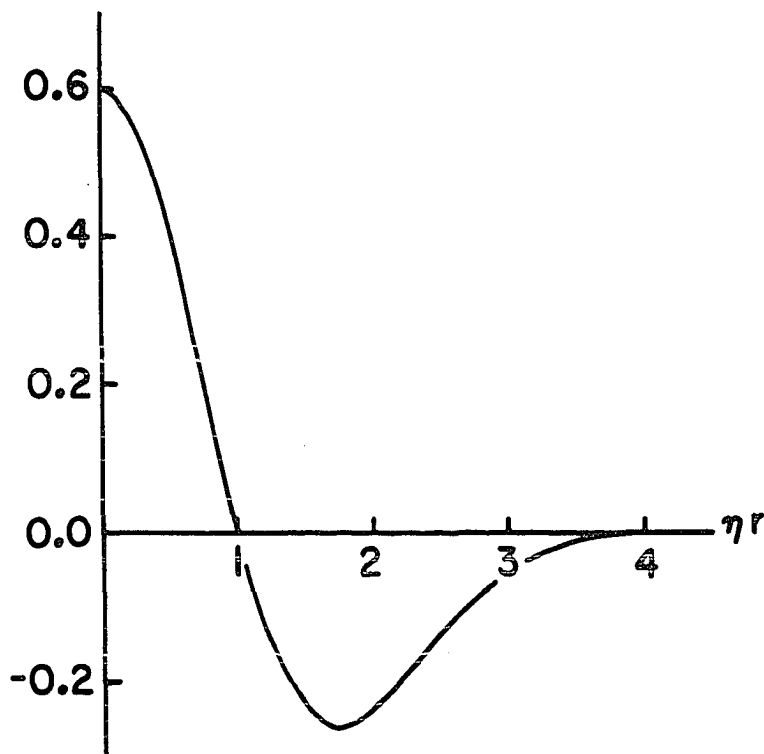
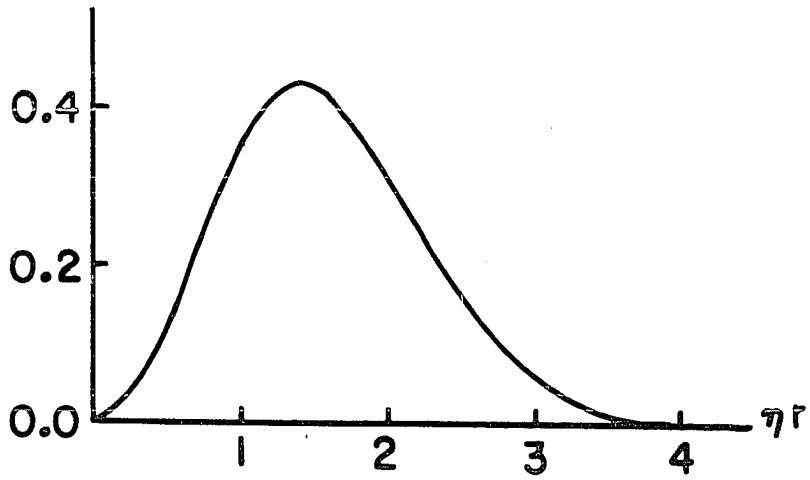
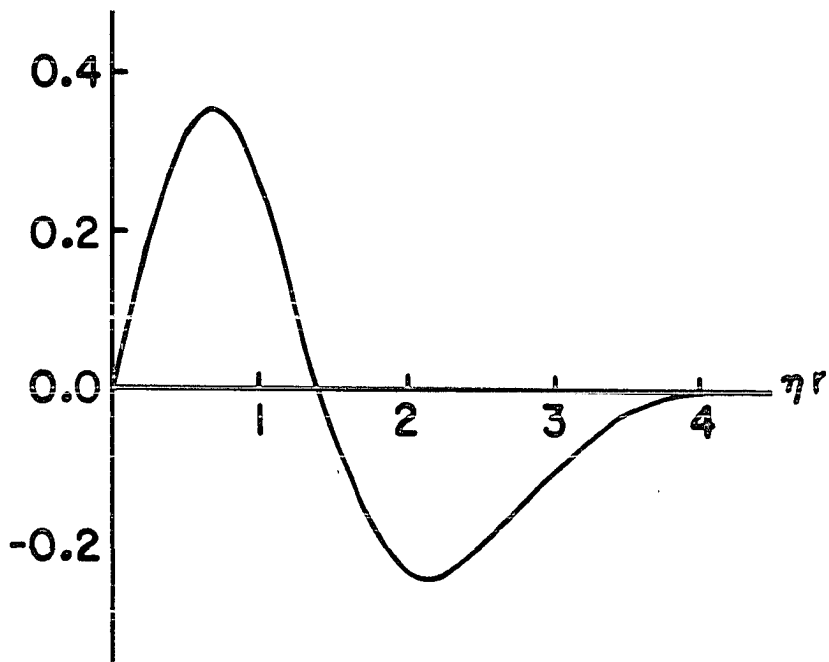


Fig. 3b. $\frac{d}{dr} R_{01}(r)$

Figure 4a. $R_{02}(r)$ Figure 4b. $\frac{d}{dr} R_{02}(r)$

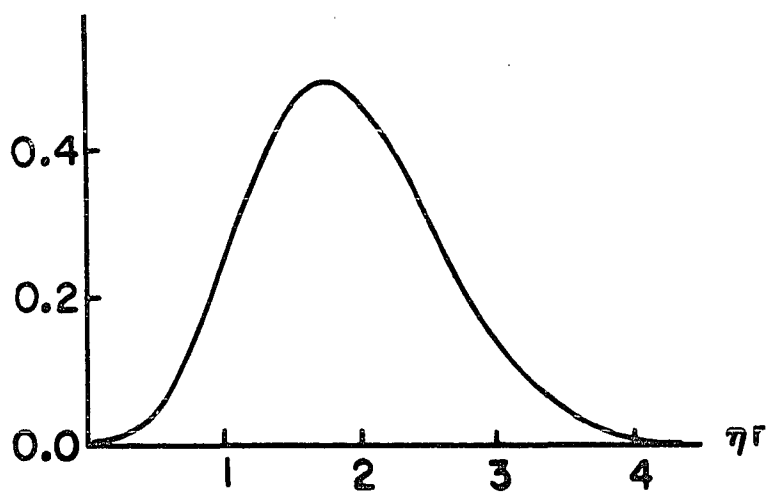


Figure 5a. $R_{03}(r)$

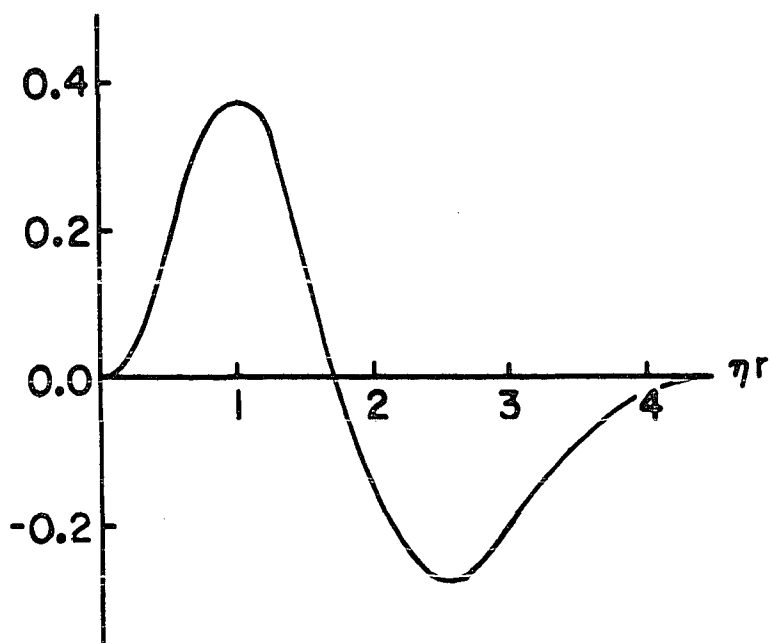
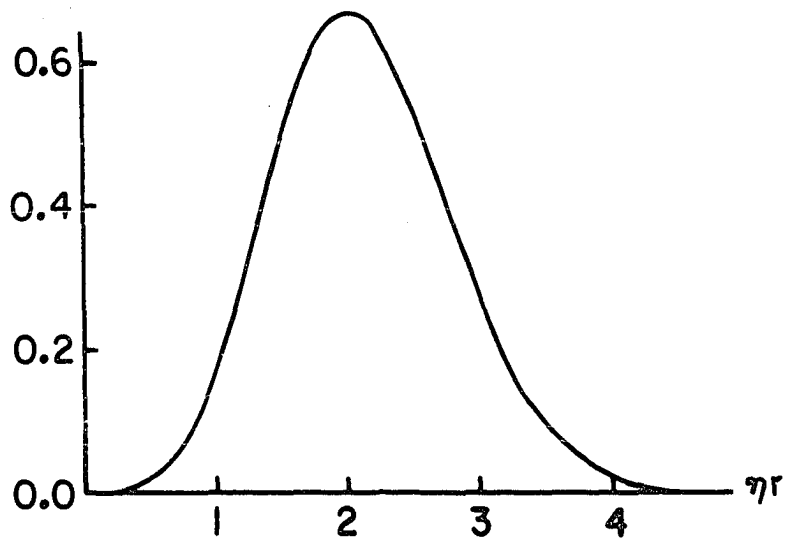
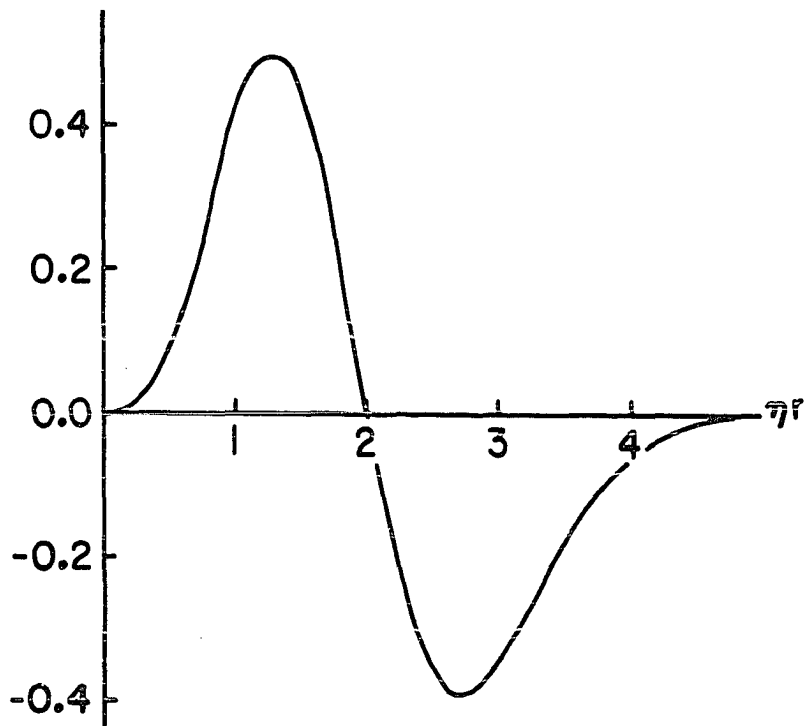


Figure 5b. $\frac{d}{dr} R_{03}(r)$

Figure 6a. $R_{04}(r)$ Figure 6b. $\frac{d}{dr} R_{04}(r)$

For mesons lying on the above mentioned leading trajectories, the radii are evaluated in units of Fermi, $F \equiv 10^{-13}$ cm as

$$\begin{aligned}
 \bar{r}_{01} &= 0.9F & \rho, \omega, K^*, \varphi \\
 \bar{r}_{02} &= 1.5F & f, A_2, K^{**}, f' \\
 \bar{r}_{03} &= 2.3F & \omega^*, g, K^{***} \\
 \bar{r}_{04} &= 3.2F & A_2^*, h
 \end{aligned} \tag{6.30}$$

Note that the radii of particles increase with spin. This is a consequence of the fact that the relative angular momentum of the quarks which increases with the radii is the spin of the meson in the present model.

E. Charmed Mesons

Finally let us consider the spectra of the charmed mesons. Since D^* belongs to the same 15-multiplet as K^* , take $p = 2$ and $q = 0$ for this meson. Substituting

$$D^* = c\bar{d}, \quad s = 1, \quad \mu_D^* = 2.01 \text{ GeV} \tag{6.31}$$

into Eq. (6.13) gives the mass of the charmed quark

$$m_c = 1.37 \text{ GeV} \tag{6.32}$$

Using this value, the spectra of the charmonium states are given by

$$\mu^2 = s + 2q - p + 8.5 \tag{6.33}$$

where η^2 is chosen to be 0.5 GeV^2 . By assigning the proper values of s and p and varying q , one can generate the mass spectra of the natural parity charmonium states. Comparison of our results with experimental

vales is given in Fig. 7 (25). Even though the mass spectra differ from those of the standard model (26), they include the experimentally known charmonium states. A peculiar feature is that J/ψ does not appear to be the ground state of 1^- spectrum. Also the present model predicts more than one χ states with 0^+ and 2^+ .

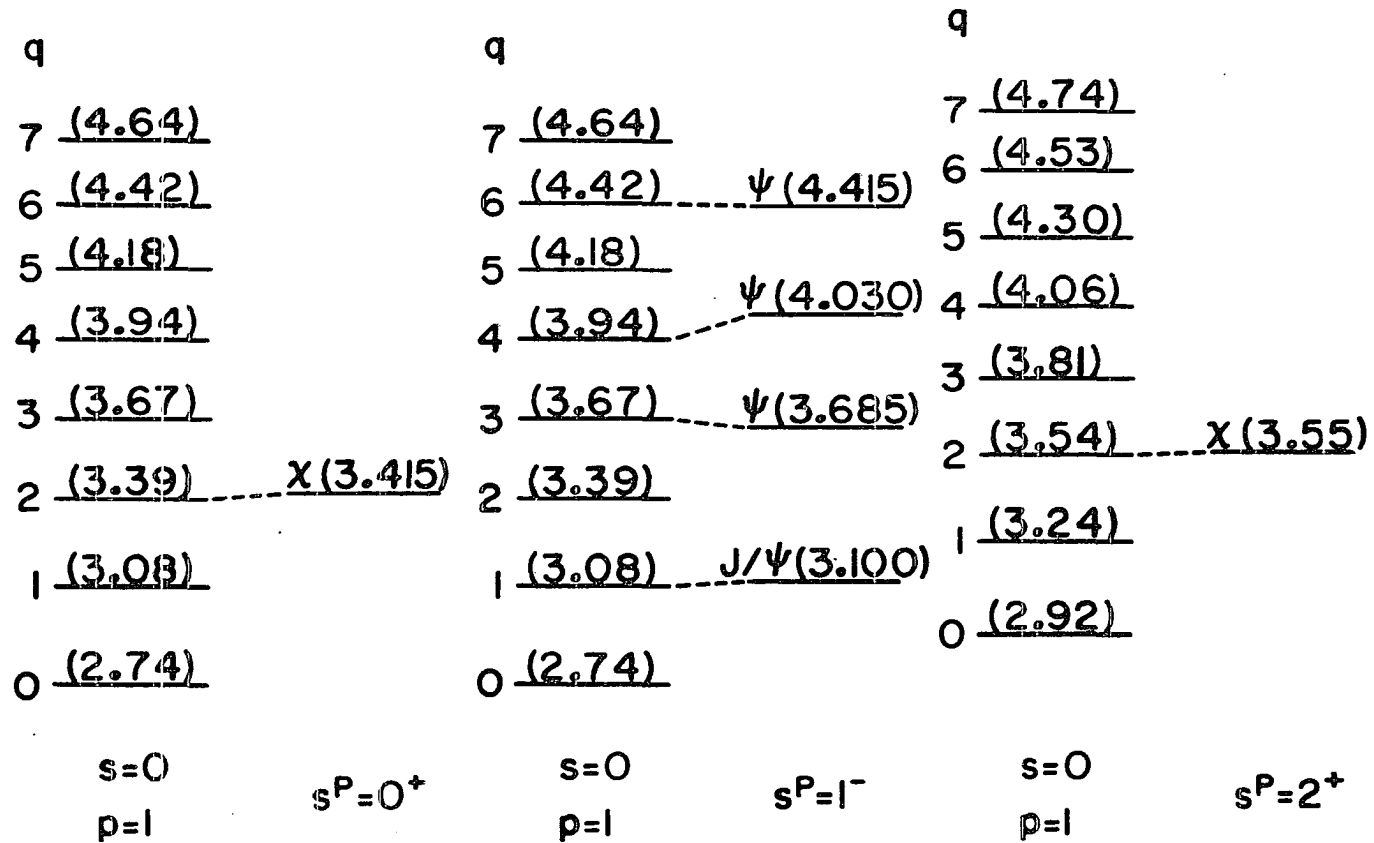


Figure 7. Mass spectra of natural parity charmonium states. In GeV units.

VII. CONCLUSION

To conclude let us summarize the results obtained from the present model.

i.) The Euler-Lagrange equation is a simple generalization of the local equation for a special class of Lagrangian densities satisfying the boundary condition on the cell.

ii.) For such Lagrangian densities there are appropriate conservation laws of energy-momentum and angular momentum.

iii.) The covariant harmonic oscillator interaction yields the linear Chew-Frautschi plots with the even daughter trajectories.

iv.) The quark masses appropriate to the meson mass spectra are in agreement with the phenomenological estimates.

v.) The radii of the mesons lying on the well-established leading trajectories are evaluated to be of the order of a fermi.

vi.) The mass spectra of the charmonium states seem to be in general agreement with the existing experimental values.

Considering the above results it seems as though the present model is appropriate to describe the static properties of the mesons. A crucial test of the model is the experimental verification of the existence of the other low lying charmonium states predicted. As with any physical model, however, our model has its limitations. The quarks are treated as bosons and their spins are neglected. It may be for this reason that the model is not appropriate to describe the unnatural parity mesons and the odd daughter trajectories are absent from the

Chew-Frautschi plots. The generalization of the model to describe baryons is not possible unless one treats quarks as fermions.

One may argue that the desired results of meson spectroscopy could be obtained solely from covariant harmonic oscillators without the framework of bilocal field theory. However, the significance of the present theory is that it has a proper framework for future developments. In analogy with local field theory, one may be able to define a suitable canonical conjugate momentum and quantize the field. It is also hoped that an appropriate S-matrix can be constructed without the divergence difficulties associated with the perturbative treatment of the conventional field theory. These points will be further investigated.

VIII. BIBLIOGRAPHY

1. H. Yukawa, Phys. Rev. 77, 219 (1950); Phys. Rev. 80, 1047 (1950).
2. H. Yukawa, Phys. Rev. 91, 415, 416 (1953).
3. M. Born, Nature 163, 207 (1949); H. S. Green, Nature 163, 208 (1949); M. Born and H. S. Green, Proc. Roy. Soc. Edinburgh A92, 470 (1949).
4. D. R. Yennie, Phys. Rev. 80, 1053 (1950).
5. J. Rayski, Proc. Phys. Soc. 64A, 957 (1951).
6. J. Rayski, Nuovo Cimento 2, 255 (1955).
7. M. Markov, Nuovo Cimento Suppl. 3, 760 (1956).
8. G. Pócsik, Acta Phys. Hung. 9, 261 (1959).
9. T. Takabayashi, Prog. Theor. Phys. 48, 1718 (1972).
10. Actually there is an exception to this statement. Markov suggested a model of elementary particles "consisting of two point <<particles>> connected by the relativistic interaction law." See Ref. 7 for detail.
11. G. Preparata and N. S. Craigie, Nuc. Phys. B102, 478 (1976).
12. C. C. Chiang, Phys. Lett. 62B, 419 (1976).
13. A. Z. Capri and C. C. Chiang, Nuovo Cimento 36A, 331 (1976).
14. T. J. Karr, Ph.D. Thesis, University of Maryland, 1976 (unpublished). I would like to thank Dr. Y. S. Kim for pointing out this work to me. I was not aware of Dr. Karr's dissertation before the completion of the present work.

15. L. L. Foldy, Phys. Rev. 122, 275 (1961).
16. J. Rzewuski, "Field Theory", Polish Scientific Publishers, Warszawa, Poland, 1964, Ch. 2.
17. Y. S. Kim and M. E. Noz, Phys. Rev. D12, 122 (1975).
18. S. S. Schweber, "An Introduction to Relativistic Quantum Field Theory", Harper and Row Publishers, New York, 1962, Ch. 17.
19. T. Takabayashi, Prog. Theor. Phys. 42, 423 (1969).
20. Y. S. Kim and M. E. Noz, Phys. Rev. D8, 3521 (1973); Phys. Rev. D12, 129 (1975); Y. S. Kim, Phys. Rev. D14, 273 (1976) and references cited therein.
21. R. M. Santilli, Nuovo Cimento 44A, 1284 (1966); K. Mita, Nuovo Cimento, 41A, 505 (1977).
22. P. M. Morse and H. Feshbach, "Methods of Theoretical Physics", McGraw-Hill Book Company, New York, 1953, Ch. 12.
23. P. D. B. Collins, "An Introduction to Regge Theory and High Energy Physics", Cambridge University Press, Cambridge, England, 1977, Ch. 5.
24. Here we are referring to the quark masses estimated from the mesonic decay processes and not those in the gauge models. See H. Suura and B. L. Young, Nuovo Cimento 11A, 101 (1972); B. L. Young, associate professor of physics at Iowa State Univ., lecture note, 1977 (unpublished).
25. Taken from Particle Data Group, Phys. Lett. 68B, 1 (1977).
26. T. Applequist, A. DeRújula, H. D. Politzer, and S. L. Glashow, Phys. Rev. Lett. 34, 365 (1975); E. Eichten, K. Gottfried, T. Kinoshita,

J. Kogut, K. D. Lane, and T. M. Yan, Phys. Rev. Lett., 34, 369
(1975).

IX. ACKNOWLEDGEMENT

I would like to thank Professor Bing-Lin Young for his support and guidance. I am grateful to Professor Derek Pursey for many helpful discussions. Without these, the present work would not have been completed. Special thanks to Mr. Douglas Peterman for his support.

PART II. TRIDENT PRODUCTION BY HIGH ENERGY
CHARGED PARTICLES ON NUCLEI

I. INTRODUCTION

The process of lepton-pair production in high energy lepton-hadron and hadron-hadron interactions is an important phenomenon in the exploration of new physics, such as the J/ψ and T production and the Drell-Yan process. In these processes high invariant mass lepton-pairs are involved. The physics of lepton-pairs, particularly electron-positron pair production, dates back to the early days of quantum theory of radiation. This "old" physics, involving quantum electrodynamics (QED), could be a potential background of the new physics. For example, the recent result on trimuon production in neutrino reactions can be partially accounted by the conventional QED bremsstrahlung effect.

Electron-positron pair production induced by fast electrons near the Coulomb field of an atom, called the trident process or direct pair production, was first suggested by Furry and Carlson in 1933 (1). In the following year, Skobel'tzyn reported the observation of pair production by β -rays in a cloud chamber (2). This proposal by Furry and Carlson was a variant of the idea of Oppenheimer and Plesset (3) who discussed pair production by high energy γ -rays observed by Curie and Joliot (4). All of the above workers sought to use pair production as a verification of Dirac's "hole theory" (5).

Various calculations of this process, using the virtual photon method of Weizsäcker and Williams (6), were carried out by Bhabha (7) and many others (8) in the 1930's. In his paper Bhabha made a distinction of the two kinds of lowest order pair production processes (7). The one in which the atomic Coulomb field interacts with the incident or

out-going charged primaries is called the "first-order process". In the other process, named the "second-order process", the presence of the Coulomb field affects either the created electron or positron. Note that the separation is gauge invariant. He further showed that the first-order process is dominant when the kinetic energy of the incident charged particle is small compared with its rest energy. As the energy of the incident particle increases, the second-order process becomes more important and eventually dominates over the first-order process at sufficiently high energies. Results obtained by Bhabha, however, are valid for small pair energies.

The first treatment on pair production in the framework of covariant perturbation theory of QED was presented by Murota, Ueda and Tanaka (9). However, their cross section formulae contain an undetermined parameter. Since then the calculations have been redone using various approximation schemes by Ternovskii (10), Kelner (11) and several others (12). The results obtained by these workers are valid only for the case in which the energies of participant particles are large compared with their masses. These results, however, do not contain any free parameter to be determined phenomenologically. A summary and comparison of these works is given by Wright (13). More recently, detailed calculations involving hadron primaries have been carried out by Young, Crawley, and the present author (14).

Most of the above mentioned works were done for the analysis of electromagnetic phenomena of high energy particles in dense media; e.g. energy loss of cosmic rays in emulsions. In their treatments, the

authors concerned themselves with trident processes with small invariant masses of lepton pair, all three out-going particles (the lepton pair and the primary) being close to the forward direction. More recently, direct pair production was discussed in the context of testing the validity of QED at small distances (15). Deviation from QED predictions, if any, can be investigated through wide-angle pair productions with large lepton pair invariant masses arising from highly off-mass shell virtual photons.

The QED calculations of pair production become somewhat complicated when the presence of atomic electrons is taken into consideration. The atomic electrons may enter the interaction in the following ways:

(i) They serve to screen the Coulomb field of the atomic nucleus and therefore reduce the effective nuclear electric charge.

(ii) They interact directly with the incident charged particle or one of the produced lepton pair.

The former effect gives rise to the elastic cross section. The latter adds incoherently to increase the cross section. The significance of this inelastic effect was pointed out by Perrin and expounded by Wheeler and Lamb (16). A detailed account of the effects of atomic electrons can be found in the article by Tsai (17).

Numerous experimental works on pair production are found in the literature (14). The status of these experiments is not clear owing to the fact that it is difficult to obtain clean data with good enough statistics to make a comparison with theoretical predictions. However, in the last several years, accelerator experiments with reasonably good statistics have been performed.

Early experiments were done in cloud chambers and other similar devices. β -rays derived from radiative sources were used as primaries. The majority of these experiments reported cross sections larger than the theoretical ones. A summary of experiments done up to 1939 was given by Crane and Halpern (18). In 1940, Feldmeier and Collins studied pair production by electrons from the Notre Dame Van de Graaff (19). In the late 1940's, the observation of pair production by high energy electrons from cosmic rays in photographic emulsions was reported by Occhialini and by Bradt, Kaplon and Peters (20). References on experimental works between 1940 and 1954, mainly on cosmic ray experiments, can be found in the article by Block, King, and Wada (21). Barkas, Deutsch, Gilbert and Violet reported the observation of pair production by electrons at the Berkeley synchrotron (22). Systematic studies of pair production from accelerator electrons were then carried out by Camac and by Shiren and Post (23).

Studies of trident processes by hadronic beams started about a decade and a half ago. An experiment on direct pair production using a π^- beam at 16 GeV/c in nuclear emulsions was performed by Mora in 1963 (24). Many investigations with primary e^- , μ^- , π^- , and p beams from accelerators have been done since then (25).

In App. A we list all the experiments using primary particles from accelerators, together with their targets, detection schemes and numbers of events, if available. Also included is a short listing of the comparisons with theory. Here it is useful to make a summary of the experiments prior to the middle of 1976.

1. Cloud chamber observations of the trident processes at low energies (primary energy $\lesssim 15$ MeV) are in general agreement with theory (26).

2. Pair production by cosmic ray electrons at primary energies $E_1 > 1$ GeV are in general variance with theory, yielding $\sigma_{\text{exp}} \approx 2 - 5 \sigma_{\text{theory}}$ (27). This discrepancy could be due to the limited number of trident events and possible systematic errors introduced in estimating the primary electron energy.

3. Experiments with cosmic ray muons are in general agreement with theory (28).

4. Counter experiments at primary electron energies $\lesssim 55$ MeV from accelerators are in good agreement with theory (23,29).

5. High energy electron and muon experiments, with primary electron energies of 4 GeV/C and 13.75 GeV/C and primary muon energy of 4 GeV/C, using both counter and emulsion techniques are in good agreement with theory (25). However, a μ emulsion experiment at a primary energy of 15.8 GeV/C is at variance with theory.

6. Experiments using hadron beams can be divided into two groups: emulsion experiments (30), which show large deviations from theoretical predictions and bubble chamber experiments, which are in good agreement with theory (31).

The calculations of the present work were done in the framework of covariant perturbation theory. The dominant contribution to the cross section comes from the lowest order diagrams and the higher order radiative corrections yield a very small part. We describe the lowest order calculations in detail for pair production by charged bosons, in particu-

lar by π^- , following the approach of Kelner (11). Cross section formulae for the fermion primary, which we take to be the proton for concreteness, are also presented. For the high energy lepton pairs, the second-order process dominates over the first-order process, as we shall see in the cross sections obtained by numerical computations. The interference term between the first and second-order process is shown to vanish. An attempt is made to calculate the radiative corrections to the second-order process.

The organization of the present work is as follows. In Sec. II, we describe the calculations for the second-order processes. Those for the first-order processes are given in Sec. III, in which the interference term between the first and second-order processes is also discussed. In Sec. IV, we present the radiative matrix elements which are free from the infrared divergences. The elimination of the infrared divergences is described in detail. Sec. V gives numerical evaluations of cross sections for the π^- primary at different incident energies. In particular, the pair energy distribution and the pair energy partition distribution are compared with the experimental data obtained by the Iowa State University group and its collaborators (32). We give concluding remarks in Sec. VI. App. A lists the experimental works on pair production. App. B through G supplement calculations presented in the main text.

II. SECOND-ORDER PROCESSES

In this section we shall calculate the differential cross section for the trident processes

$$B + A \rightarrow B + A^* + e^+ + e^-$$

where B represents a charged particle and A is an atom. A^* is the excited or ionized state of A . In general the results obtained in the present work are applicable to spin 0 bosons (π^\pm , K^\pm , etc.) and spin 1/2 fermions (e^\pm , μ^\pm , p , etc.) for the case that the momentum transfer between the in-coming and out-going B particle is small. Since we are particularly interested in the direct lepton pair production by hadrons, we shall refer to B as π^\pm or p . To the lowest order in the fine structure constant, the second order processes are depicted in diagrams of Fig. 1. In Fig. 1a, the incident particle (dotted line) is π^- and in 1b, p (solid line).

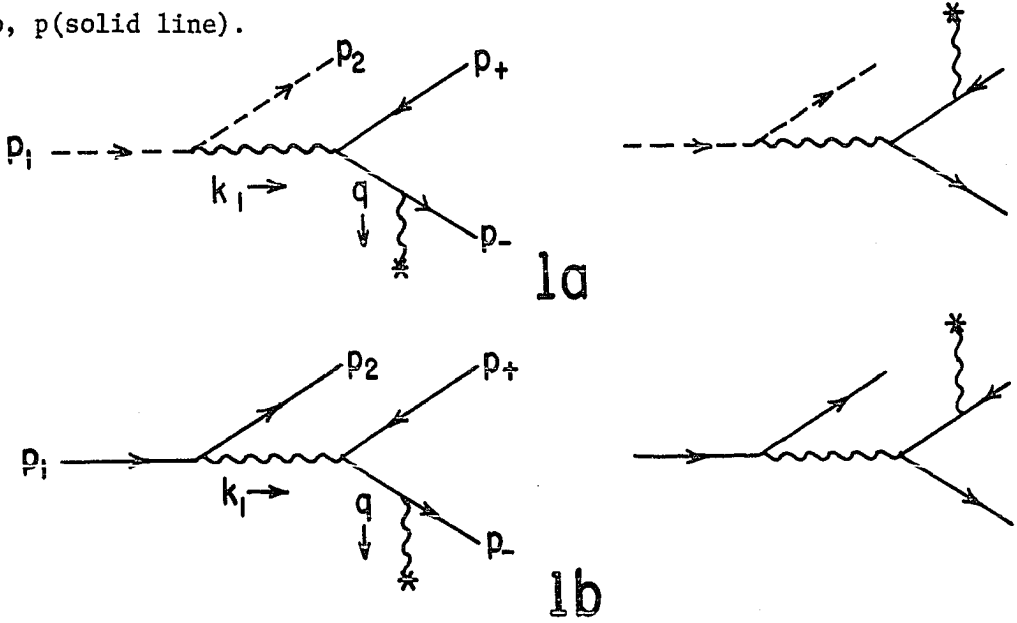


Figure 1. Feynman diagrams for second-order processes

A. Notations

Throughout the present work we will use the following notations:

$p_1(p_2)$; four-momentum of the incident (out-going) charged particle.

k_1 ; four-momentum of the intermediate virtual photon. For the

first order process in Sec. III, this will be denoted as k_2 .

$p_+(p_-)$; four-momentum of the positron (electron).

q ; four-momentum transfer to the atom.

$$\Delta^2 = -q^2$$

$u_\mu = (u_0, \vec{u})$, it takes the particular form $(1, \vec{0})$ in the lab frame.

\bar{a} ; length of the spacial part of a four-vector a_μ .

We will employ the convention of Bjorken and Drell (33). In particular, the metric is given by $g_{00} = -g_{11} = -g_{22} = -g_{33} = 1$.

B. Differential Cross Section

According to the Feynman rules of quantum electrodynamics, the T-matrix element for the pair of diagrams 1a is written as

$$T_{II} = i \frac{Ze^4}{k_1^2} (p_1 + p_2)_\alpha u^\mu \frac{F(\vec{q})}{q^2} \times \bar{u}(p_-) \left[\gamma^\alpha \frac{\not{q} - \not{p}_+ + m_e}{D_+} \gamma_\mu + \gamma_\mu \frac{\not{p}_- - \not{q} + m_e}{D_-} \gamma^\alpha \right] v(p_+) \quad (2.1)$$

where

$$\begin{cases} D_\pm = -\Delta^2 = 2(q \cdot p_\pm) \\ u \cdot q = 0 \end{cases} \quad (2.2)$$

and $F(\vec{q})/q^2$ is the form factor of the atom.

To proceed further, we need to qualify the expression of Eq. (2.1). We treat the particle B as point-like. It is known that hadrons have internal structures which manifest themselves as electromagnetic (em) form factors when they interact with high mass virtual photons. At the present time, there is no reliable theory for the em form factor. However, the vector meson dominance model provides a good guidance, especially for time-like virtual photons. The em form factor effect in this model is to modify the photon propagator according to

$$\frac{1}{k_1^2} \rightarrow \sum_i \frac{1}{k_1^2} \frac{1}{k_1^2 - m_i^2 + im_i \Gamma_i}$$

where the m_i 's are the masses of the neutral vector mesons which can couple to the photon and the B and the Γ_i 's are their widths. It is clear from the above modification that the dominant contributions come from small values of k_1^2 or $k_1^2 \approx m_i^2$. The former corresponds to QED processes and the latter, vector meson dominance predictions. In the present work, we shall concern ourselves only with the QED process, i.e., small k_1^2 and approximate the em form factor by unity.

Taking the absolute square of T_{II} and summing over polarizations of the electron-positron pair, we obtain the differential cross section

$$d\sigma_{II} = \frac{Z^2 \alpha^4}{\pi} [(u \cdot p_1)^2 - m_\pi^2]^{-1/2} \frac{|F(\Delta^2)|^2}{k_1^4 \Delta^4} \times A_{\alpha\beta} B^{\alpha\beta}_{\mu\nu} u^\mu u^\nu \frac{d^3 p_+}{p_+^0} \frac{d^3 p_-}{p_-^0} \frac{d^3 p_2}{p_2^0} \frac{d^3 q}{q^0} \delta(q + k_1 - p_+ - p_-) \quad (2.3)$$

where $\alpha = e^2/4\pi$ denotes the fine structure constant and the tensors $A_{\alpha\beta}$ and $B_{\mu\nu}^{\alpha\beta}$ are defined by

$$\begin{cases} A_{\alpha\beta} = \frac{1}{2} (p_1 + p_2)_\alpha (p_1 + p_2)_\beta \\ B_{\mu\nu}^{\alpha\beta} = \frac{1}{8} \text{Tr} \left\{ \left[\gamma^\alpha \frac{\not{d} - \not{p}_+ + m_e}{D_+} \gamma_\mu + \gamma_\mu \frac{\not{p}_- - \not{d} + m_e}{D_-} \gamma^\alpha \right] (\not{p}_+ - m_e) \right. \\ \quad \times \left. \left[\gamma^\beta \frac{\not{p}_- - \not{d} + m_e}{D_-} \gamma_\nu + \gamma_\nu \frac{\not{d} - \not{p}_+ + m_e}{D_+} \gamma^\beta \right] (\not{p}_- + m_e) \right\}. \end{cases} \quad (2.4)$$

For the proton case, we replace $A_{\alpha\beta}$ by $A'_{\alpha\beta}$:

$$A'_{\alpha\beta} = \frac{1}{4} \text{Tr} [\gamma_\alpha (\not{p}_1 + m_p) \gamma_\beta (\not{p}_2 + m_p)] \quad (2.5)$$

To fix the energies of the electron, the positron, and the virtual photon, we introduce the appropriate δ -functions in the differential cross section. Then Eq. (2.3) is rewritten in the form

$$\frac{d\sigma_{II}}{d\varepsilon_+ d\varepsilon_-} = \frac{2Z^2 \alpha^4}{\pi^2} [(u \cdot p_1)^2 - m_\pi^2]^{-1/2} \frac{1}{k_1^4} A_{\alpha\beta} \ell^{\alpha\beta} \frac{d^3 p_2}{p_2^0} \delta(u \cdot k_1 - \varepsilon_+ - \varepsilon_-) \quad (2.6)$$

where

$$\begin{aligned} & 2\pi^2 \ell^{\alpha\beta} \delta(u \cdot k_1 - \varepsilon_+ - \varepsilon_-) \\ &= \int \frac{|F(\Delta^2)|^2}{\Delta^4} B_{\mu\nu}^{\alpha\beta} u^\mu u^\nu \frac{d^3 p_+}{p_+^0} \frac{d^3 p_-}{p_-^0} \frac{d^3 q}{u^0} \delta(q + k_1 - p_+ - p_-) \\ & \times \delta(\varepsilon_+ - u \cdot p_+) \delta(\varepsilon_- - u \cdot p_-) \quad (2.7) \end{aligned}$$

The Lorentz invariant quantities $\varepsilon_{\pm} = u \cdot p_{\pm}$ introduced here represent the energies of positron and electron in the lab frame in which $u = (1, 0, 0, 0)$.

As seen from its definition above, the tensor $\ell^{\alpha\beta}$ is symmetric in α and β . Since the momenta p_+ , p_- , and q are integrated over, the available tensors to expand $\ell^{\alpha\beta}$ are k_1 , u , and $g^{\alpha\beta}$. Thus the general form of $\ell^{\alpha\beta}$ is written as

$$\ell^{\alpha\beta} = A_1 g^{\alpha\beta} + A_2 k_1^{\alpha} k_1^{\beta} + A_3 u^{\alpha} u^{\beta} + A_4 (k_1^{\alpha} u^{\beta} + u^{\alpha} k_1^{\beta}). \quad (2.8)$$

To determine A_1 through A_4 , let us employ the gauge invariance condition

$$k_{1\alpha} \ell^{\alpha\beta} = 0 \quad \text{or} \quad k_{1\beta} \ell^{\alpha\beta} = 0. \quad (2.9)$$

Either of the above implies

$$\begin{aligned} A_1 &= -k_1^2 A_2 - \omega A_4 \\ A_3 &= -\frac{k_1^2}{\omega} A_4 \end{aligned} \quad (2.10)$$

where $\omega = u \cdot k_1 = \varepsilon_+ + \varepsilon_-$ is the energy of the virtual photon in the lab frame. We can now write

$$-\ell^{\alpha\beta} = (k_1^2 g^{\alpha\beta} - k_1^{\alpha} k_1^{\beta}) A_2 + (\omega g^{\alpha\beta} + \frac{k_1^2}{\omega} u^{\alpha} u^{\beta} - k_1^{\alpha} u^{\beta} - u^{\alpha} k_1^{\beta}) A_4. \quad (2.11)$$

We can further express A_2 and A_4 in terms of the contraction of $\ell^{\alpha\beta}$

with $g_{\alpha\beta}$ and $u_{\alpha} u_{\beta}$:

$$A_2 = \frac{1}{\frac{2}{\omega - k_1^2}} u_{\alpha} u_{\beta} \ell^{\alpha\beta} + \frac{1}{2(\omega - k_1^2)} (g_{\alpha\beta} \ell^{\alpha\beta} + \frac{3k_1^2}{\frac{2}{\omega - k_1^2}} u_{\alpha} u_{\beta} \ell^{\alpha\beta})$$

$$A_4 = - \frac{\omega}{2(\omega^2 - k_1^2)} (g_{\alpha\beta} \ell^{\alpha\beta} + \frac{3k_1^2}{\omega^2 - k_1^2} u_\alpha u_\beta \ell^{\alpha\beta}) \quad (2.12)$$

Inserting the above expressions into Eq. (2.11) and rearranging terms, $\ell^{\alpha\beta}$ is now represented in the form

$$\ell^{\alpha\beta} = \frac{1}{2(\omega^2 - k_1^2)} (g_{\mu\nu} \ell^{\mu\nu} f_1^{\alpha\beta} + \frac{k_1^2}{\omega^2 - k_1^2} u_\mu u_\nu \ell^{\mu\nu} f_1^{\alpha\beta}) \quad (2.13)$$

where

$$\begin{cases} f_1^{\alpha\beta} = (\omega^2 - k_1^2) g^{\alpha\beta} + k_1^\alpha k_1^\beta + k_1^2 u^\alpha u^\beta - \omega(k_1^\alpha u^\beta + u^\alpha k_1^\beta) \\ f_2^{\alpha\beta} = (\omega^2 - k_1^2) g^{\alpha\beta} + (1 + \frac{2\omega^2}{k_1^2}) k_1^\alpha k_1^\beta + 3k_1^2 u^\alpha u^\beta - 3\omega(k_1^\alpha u^\beta + u^\alpha k_1^\beta) \end{cases} \quad (2.14)$$

The above representation shows that, to determine $\ell^{\alpha\beta}$, it is sufficient to evaluate the two scalar integrals $g_{\alpha\beta} \ell^{\alpha\beta}$ and $u_\alpha u_\beta \ell^{\alpha\beta}$. For this task we first need to evaluate $g_{\alpha\beta} B_{\mu\nu}^{\alpha\beta} u^\mu u^\nu$ and $u_\alpha u_\beta B_{\mu\nu}^{\alpha\beta} u^\mu u^\nu$ which involves trace calculations. The details are given in App. B. Here we give the final expressions.

$$\begin{aligned} g_{\alpha\beta} B_{\mu\nu}^{\alpha\beta} u^\mu u^\nu &= -4 \left(\frac{\epsilon_+}{D_+} - \frac{\epsilon_-}{D_-} \right)^2 [(p_+ \cdot p_-) + 2m_e^2] \\ &\quad + 4 \left(\frac{1}{D_+} + \frac{1}{D_-} \right) \left(\frac{\epsilon_+}{D_+} - \frac{\epsilon_-}{D_-} \right) [\epsilon_+ (q \cdot p_-) - \epsilon_- (q \cdot p_+)] \\ &\quad + 2 \left(\frac{1}{D_+} + \frac{1}{D_-} \right) \left\{ (q \cdot p_+) (q \cdot p_-) - \Delta^2 \epsilon_+ \epsilon_- + \frac{1}{2} \Delta^2 [(p_+ \cdot p_-) + 2m_e^2] \right\} \\ &\quad - \frac{2\Delta^2 (p_+ \cdot p_-)}{D_+ D_-} \end{aligned} \quad (2.15)$$

and

$$\begin{aligned}
 u_{\alpha} u_{\beta} B_{\mu\nu}^{\alpha\beta} u^{\mu} u^{\nu} &= 2 \left(\frac{\varepsilon_+}{D_+} - \frac{\varepsilon_-}{D_-} \right)^2 [2\varepsilon_+ \varepsilon_- - (p_+ \cdot p_-) - m_e^2] \\
 &+ \frac{1}{2} \left(\frac{1}{D_+} - \frac{1}{D_-} \right)^2 \left\{ 2(q \cdot p_+) (q \cdot p_-) + \Delta^2 [(p_+ \cdot p_-) + m_e^2] \right\} \\
 &+ 2 \left(\frac{1}{D_+} - \frac{1}{D_-} \right) \left(\frac{\varepsilon_+}{D_+} - \frac{\varepsilon_-}{D_-} \right) [\varepsilon_+ (q \cdot p_-) + \varepsilon_- (q \cdot p_+)] \quad (2.16)
 \end{aligned}$$

C. Integrations Over Kinematic Variables

We continue the evaluation of $\ell^{\alpha\beta}$ carrying out the integrations with respect to the electron and positron momenta. Denote

$$d\Gamma = \frac{d^3 p_+}{0} \frac{d^3 p_-}{0} \delta(q + k_1 - p_+ - p_-) \delta(\varepsilon_+ - u \cdot p_+) \delta(\varepsilon_- - u \cdot p_-) \quad (2.17)$$

It is convenient to integrate in the center of mass frame of the electron and positron. For this purpose, define the new variables

$$P = p_+ + p_- , \quad K = p_+ - p_- . \quad (2.18)$$

Let us rewrite the infinitesimal volume element as

$$\frac{d^3 p}{0} = 2 d^4 p \delta_+(p^2 - m^2) \quad (2.19)$$

where δ_+ denotes

$$\delta_+(x^2 - a^2) = \frac{1}{2a} \delta(x - a) . \quad (2.20)$$

Since

$$d^4 p_+ d^4 p_- = 2^{-4} d^4 P d^4 K , \quad (2.21)$$

we represent $d\Gamma$ in the form

$$\begin{aligned}
d\Gamma = & 2d^4K d^4P \delta(q+k_1-P)\delta_+(P^2+K^2-4m_e^2) \\
& \times \delta(P \cdot K) \delta(u \cdot P - (\epsilon_+ + \epsilon_-)) \delta(u \cdot K - (\epsilon_+ - \epsilon_-))
\end{aligned} \tag{2.22}$$

where the identity for the δ -function

$$f(x)\delta(x-a) = f(a)\delta(x-a) \tag{2.23}$$

is used to obtain Eq. (2.22). In the center of mass frame of electron and positron

$$P = (P_0, \vec{0}), \quad K = (0, \vec{K}). \tag{2.24}$$

Note that in this frame $u \neq (1, \vec{0})$. The δ -function appearing in Eq. (2.22) allow us to perform several of integrations trivially and we have

$$d\Gamma = \frac{1}{\bar{u} P_0} d\Omega_K \delta(\cos \theta - \frac{\epsilon_- - \epsilon_+}{\bar{u} \bar{K}}) \delta(u \cdot k_1 - \omega) \tag{2.25}$$

where

$$P = q + k_1, \quad \bar{K} = \sqrt{P^2 - 4m_e^2} \tag{2.26}$$

Since $P^2 = P_0^2$ in this frame, we have

$$\bar{u} P_0 = \sqrt{(u \cdot P)^2 - u^2 P^2} = \sqrt{\omega^2 - (q+k_1)^2}. \tag{2.27}$$

Choosing the z-axis along u direction, we describe the appropriate coordinate system as indicated in Fig. 2.

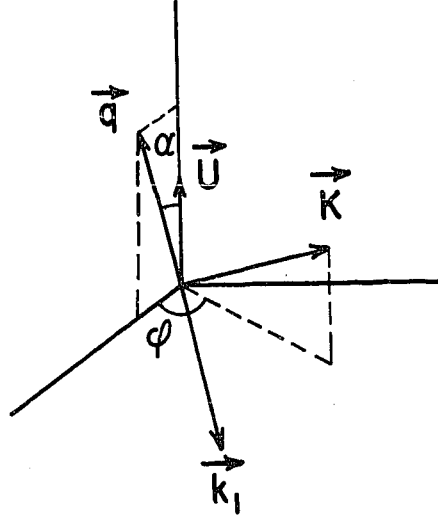


Figure 2. Center of mass frame of e^+ and e^-

In such a coordinate system, the calculation reduces to integration over the azimuthal angle ϕ .

$$d\Gamma = R^{-1/2} \delta(u \cdot k_1 - \omega) d\phi \quad (2.28)$$

where

$$\begin{cases} R = \omega^2 - (q + k_1)^2 \\ \cos \theta = \frac{\varepsilon_- - \varepsilon_+}{\bar{u}\bar{K}} \end{cases} \quad (2.29)$$

To proceed further, let us note the relations

$$(q \cdot p_{\pm}) = -\frac{1}{2} (\Delta^2 + D_{\pm})$$

$$D_+ + D_- = -2(q \cdot k_1)$$

$$\frac{1}{D_+ D_-} = - \frac{1}{2(q \cdot k_1)} \left(\frac{1}{D_+} + \frac{1}{D_-} \right)$$

$$(p_+ p_-) + m_e^2 = - \frac{1}{2} (D_+ + D_- + \Delta^2 - k_1^2) \quad . \quad (2.30)$$

Then

$$g_{\alpha\beta} B_{\mu\nu}^{\alpha\beta} u^\mu u^\nu = \omega^2 (X_+^2 + X_-^2) \frac{\Delta^2}{(q \cdot k_1)} \left(\frac{1}{D_+} + \frac{1}{D_-} \right)$$

$$- 4\omega^2 \left(m_e^2 + \frac{1}{2} k_1^2 \right) \left[\frac{X_+^2}{D_+^2} + \frac{X_-^2}{D_-^2} + \frac{X_+ X_-}{(q \cdot k_1)} \left(\frac{1}{D_+} + \frac{1}{D_-} \right) \right]$$

$$- \left[(q \cdot k_1) - \Delta^2 + \frac{\Delta^2}{2(q \cdot k_1)} (\Delta^2 - k_1^2 + 2m_e^2) \right] \left(\frac{1}{D_+} + \frac{1}{D_-} \right)$$

$$+ \Delta^2 \left(m_e^2 + \frac{1}{2} k_1^2 \right) \left(\frac{1}{D_+} + \frac{1}{D_-} \right) - 1 \quad (2.31)$$

and

$$u_\alpha u_\beta B_{\mu\nu}^{\alpha\beta} u^\mu u^\nu = 4\omega^4 X_+ X_- \left[\frac{X_+^2}{D_+^2} + \frac{X_-^2}{D_-^2} + \frac{X_+ X_-}{(q \cdot k_1)} \left(\frac{1}{D_+} + \frac{1}{D_-} \right) \right]$$

$$- \omega^2 \left[\left(\frac{X_+^2 k_1^2 + X_+ X_- \Delta^2}{D_+^2} + \frac{X_-^2 k_1^2 + X_+ X_- \Delta^2}{D_-^2} \right) - 2(X_+ - X_-) \left(\frac{X_+}{D_+} - \frac{X_-}{D_-} \right) \right]$$

$$+ \frac{2X_+ X_- k_1^2 + (X_+^2 + X_-^2) \Delta^2}{2(q \cdot k_1)} \left(\frac{1}{D_+} + \frac{1}{D_-} \right) + \frac{1}{4} \Delta^2 k_1^2 \left(\frac{1}{D_+^2} + \frac{1}{D_-^2} \right)$$

$$- \frac{1}{2} \left[(q \cdot k_1) - \frac{\Delta^2 k_1^2}{2(q \cdot k_1)} \right] \left(\frac{1}{D_+} + \frac{1}{D_-} \right) - 1 \quad (2.32)$$

where $X_\pm = \epsilon_\pm / \omega$. From these expressions, we see that the following

three integrals need to be evaluated.

$$\int d\Gamma, \int \frac{d\Gamma}{D_\pm}, \int \frac{d\Gamma}{D_\pm^2} \quad .$$

Integration of the first integral is trivial and is given by

$$\int d\Gamma = 2\pi R^{-1/2} \delta(u \cdot k_1 - \omega) \quad (2.33)$$

We shall carry out the second and the third integral separately.

The second integral $\int d\Gamma/D_{\pm}$:

We write

$$D_{\pm} = - (a_{\pm} + b_{\pm} \cos \phi) \quad (2.34)$$

where

$$\begin{cases} a_{\pm} = (q \cdot k_1) \mp \bar{q} \bar{K} \cos \alpha \cos \theta \\ b_{\pm} = \mp \bar{q} \bar{K} \sin \alpha \sin \theta \end{cases} \quad (2.35)$$

so that

$$\begin{aligned} \int \frac{d\Gamma}{D_{\pm}} &= - R^{-1/2} \delta(u \cdot k_1 - \omega) \int_0^{2\pi} \frac{d\phi}{a_{\pm} + b_{\pm} \cos \phi} \\ &= \frac{-2\pi}{\sqrt{a_{\pm}^2 - b_{\pm}^2}} R^{-1/2} \delta(u \cdot k_1 - \omega) . \end{aligned} \quad (2.36)$$

The quantity $(a_{\pm}^2 - b_{\pm}^2)$ can be calculated using Eqs. (2.26), (2.27), (2.29), and

$$\begin{cases} \bar{q} = \sqrt{\frac{(q \cdot P)^2 - q^2 P^2}{P^2}} \\ \cos \alpha = \frac{(u \cdot P)(q \cdot P)}{\bar{u} \bar{q} P^2} \end{cases} \quad (2.37)$$

Note that the right-hand sides of Eq. (2.37) can be expressed in terms of Lorentz invariant quantities, as we can write $\bar{u} = \sqrt{(u \cdot p)^2 / p^2 - 1}$.

After a tedious algebraic manipulation, we obtain

$$a_{\pm}^2 - b_{\pm}^2 = R^{-1} Q_{\pm} \quad (2.38)$$

where

$$\begin{aligned} Q_{\pm} = & 4 \varepsilon_{\pm}^2 (q \cdot k_1)^2 + \omega^2 \Delta^2 (4m_e^2 + \Delta^2) - 4\Delta^2 [\varepsilon_+ \varepsilon_- k_1^2 + \omega \varepsilon_{\pm} (q \cdot k_1)] \\ & - 4 m_e^2 [(q \cdot k_1)^2 + \Delta^2 k_1^2] + \Delta^2 k_1^2 (q + k_1)^2. \end{aligned} \quad (2.39)$$

The integral is now given by

$$\int \frac{d\Gamma}{D_{\pm}} = -2\pi Q_{\pm}^{-1/2} \delta(u \cdot k_1 - \omega). \quad (2.40)$$

The third integral $\int d\Gamma / D_{\pm}^2$:

With the knowledge of the second integral, the third integral can be evaluated as

$$\int \frac{d\Gamma}{D_{\pm}^2} = \frac{\partial}{\partial a_{\pm}} \int \frac{d\Gamma}{D_{\pm}} = 2\pi S_{\pm} Q_{\pm}^{-3/2} \delta(u \cdot k_1 - \omega) \quad (2.41)$$

where (34)

$$S_{\pm} = a_{\pm} R = 2\omega \varepsilon_{\pm} (q \cdot k_1) \pm \omega \Delta^2 (\varepsilon_- - \varepsilon_+) - (q \cdot k_1)(q + k_1)^2. \quad (2.42)$$

The expressions obtained so far are exact without any approximations. In the subsequent calculations we will make the following approximations for the high energy leptons.

- (i) Neglect the terms proportional to $1/\omega^4$.
- (ii) Neglect Δ^2 and k_1^2 compared with ω^2 .

Note that the dominant contributions to the cross section come from the lower limits of Δ^2 and k_1^2 integrations. At these limits

$$\frac{\Delta^2}{\omega^2} \sim \frac{\gamma_1^2}{\omega^4}, \quad \frac{k_1^2}{\omega^2} \sim \frac{m_\pi^2}{E_1 E_2}.$$

The integration limits of Δ^2 and k_1^2 will be given shortly. (See Eqs. (2.59) and (2.68).)

It is convenient to denote

$$(q \cdot k_1) = \gamma_1 t, \quad \Delta^2 = \gamma_1 y. \quad (2.43)$$

with

$$\gamma_1 = m_e^2 - k_1^2 X_+ X_- . \quad (2.44)$$

Using the above definitions and approximations, R , S_\pm , and Q_\pm are rewritten as

$$\begin{cases} R = \omega^2 \left(1 - \frac{2\gamma_1 t}{\omega^2}\right) \\ S_\pm = \gamma_1 \omega^2 (\sigma_\pm - \tilde{\sigma}) \\ Q_\pm = 4 \gamma_1^2 \omega^2 (q_\pm - \tilde{q}) \end{cases} \quad (2.45)$$

where

$$\begin{cases} \sigma_\pm = 2X_\pm t \pm (X_- - X_+)y \\ q_\pm = \frac{1}{4} y^2 + (1 - X_\pm t)y + X_\pm^2 t^2 \end{cases} \quad (2.46)$$

and

$$\begin{cases} \tilde{\sigma} = \frac{2\gamma_1 t^2}{\omega^2} \\ \tilde{q} = \frac{\gamma_1 t^2}{\omega^2} \end{cases} . \quad (2.47)$$

With the above integrals and quantities given, we can now perform the Γ -integration of $g_{\alpha\beta}^{\mu\nu} u^\mu u^\nu$ and $u_\alpha u_\beta B_{\mu\nu}^{\alpha\beta} u^\mu u^\nu$. These are expressed in the form

$$\left\{ \begin{aligned} & -\int d\Gamma g_{\alpha\beta}^{\mu\nu} u^\mu u^\nu = \omega \pi \left[\frac{1}{\gamma_1} (X_+^2 + X_-^2) \mathcal{J}_1 + \frac{1}{\gamma_1} (m_e^2 + \frac{1}{2} k_1^2) \mathcal{J}_2 \right] \\ & \quad \times \delta(u \cdot k_1 - \omega) \\ & \int d\Gamma u_\alpha u_\beta B_{\mu\nu}^{\alpha\beta} u^\mu u^\nu = \omega^3 \pi \frac{X_+ X_-}{\gamma_1^2} \mathcal{J}_2 \delta(u \cdot k_1 - \omega) \end{aligned} \right. \quad (2.48)$$

where

$$\left\{ \begin{aligned} \mathcal{J}_1 &= \frac{\gamma}{t} \left(\frac{1}{\sqrt{q_+}} + \frac{1}{\sqrt{q_-}} \right) - \frac{\gamma_1}{\omega^2 X_+ X_-} \\ \mathcal{J}_2 &= \frac{X_+^2}{\sqrt{q_+^3}} + \frac{X_-^2}{\sqrt{q_-^3}} - \frac{4X_+ X_-}{t} \left(\frac{1}{\sqrt{q_+}} + \frac{1}{\sqrt{q_-}} \right) \\ & \quad + \frac{\gamma_1}{\omega^2} \left(\frac{1}{X_+^2 X_-^2 t} - \frac{2}{X_+ X_- t} \right) . \end{aligned} \right. \quad (2.49)$$

To obtain ℓ^α and $u_\alpha u_\beta \ell^{\alpha\beta}$, we have to perform the integration with respect to q . The q -dependence can be expressed in terms of Δ^2 and $(q \cdot k_1)$. In the lab frame $u_0 = 1$ and taking \vec{k}_1 along Z-axis, we have

$$\begin{aligned} \frac{d^3 q}{u_0} &= \frac{-2}{q} d\bar{q} d(\cos \theta_q) d\phi_q = \frac{\pi}{\sqrt{\omega^2 - k_1^2}} d\Delta^2 d(q \cdot k_1) \\ &\approx \frac{\gamma_1^2 \pi}{\omega} dy dt . \end{aligned} \quad (2.50)$$

Hence

$$\left\{ \begin{aligned} -\ell^\alpha_\alpha &= \frac{1}{\gamma_1} (X_+^2 + X_-^2) I_1 + \frac{1}{\gamma_1^2} (m_e^2 + \frac{1}{2} k_1^2) I_2 \\ \frac{1}{\omega^2} u_\alpha u_\beta \ell^{\alpha\beta} &= \frac{X_+ X_-}{\gamma_1^2} I_2 \end{aligned} \right. \quad (2.51)$$

where

$$\left\{ \begin{aligned} I_1 &= \frac{1}{2} \iint \frac{dy}{y} dt |F(y)|^2 \mathcal{J}_1 \\ I_2 &= \frac{1}{2} \iint \frac{dy}{y} dt |F(y)|^2 \mathcal{J}_2 . \end{aligned} \right. \quad (2.52)$$

To determine the ranges of $(q \cdot k_1)$ and Δ^2 , we start with

$$(q + k_1)^2 = (p_+ + p_-)^2$$

which gives

$$(q \cdot k_1) = m_e^2 + (p_+ \cdot p_-) + \frac{1}{2} (\Delta^2 - k_1^2) . \quad (2.53)$$

For the high energy electron and positron

$$(p_+ \cdot p_-)_{\min} = \varepsilon_+ \varepsilon_- - \bar{p}_+ \bar{p}_- \approx m_e^2 \left(\frac{1}{2X_+ X_-} - 1 \right) + \frac{m_e^4}{\omega^2} \frac{(X_+ - X_-)^2}{X_+^3 X_-^3} \quad (2.54)$$

The above two equations imply

$$(q \cdot k_1)_{\min} = \frac{1}{2} \Delta^2 + \frac{\gamma_1}{2X_+ X_-} + \frac{m_e^4}{8\omega^2} \frac{(X_+ - X_-)^2}{X_+^3 X_-^3} . \quad (2.55)$$

Also in the lab frame

$$(q \cdot k_1) = -\vec{q} \cdot \vec{k}_1 \leq \Delta \bar{k}_1$$

from which it follows

$$(q \cdot k_1)_{\max} = \sqrt{\Delta^2 (\omega^2 - k_1^2)} . \quad (2.56)$$

Thus the integration limits of t are given by

$$t_1 \leq t \leq t_2$$

where

$$\begin{cases} t_1 = \frac{1}{2} y + \frac{1}{2X_+X_-} + \frac{m_e^4}{8\gamma_1\omega^2} \frac{(X_+ - X_-)^2}{X_+^3 X_-^3} \\ t_2 = \sqrt{\frac{(\omega^2 - k_1^2)}{\gamma_1}} y \end{cases} \quad (2.57)$$

The cross-hatched area on the t - y plane in Fig. 3 represents the integration region.

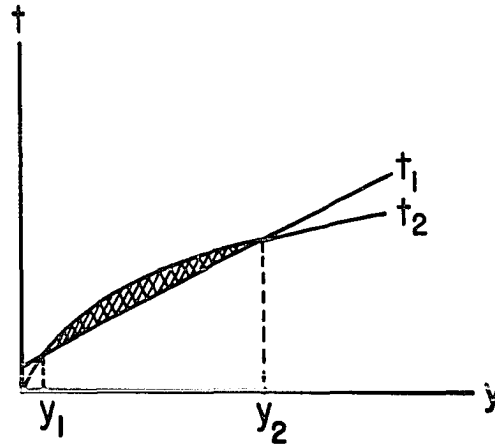


Figure 3. Integration region of t and y

To find the limits of y , solve for

$$t_1 = t_2 \quad (2.58)$$

which gives

$$y_1 \leq y \leq y_2$$

where

$$\begin{cases} y_1 = \frac{\gamma_1}{4(\omega^2 - k_1^2)} \frac{1}{x_+^2 x_-^2} \\ y_2 = \frac{4(\omega^2 - k_1^2)}{\gamma_1} - \frac{2}{x_+ x_-} - \frac{\gamma_1}{4(\omega^2 - k_1^2)} \frac{1}{x_+^2 x_-^2} - \frac{m_e^4}{2\gamma_1 \omega^2} \frac{(x_+ - x_-)^2}{x_+^3 x_-^3} \end{cases} \quad (2.59)$$

In the integration of t and y , we retain the terms proportional to $m_e^4 \omega^4$ and keep k_1^2 in comparison with ω^2 . The reason for doing these is that, at not too large values of ω still satisfying $m_e^2 < \omega^2$, the lower limits may exceed the upper limits for certain kinematic configurations unless these terms are included.

The t -integration in I_1 and I_2 can be carried out analytically for arbitrary $F(y)$. These integrals after the t -integration are given in App. C.

D. Cross Section Formula

It remains to integrate over p_2 in order to obtain the expression for the cross section. Take \vec{p}_1 along the Z -axis, then

$$d^3 p_2 = \bar{p}_2^2 d\bar{p}_2 d(\cos \theta_p) d\phi_p \quad (2.60)$$

From

$$k_1^2 = (p_1 - p_2)^2 = 2(m_\pi^2 - E_1 E_2 + \bar{p}_1 \bar{p}_2 \cos \theta_p) \quad (2.61)$$

we get

$$d(\cos \theta_p) = \frac{2 dk_1}{2\bar{p}_1 \bar{p}_2} \quad (2.62)$$

which leads to

$$\frac{d^3 p_2}{0} \delta(u k_1 - \omega) \approx \frac{\pi}{E_1} dk_1^2 \quad (2.63)$$

where $\omega = E_1 - E_2$ is used and m_π^2 are neglected compared with E_1^2 and E_2^2 .

Using Eqs. (2.4), (2.6) and (2.63), we obtain the differential cross section

$$\frac{d\sigma_{II}}{d\varepsilon_+ d\varepsilon_-} = \frac{2Z^2 \alpha^4}{\pi} \frac{1}{\omega^2} \frac{E_2}{E_1} \frac{ds}{s^2} F_{II} \quad (2.64)$$

where

$$F_{II} = (s - \frac{\xi}{X_+ X_-}) (-\ell^\alpha \alpha) + s \frac{m_e^2}{\omega^2} (3s - \frac{\xi}{X_+ X_-} + \frac{\omega^2}{2E_1 E_2} s) (u_\alpha u_\beta \ell^{\alpha\beta}) \quad (2.65)$$

and the quantities $-\ell^\alpha \alpha$ and $u_\alpha u_\beta \ell^{\alpha\beta}$ are given by Eq. (2.51). The symbols s and ξ here denote

$$\left\{ \begin{array}{l} s = -\frac{k_1^2}{2m_e} \\ \xi = \frac{m_\pi^2 \varepsilon_+ \varepsilon_-}{m_e^2 E_1 E_2} \end{array} \right. \quad (2.66)$$

We neglect k_1^2 compared with E_1^2 and ω^2 in the above expression of F_{II} .

One can find the range of k_1^2 from Eq. (2.61). Since

$$\bar{p}_1 \bar{p}_2 \approx E_1 E_2 - \frac{1}{2} \frac{E_1^2 + E_2^2}{E_1 E_2} m_\pi^2, \quad (2.67)$$

we have

$$\frac{m_\pi^2 \omega^2}{E_1 E_2} \leq -k_1^2 \leq 4E_1 E_2 \quad (2.68)$$

Or expressed in terms of s

$$s_1 \leq s \leq s_2$$

where

$$\begin{cases} s_1 = \frac{\xi}{X_+ X_-} \\ s_2 = \frac{4E_1 E_2}{m_e^2} \end{cases} \quad (2.69)$$

E. Proton Case

For the proton case, the cross section formula can be obtained with the use of $A'_{\alpha\beta}$ given by Eq. (2.5).

$$\frac{d\sigma'_{II}}{d\epsilon_+ d\epsilon_-} = \frac{2Z^2 \alpha}{\pi} \frac{1}{\omega^2} \frac{E_2}{E_1} \frac{ds}{s^2} F'_{II} \quad (2.70)$$

where

$$\begin{aligned} F'_{II} = & \left(s - \frac{\xi'}{X_+ X_-} - \frac{\omega^2}{2E_1 E_2} s \right) (-\ell^\alpha{}_\alpha) \\ & + s \frac{m_e^2}{\omega^2} \left(3s - \frac{\xi'}{X_+ X_-} + \frac{\omega^2}{2E_1 E_2} s \right) (u_\alpha u_\beta \ell^{\alpha\beta}) \end{aligned} \quad (2.71)$$

and

$$\xi' = \frac{m_p^2 \epsilon_+ \epsilon_-}{2 m_e E_1 E_2} \quad (2.72)$$

The other necessary quantities are previously given in this section.

III. FIRST-ORDER PROCESSES

In this section we shall consider the contribution to the cross section due to the diagrams 4a and 4b. In the diagrams of 4a, the incident particle is π^- and in 4b, p.

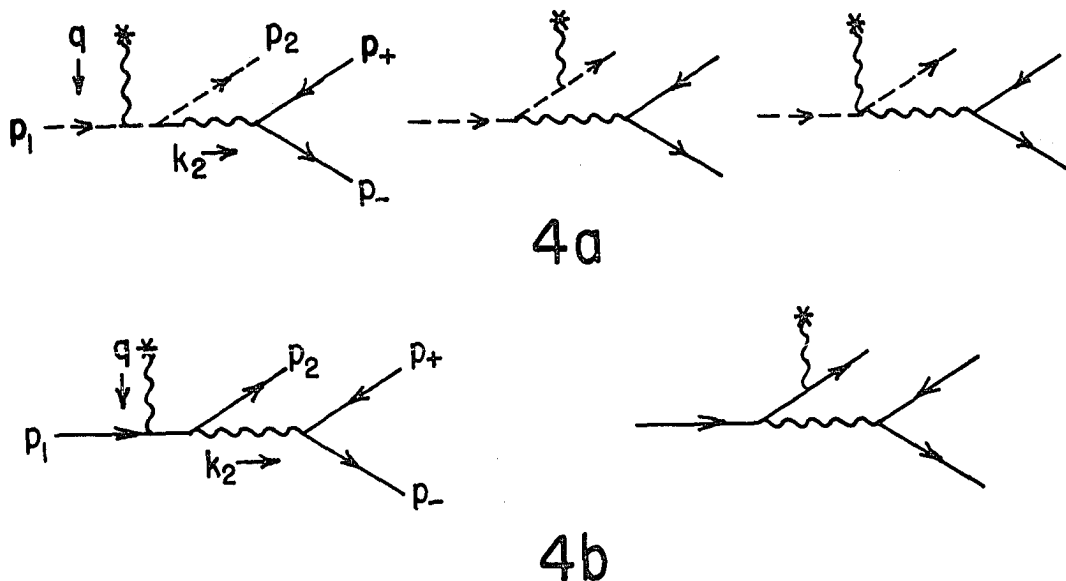


Figure 4. Feynman diagrams for first-order processes

The third diagram in 4a, called the contact term, is necessary to maintain the gauge invariance. The calculations will be carried out in a similar way to those of Sec. II. We describe the detail of calculations for the pion case. For the proton case, we give summary of the results. The interference term between the first and the second order processes is discussed at the end of this section.

A. Differential Cross Section

The T-matrix element for the diagrams 4a is written as

$$T_I = -i \frac{Ze^4}{k_2^2} \bar{u}(p_-) \gamma_\alpha v(p_+) u^\mu \frac{F(\vec{q})}{\vec{q}^2} \times \left[\frac{(p_1+p_2+q)^\alpha (2p_1+q)_\mu}{D_1} + \frac{(p_1+p_2-q)^\alpha (2p_2-q)_\mu}{D_2} - 2g_\mu^\alpha \right] \quad (3.1)$$

where

$$D_1 = (p_1+q)^2 - m_\pi^2, \quad D_2 = (p_2-q)^2 - m_\pi^2. \quad (3.2)$$

Taking the absolute square of T_I and summing over the polarizations of electron and positron, the differential cross section can be expressed in the form

$$d\sigma_I = \frac{Z^2 \alpha^4}{\pi^4} [(u \cdot p_1)^2 - m_\pi^2]^{-1/2} \frac{|F(\vec{q})|^2}{k_2^4 \Delta^4} K_{\alpha\beta} M_{\mu\nu}^{\alpha\beta} u^\mu u^\nu \times \frac{d^3 p_+}{p_+} \frac{d^3 p_-}{p_-} \frac{d^3 p_2}{p_2} \frac{d^3 q}{u} \delta(q+p_1-p_2-p_+-p_-) \quad (3.3)$$

where the tensors $K_{\alpha\beta}$ and $M_{\mu\nu}^{\alpha\beta}$ are given by

$$\left\{ \begin{aligned} K_{\alpha\beta} &= \frac{1}{4} \text{Tr}[\gamma_\alpha (\not{p}_+ - m_e) \gamma_\beta (\not{p}_- + m_e)] \\ M_{\mu\nu}^{\alpha\beta} &= \frac{1}{8} \left[\frac{(p_1+p_2+q)^\alpha (2p_1+q)_\mu}{D_1} + \frac{(p_1+p_2-q)^\beta (2p_2-q)_\mu}{D_2} - 2g_\mu^\alpha \right] \\ &\times \left[\frac{(p_1+p_2+q)^\beta (2p_1+q)_\nu}{D_1} + \frac{(p_1+p_2-q)^\beta (2p_2-q)_\nu}{D_2} - 2g_\nu^\beta \right]. \end{aligned} \right. \quad (3.4)$$

To facilitate the calculation, we separate the contributions from two parts of the diagrams connected by the intermediate virtual photon. This is achieved by introducing an additional δ -function to fix the four-momentum k_2 . As in Sec. II, we also fix the energies of the lepton pair. Then the cross section is represented in the form

$$\frac{d\sigma_I}{d\varepsilon_+ d\varepsilon_-} = \frac{Z^2 \alpha^4}{\pi^4} [(u \cdot p_1)^2 - m_\pi^2]^{-1/2} L_{\alpha\beta} N^{\alpha\beta} \frac{d^4 k_2}{k_2^4} \quad (3.5)$$

where

$$\begin{cases} L_{\alpha\beta} = \int K_{\alpha\beta} \frac{d^3 p_+}{p_+^0} \frac{d^3 p_-}{p_-^0} \delta(k_2 - p_+ - p_-) \delta(u \cdot p_+ - \varepsilon_+) \delta(u \cdot p_- - \varepsilon_-) \\ N^{\alpha\beta} = \int \frac{|F(\vec{q})|^2}{\Delta^4} M_{\mu\nu}^{\alpha\beta} u^\mu u^\nu \frac{d^3 p_2}{p_2^0} \frac{d^3 q}{q^0} \delta(q + p_1 - p_2 - k_2) \end{cases} \quad (3.6)$$

B. Bremsstrahlung Part

The tensor $L_{\alpha\beta}$ describes the parts of the diagrams associated with the virtual photon dissociation into e^+ and e^- . As in Sec. II, the general form of the symmetric tensor $L_{\alpha\beta}$ is given by

$$L_{\alpha\beta} = B_1 g_{\alpha\beta} + B_2 k_{2\alpha} k_{2\beta} + B_3 u_\alpha u_\beta + B_4 (k_{2\alpha} u_\beta + u_\alpha k_{2\beta}) \quad (3.7)$$

The gauge invariance condition

$$k_2^\alpha L_{\alpha\beta} = 0 \quad \text{or} \quad k_2^\beta L_{\alpha\beta} = 0 \quad (3.8)$$

implies

$$\begin{cases} B_1 = -k_2^2 B_2 - \omega B_4 \\ B_3 = -\frac{k_2^2}{\omega} B_4 \end{cases} \quad (3.9)$$

where the invariant quantity $\omega = u \cdot k_2 = \epsilon_+ + \epsilon_-$ is the lepton pair energy in the lab frame. Using Eq. (3.9) in Eq. (3.8), we have

$$-L_{\alpha\beta} = (k_2^2 g_{\alpha\beta} - k_{2\alpha} k_{2\beta}) B_2 + (\omega g_{\alpha\beta} + \frac{k_2^2}{\omega} u_\alpha u_\beta - k_{2\alpha} u_\beta - u_\alpha k_{2\beta}) B_4 \quad (3.10)$$

In terms of the contractions $g^{\alpha\beta} L_{\alpha\beta}$ and $u^\alpha u^\beta L_{\alpha\beta}$, B_2 and B_4 are given by

$$\begin{cases} B_2 = \frac{1}{\omega^2 - k_2^2} u^\alpha u^\beta L_{\alpha\beta} + \frac{1}{2(\omega^2 - k_2^2)} (g^{\alpha\beta} L_{\alpha\beta} + \frac{3k_2^2}{\omega^2 - k_2^2} u^\alpha u^\beta L_{\alpha\beta}) \\ B_4 = -\frac{\omega}{2(\omega^2 - k_2^2)} (g^{\alpha\beta} L_{\alpha\beta} + \frac{3k_2^2}{\omega^2 - k_2^2} u^\alpha u^\beta L_{\alpha\beta}). \end{cases} \quad (3.11)$$

Thus we can express Eq. (3.10) in the form

$$L_{\alpha\beta} = \frac{1}{2(\omega^2 - k_2^2)} (g^{\mu\nu} L_{\mu\nu} j_{1\alpha\beta} + \frac{k_2^2}{\omega^2 - k_2^2} u^\mu u^\nu L_{\mu\nu} j_{2\alpha\beta}) \quad (3.12)$$

where

$$\begin{cases} j_{1\alpha\beta} = (\omega^2 - k_2^2) g_{\alpha\beta} + k_{2\alpha} k_{2\beta} + k_2^2 u_\alpha u_\beta - \omega(k_{2\alpha} u_\beta + k_{2\beta} u_\alpha) \\ j_{2\alpha\beta} = (\omega^2 - k_2^2) g_{\alpha\beta} + (1 + \frac{2\omega^2}{k_2^2}) k_{2\alpha} k_{2\beta} + 3k_2^2 u_\alpha u_\beta \\ \quad - 3\omega(k_{2\alpha} u_\beta + k_{2\beta} u_\alpha) \end{cases} \quad (3.13)$$

From the first expression of Eq. (3.4)

$$K_{\alpha\beta} = (p_{+\alpha} p_{-\beta} + p_{-\alpha} p_{+\beta}) - g_{\alpha\beta} [m_e^2 + (p_+ \cdot p_-)] \quad (3.14)$$

which gives

$$\begin{cases} g^{\alpha\beta} K_{\alpha\beta} = -(2m_e^2 + k_2^2) \\ u^\alpha u^\beta K_{\alpha\beta} = 2\epsilon_+ \epsilon_- - \frac{1}{2} k_2^2 \end{cases} \quad (3.15)$$

To determine $L_{\alpha\beta}$ it remains to integrate over the pair momenta p_+ and p_- . Denoting

$$d\Gamma' = \frac{d^3 p_+}{p_+} \frac{d^3 p_-}{p_-} \delta(k_2 - p_+ - p_-) \delta(u \cdot p_+ - \varepsilon_+) \delta(u \cdot p_- - \varepsilon_-) , \quad (3.16)$$

we notice that $d\Gamma'$ reduces to $d\Gamma$, Eq. (2.17), when $(q+k_1)$ is replaced by k_2 . Hence

$$d\Gamma' = (\omega^2 - k_2^2)^{-1/2} \delta(u \cdot k_2 - \omega) d\phi \quad (3.17)$$

The Γ' -integration is now straightforward to give

$$\begin{cases} -L_{\alpha}^{\alpha} = 2\pi(\omega^2 - k_2^2)^{-1/2} (2m_e^2 + k_2^2) \delta(u \cdot k_2 - \omega) \\ u^{\alpha} u^{\beta} L_{\alpha\beta} = 2\pi(\omega^2 - k_2^2)^{-1/2} (2\varepsilon_+ \varepsilon_- - \frac{1}{2} k_2^2) \delta(u \cdot k_2 - \omega) \end{cases} . \quad (3.18)$$

Now $L_{\alpha\beta}$ takes the form

$$L_{\alpha\beta} = \frac{\pi}{(\omega^2 - k_2^2)^{3/2}} \left[-(2m_e^2 + k_2^2) j_{1\alpha\beta} + \frac{k_2^2}{\omega^2 - k_2^2} (2\varepsilon_+ \varepsilon_- - \frac{1}{2} k_2^2) j_{2\alpha\beta} \right] \\ \times \delta(u \cdot k_2 - \omega) . \quad (3.19)$$

In order to separate in $d\sigma_I$ the factor proportional to the bremsstrahlung cross section of the virtual photon, we make use of the gauge invariance constraints:

$$k_{2\alpha} M_{\mu\nu}^{\alpha\beta} = 0 , \quad k_{2\beta} M_{\mu\nu}^{\alpha\beta} = 0 . \quad (3.20)$$

Therefore, the terms proportional to $k_{2\alpha}$ or $k_{2\beta}$ in $j_{1\alpha\beta}$ and $j_{2\alpha\beta}$ do not contribute to the cross section. For this reason, we can leave out from $L_{\alpha\beta}$ the terms proportional to $k_{2\alpha}$ or $k_{2\beta}$. Also we write

$$d^4 k_2 = \frac{d^3 k_2}{2k_2} d k_2^2 \quad (3.21)$$

where k_2^2 is the lepton pair invariant mass. Then the cross section can be represented in the form

$$\frac{d\sigma_I}{d\varepsilon_+ d\varepsilon_-} = \frac{Z_\alpha^2}{\pi^3} [(u \cdot p_1)^2 - m_\pi^2]^{-1/2} F_{\alpha\beta} G^{\alpha\beta} \frac{dk_2^2}{k_2^4} \quad (3.22)$$

where

$$F_{\alpha\beta} = \frac{1}{2(\omega^2 - k_2^2)^{3/2}} \left[-(2m_e^2 + k_2^2) j'_{1\alpha\beta} + \frac{k_2^2}{\omega^2 - k_2^2} (2\varepsilon_+ \varepsilon_- - \frac{1}{2} k_2^2) j'_{1\alpha\beta} \right] \quad (3.23)$$

with

$$\begin{cases} j'_{1\alpha\beta} = (\omega^2 - k_2^2) g_{\alpha\beta} + k_2^2 u_\alpha u_\beta \\ j'_{2\alpha\beta} = (\omega^2 - k_2^2) g_{\alpha\beta} + 3k_2^2 u_\alpha u_\beta \end{cases} \quad (3.24)$$

and

$$G^{\alpha\beta} = \int \frac{|F(\vec{q})|^2}{\Delta^4} M_{\mu\nu}^{\alpha\beta} u^\mu u^\nu \frac{d^3 p_2}{p_2} \frac{d^3 k_2}{k_2} \frac{d^3 q}{u} \delta(u \cdot k_2 - \omega) \times \delta(q + p_1 - p_2 - k_2) \quad (3.25)$$

C. Primary Part

The tensor $G^{\alpha\beta}$ describes the interaction of the incident and outgoing charged particle with the atom. In the cross section formula given above, we need to know only two scalar integrals $g_{\alpha\beta} G^{\alpha\beta}$

and $u_\alpha u_\beta G^{\alpha\beta}$. For this purpose, we first evaluate the integrands $g_{\alpha\beta} M_{\mu\nu}^{\alpha\beta} u^\mu u^\nu$ and $u_\alpha u_\beta M_{\mu\nu}^{\alpha\beta} u^\mu u^\nu$. From the definition of $M_{\mu\nu}^{\alpha\beta}$ given by the second expression of Eq. (3.4), it immediately follows that

$$\begin{aligned} g_{\alpha\beta} M_{\mu\nu}^{\alpha\beta} u^\mu u^\nu &= \left(\frac{E_1}{D_1} + \frac{E_2}{D_2} \right)^2 [(p_1 \cdot p_2) + m_\pi^2 + \frac{1}{2} \Delta^2] \\ &\quad + \left(\frac{E_1^2}{D_1^2} - \frac{E_2^2}{D_2^2} \right) [(q \cdot p_1) + (q \cdot p_2)] - \left(\frac{E_1^2}{D_1^2} + \frac{E_2^2}{D_2^2} \right) \Delta^2 \\ &\quad - \left(\frac{E_1}{D_1} + \frac{E_2}{D_2} \right) (E_1 + E_2) + \frac{1}{2} \end{aligned} \quad (3.26)$$

and

$$\begin{aligned} u_\alpha u_\beta M_{\mu\nu}^{\alpha\beta} u^\mu u^\nu &= \frac{1}{2} \left(\frac{E_1}{D_1} + \frac{E_2}{D_2} \right)^2 (E_1 + E_2)^2 \\ &\quad - \left(\frac{E_1}{D_1} + \frac{E_2}{D_2} \right) (E_1 + E_2) + \frac{1}{2} \end{aligned} \quad (3.27)$$

Using the relations

$$\begin{cases} (q \cdot p_1) = \frac{1}{2} (\Delta^2 + D_1) & , \quad (q \cdot p_2) = -\frac{1}{2} (\Delta^2 + D_2) \\ (p_1 \cdot p_2) - m_\pi^2 = \frac{1}{2} (D_1 + D_2 + \Delta^2 - k_1^2) & , \end{cases} \quad (3.28)$$

Eq. (3.26) can be rewritten in the form

$$g_{\alpha\beta} M_{\mu\nu}^{\alpha\beta} u^\mu u^\nu = \frac{2E_1 E_2}{D_1 D_2} \Delta^2 + 2 \left(m_\pi^2 - \frac{1}{4} k_2^2 \right) \left(\frac{E_1}{D_1} + \frac{E_2}{D_2} \right)^2 + \frac{1}{2} . \quad (3.29)$$

Eq. (3.27) is already in the desired form.

Next we shall consider integration with respect to p_2 and k_2 . Let us define

$$d\Sigma = \frac{d^3 p_2}{p_2^0} \frac{d^3 k_2}{k_2^0} \delta(q+p_1-p_2-k_2) \delta(u \cdot k_2 - \omega) \quad (3.30)$$

With the new variables

$$P = p_2 + k_2, \quad Q = p_2 - k_2, \quad (3.31)$$

we rewrite Eq. (3.30) in the form

$$d\Sigma = d^4 P d^4 Q \delta_+(P^2 + Q^2 - 2\rho_+^2) \delta_+(P \cdot Q - \rho_-^2) \\ \times \delta(P - p_1 - q) \delta(u \cdot k_2 - \omega) \quad (3.32)$$

where $\rho_{\pm}^2 = m_{\pi}^2 \pm k_2^2$. In the frame in which

$$P = (P_0, \vec{0}), \quad (3.33)$$

$d\Sigma$ can be further represented as

$$d\Sigma = \frac{1}{\bar{u}P_0} d\Omega_Q \delta \left[\cos \theta - \frac{1}{\bar{u}Q} \left(2\omega - u_0 P_0 \left(1 - \frac{\rho_-^2}{P^2} \right) \right) \right] \quad (3.34)$$

where $P = q + p_1$ and

$$\begin{cases} \bar{Q} = P_0 \sqrt{1 - 2 \frac{\rho_+^2}{P^2} + \frac{\rho_-^2}{P^4}} \\ \bar{u}P_0 = \sqrt{(u \cdot P)^2 - u^2 P^2} = \sqrt{E_1^2 - (q+p_1)^2} \end{cases} \quad (3.35)$$

Note that in general $k_2^2 \neq m_{\pi}^2$, hence $\rho_- \neq 0$ and $Q_0 \neq 0$. Fig. 5 gives the coordinate system in which the Σ -integration reduces to integration over the azimuthal angle ϕ .

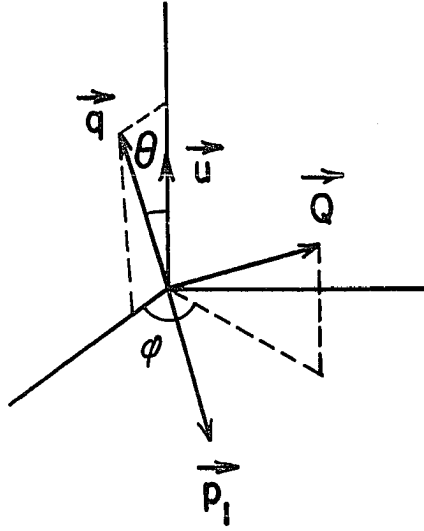


Figure 5. Coordinate system for the Σ -integration

This gives

$$d\Sigma = W^{-1/2} d\phi \quad (3.36)$$

where

$$\begin{cases} \bar{W} = E_1^2 - (q+p_1)^2 \\ \cos \theta = \frac{1}{\bar{u}\bar{Q}} \left[2\omega - u_0 P_0 \left(1 - \frac{\rho^2}{P^2} \right) \right] \end{cases} \quad (3.37)$$

Since D_1 is independent of p_2 and k_2 , we only need to do the following integrals:

$$\int d\Sigma, \quad \int \frac{d\Sigma}{D_2}, \quad \int \frac{d\Sigma}{D_2^2}.$$

The first integral is trivial and given by

$$\int d\Sigma = 2\pi W^{-1/2} . \quad (3.38)$$

To evaluate the second integral $\int d\Sigma/D_2$, we write D_2 in the form

$$D_2 = - (c + d \cos \phi) \quad (3.39)$$

where

$$\begin{cases} c = (q \cdot p_1) + q_0 Q_0 - \bar{q} \bar{Q} \cos \alpha \cos \theta \\ d = - \bar{q} \bar{Q} \sin \alpha \sin \theta . \end{cases} \quad (3.40)$$

With these definitions

$$\int \frac{d\Sigma}{D_2} = -W^{-1/2} \int_0^{2\pi} \frac{d\phi}{c+d \cos \phi} = - \frac{2\pi}{\sqrt{c^2-d^2}} W^{-1/2} . \quad (3.41)$$

Using Eqs. (3.35) and (3.37) and expressing other quantities in the invariant form as in Eq. (2.37), we can write

$$c^2 - d^2 = W^{-1} V \quad (3.42)$$

where

$$\begin{aligned} V = & 4[E_2^2(q \cdot p_1)^2 - E_1 E_2 (q \cdot p_1) \Delta^2 + \omega^2 m_\pi^2 \Delta^2 + E_1 E_2 k_2^2 \Delta^2 + \frac{1}{4} E_1^2 \Delta^4] \\ & - m_\pi^2 [2(q \cdot p_1) - \Delta^2]^2 - k_2^2 \Delta^2 [4m_\pi^2 + 2(q \cdot p_1) - k_2^2] . \end{aligned} \quad (3.43)$$

Hence

$$\int \frac{d\Sigma}{D_2} = -2\pi V^{-1/2} . \quad (3.44)$$

Now the evaluation of the third integral is trivial.

$$\int \frac{d\Sigma}{D_2^2} = \frac{\partial}{\partial c} \int \frac{d\Sigma}{D_2} = 2\pi U V^{-3/2} \quad (3.45)$$

where

$$U = C W = 2E_1 E_2 (q \cdot p_1) - E_1 (E_2 - \omega) \Delta^2 + [m_\pi^2 + (q \cdot p_1)][2(q \cdot p_1) - \Delta^2] + k_2^2 [(q \cdot p_1) - \Delta^2] \quad (3.46)$$

It is convenient to define the energies of the out-going pion and the virtual photon in terms of the energy of the incident pion.

$$\omega = E_1 \beta_1, \quad E_2 = E_1 \beta_2 \quad (3.47)$$

In the approximation $q_0 \simeq 0$ in the lab frame, it follows that $E_1 = \omega + E_2$, hence

$$\beta_1 + \beta_2 = 1 \quad (3.48)$$

Also we denote

$$\begin{cases} (q \cdot p_1) = \gamma_2 t \\ \Delta^2 = \gamma_2 y \end{cases} \quad (3.49)$$

where

$$\gamma_2 = 1 + \frac{k_2^2 \beta_2}{m_\pi^2 \beta_1} \quad (3.50)$$

For the high energy incident pion, we now make the following approximations

- (i) Neglect the terms proportional to $1/E_1^4$.
- (ii) Neglect m_π^2 , $(q \cdot p_1)$, Δ^2 , k_1^2 , compared with E_1^2 .

Then W , U and V are simplified to

$$\begin{cases} W = E_1^2 \\ U = \gamma_2 E_1^2 \lambda \\ V = 4\gamma_2^2 E_1^2 \mu \end{cases} \quad (3.51)$$

where

$$\begin{cases} \lambda = 2\beta_2 t - (\beta_2 - \beta_1)y \\ \mu = \frac{1}{4} y^2 + (m_\pi^2 \beta_1^2 - \beta_2 t)y + \beta_2^2 t^2. \end{cases} \quad (3.52)$$

We now perform the Σ -integration

$$\begin{cases} -\int d\Sigma_{\alpha\beta} M_{\mu\nu}^{\alpha\beta} u^\mu u^\nu = \pi E_1 \left[\frac{2\beta_2}{\gamma_2} \mathcal{J}_1 - \frac{1}{2} \left(m_\pi^2 - \frac{1}{4} k_2^2 \right) \frac{1}{\gamma_2} \mathcal{J}_2 \right] \\ \int d\Sigma_{\alpha\beta} u^\alpha u^\beta M_{\mu\nu}^{\alpha\beta} u^\mu u^\nu = \pi E_1^3 \frac{(1+\beta_2)^2}{4\gamma_2^2} \mathcal{J}_2 \end{cases} \quad (3.53)$$

where

$$\begin{cases} \mathcal{J}_1 = \frac{y}{\eta\sqrt{\mu}} \\ \mathcal{J}_2 = \frac{4}{\eta^2} - \frac{4\beta_2}{\eta\sqrt{\mu}} + \frac{\beta_2^2}{2\sqrt{\mu}^3} \end{cases} \quad (3.54)$$

and

$$\eta = 2t - y. \quad (3.55)$$

To determine the two scalar integrals $g_{\alpha\beta} G^{\alpha\beta}$ and $u_\alpha u_\beta G^{\alpha\beta}$, it remains to integrate over the momentum transfer q . In the lab frame, choosing \vec{p}_1 along the z -axis, we write

$$\frac{d^3 q}{u_0} = \Delta^2 d\Delta d(\cos \theta_q) d\phi_q. \quad (3.56)$$

We use

$$d(\cos \theta_q) = \frac{d(q \cdot p_1)}{\Delta \bar{p}_1}$$

to rewrite Eq. (3.56)

$$\frac{d^3 q}{u_0} = \frac{\pi}{\bar{p}_1} d\Delta^2 d(q \cdot p_1) \approx \gamma_2^2 \frac{\pi}{E_1} dy dt. \quad (3.57)$$

Thus

$$\left\{ \begin{array}{l} -G^\alpha_\alpha = \pi^2 \left[\frac{2\beta_2}{\gamma_2} J_1 - \frac{1}{\gamma_2^2} (m_\pi^2 - \frac{1}{4} k_2^2) J_2 \right] \\ \frac{1}{E_1^2} u_\alpha u_\beta G^{\alpha\beta} = \pi^2 \frac{(1+\beta_2)^2}{4\gamma_2^2} J_2 \end{array} \right. \quad (3.58)$$

where

$$\left\{ \begin{array}{l} J_1 = \iint \frac{dy}{y^2} dt |F(y)|^2 \mathcal{J}_1 \\ J_2 = \iint \frac{dy}{y^2} dt |F(y)|^2 \mathcal{J}_2 \end{array} \right. \quad (3.59)$$

The integration limits of t and y can be found in the same fashion as in Sec. II. We start with

$$(q + p_1)^2 = (p_2 + k_2)^2$$

to obtain

$$(q \cdot p_1) = (p_2 \cdot k_2) + \frac{1}{2} (\Delta^2 + k_2^2) \quad (3.60)$$

From

$$(p_2 \cdot k_2)_{\min} = E_2 \omega - \bar{p}_2 \bar{k}_2 \simeq \frac{1}{2} \frac{E_2^2 k_2^2 + m_\pi^2 \omega^2}{E_2 \omega} \quad (3.61)$$

it follows that

$$(q \cdot p_1)_{\min} = \frac{1}{2} \Delta^2 + \frac{\gamma_2^2 m_\pi^2 \omega^2}{2E_2^2} \quad (3.62)$$

To find the maximum, rewrite $(q \cdot p_1)$ in the lab frame

$$(q \cdot p_1) = -\Delta \bar{p}_1 \cos \theta_q \leq \Delta \bar{p}_1 \quad ,$$

so that

$$(q \cdot p_1)_{\max} \simeq E_1 \Delta \quad (3.63)$$

The integration limits of t are now given by

$$t_1 \leq t \leq t_2$$

with

$$\begin{cases} t_1 = \frac{1}{2} y + \frac{m_\pi^2 \beta_1}{2\beta_2} \\ t_2 = \sqrt{\frac{E_1^2 y}{\gamma_2}} \end{cases} \quad (3.64)$$

The range of y can be obtained from $t_1 = t_2$.

$$y_1 \leq y \leq y_2$$

with

$$\begin{cases} y_1 = \frac{\gamma_2^4 m_\pi^2 \beta_1^2}{4E_1^2 \beta_2^2} \\ y_2 = \frac{4E_1^2}{\gamma_2} - \frac{2m_\pi^2 \beta_1}{\beta_2} \end{cases} \quad (3.65)$$

In App. D the integrals J_1 and J_2 after the t -integration are given.

D. Cross Section Formula

The cross section formula can be obtained from Eqs. (3.22), (3.23), (3.24), and (3.58). Denoting $k_2^2 = S$ and neglecting k_2^2 compared with ω^2 , we may write

$$\frac{d\sigma_I}{d\varepsilon_+ d\varepsilon_-} = \frac{Z^2 \alpha^4}{2\pi} \frac{1}{E_1^2 \beta_1^3} \frac{dS}{S^2} F_I \quad (3.66)$$

where

$$F_I = [2m_e^2 + (X_+^2 + X_-^2)S] \left[\frac{2\beta_1^2 \beta_2}{\gamma_2} J_1 - \frac{1}{\gamma_2^2} (m_\pi^2 \beta_1^2 + \beta_2 S) J_2 \right]$$

$$+ \frac{X_+ X_- (1 + \beta_2)^2}{\gamma_2^2} s^2 J_2 . \quad (3.67)$$

To find the range of k_2^2 , consider

$$k_2^2 = (p_+ + p_-)^2 = 2[m_e^2 + \epsilon_+ \epsilon_- - \bar{p}_+ \bar{p}_- \cos(\hat{p}_+ \cdot \hat{p}_-)] . \quad (3.68)$$

For the high energy lepton pair

$$\bar{p}_+ \bar{p}_- \approx \epsilon_+ \epsilon_- - \frac{X_+^2 + X_-^2}{2X_+ X_-} m_e^2 , \quad (3.69)$$

so that

$$s_1 \leq s \leq s_2$$

where

$$\begin{cases} s_1 = \frac{m_e^2}{X_+ X_-} \\ s_2 = 4\omega^2 X_+ X_- \end{cases} . \quad (3.70)$$

E. Proton Case

For the proton case we replace the tensor describing the primary part $M_{\mu\nu}^{\alpha\beta}$ by $M_{\mu\nu}'^{\alpha\beta}$, which reads

$$M_{\mu\nu}'^{\alpha\beta} = \frac{1}{8} \text{Tr} \left\{ \left[\gamma^\alpha \frac{\not{p}_1 + \not{q} + m_p}{D_1} \gamma_\mu + \gamma_\mu \frac{\not{p}_2 - \not{q} + m_p}{D_2} \gamma^\alpha \right] (\not{p}_1 + m_p) \right. \\ \left. \times \left[\gamma^\beta \frac{\not{p}_2 - \not{q} + m_p}{D_2} \gamma_\nu + \gamma_\nu \frac{\not{p}_1 + \not{q} + m_p}{D_1} \gamma^\beta \right] (\not{p}_2 + m_p) \right\} . \quad (3.71)$$

After trace calculations the two scalar quantities are given by

$$g_{\alpha\beta}^M{}^{\mu\nu}{}_{\mu\nu}{}^{\alpha\beta}{}^{\mu\nu}{}_{\mu\nu} = \frac{2(E_1^2 + E_2^2)}{D_1 D_2} \Delta^2 + 4(m_p^2 + \frac{1}{2} k_2^2) \left(\frac{E_1}{D_1} + \frac{E_2}{D_2} \right)^2 + 1 \quad (3.72)$$

and

$$u_{\alpha} u_{\beta}^M{}^{\mu\nu}{}_{\mu\nu}{}^{\alpha\beta}{}^{\mu\nu}{}_{\mu\nu} = 4E_1 E_2 \left(\frac{E_1}{D_1} + \frac{E_2}{D_2} \right)^2 - 2(E_1 + E_2) \left(\frac{E_1}{D_1} + \frac{E_2}{D_2} \right). \quad (3.73)$$

Using the approximations mentioned above, we represent the two scalar integrals in the form

$$\begin{cases} -G_{\alpha}^{\mu\nu}{}_{\mu\nu}{}^{\alpha\beta}{}^{\mu\nu}{}_{\mu\nu} = 2\pi^2 \frac{1}{\gamma_2} \left[(1 + \beta_2^2) J_1 - \frac{1}{\gamma_2^2} (m_p^2 + \frac{1}{2} k_2^2) J_2 \right] \\ u_{\alpha} u_{\beta}^G{}^{\mu\nu}{}_{\mu\nu}{}^{\alpha\beta}{}^{\mu\nu}{}_{\mu\nu} = \frac{2\pi^2 E_1^2 \beta_2^2}{\gamma_2^2} J_2 \end{cases} \quad (3.74)$$

Here all the expressions obtained for the pion case are valid if we replace every m_{π} by m_p . The cross section formula is given by

$$\frac{d\sigma_I'}{d\varepsilon_+ d\varepsilon_-} = \frac{Z^2 \alpha^4}{\pi} \frac{1}{E_1^2 \beta_1^3} \frac{dS}{S^2} F_I' \quad (3.75)$$

where

$$\begin{aligned} F_I' = [2m_e^2 + (X_+^2 + X_-^2)S] & \left\{ \frac{1}{\gamma_2} \beta_1^2 (1 + \beta_2^2) J_1 \right. \\ & \left. - \frac{1}{\gamma_2^2} \left[\beta_1^2 m_p^2 + \frac{1}{2} (1 + \beta_2^2) S \right] J_2 \right\} + \frac{4X_+ X_- \beta_2}{\gamma_2^2} S^2 J_2 \end{aligned} \quad (3.76)$$

F. Interference Term

We now show that the interference term $d\sigma_{I \text{ II}}$ between the first and the second process vanishes (35). To see this write $d\sigma_{I \text{ II}}$ in the form

$$d\sigma_{I II} \sim \int d\Phi F_{I II} \quad (3.77)$$

where

$$F_{I II} = (p_1 + p_2)_\alpha A_{\beta\mu}^\alpha B_{\nu}^{\beta\mu} u^\nu, \quad (3.78)$$

and $\int d\Phi$ denotes the integrations over the phase space. The tensors $A_{\beta\mu}^\alpha$ and B_{ν}^β are given by

$$A_{\beta\mu}^\alpha = \text{Tr} \left[\gamma_\beta (\not{p}_+ - m_e) \left(\gamma^\beta \frac{\not{p}_- - \not{q} + m_e}{D_-} \gamma_\mu + \gamma_\mu \frac{\not{q} - \not{p}_+ + m_e}{D_+} \gamma^\alpha \right) (\not{p}_- + m_e) \right] \quad (3.79)$$

and

$$B_{\nu}^\beta = \frac{(p_1 + p_2 + q)^\beta (2p_1 + q)_\nu}{D_1} + \frac{(p_1 + p_2 - q)^\beta (2p_2 - q)_\nu}{D_2} - 2g_{\nu}^\beta. \quad (3.80)$$

Using the charge conjugation property of the γ -matrices (See Eq. (B.4)), it is easy to see that the tensor $A_{\beta\mu}^\alpha$ is antisymmetric with respect to the interchange of p_+ and p_- . Since the rest of $F_{I II}$ does not contain the pair momenta, the entire integrand $F_{I II}$ is antisymmetric. Now the phase space integral $\int d\Phi$ contains a part

$$\iint \frac{d^3 p_+}{0_{p_+}} \frac{d^3 p_-}{0_{p_-}} \delta(q + p_1 - p_2 - p_+ - p_-).$$

Since this is symmetric under interchange of p_+ and p_- , the cross section $d\sigma_{I II}$ vanishes when the above integration is carried out.

IV. RADIATIVE CORRECTIONS

In this section we shall consider the lowest order radiative corrections to the second-order processes. Our purpose is to verify that the infrared divergences associated with the higher order radiative processes can be eliminated by the conventional procedure. This ensures us that the radiative process contribution is small. We shall concern ourselves with the radiative corrections for the electron and the positron only; the pion and the proton are much more massive and the radiative corrections to them are negligible in comparison. For the most regions of ω (except for $\omega \sim E_1$), the first-order process gives the contribution to the cross section down roughly by the factor $(m_e/m_\pi)^2 \sim 10^{-5}$ compared with the second-order process. For this reason, the radiative corrections to the first order process will not be considered.

A problem associated with the consideration of radiative corrections is the occurrence of the infrared divergences in the vertex and the electron propagator part. The divergences enter into these virtual photon radiative parts through the regularization procedure. In general the infrared divergences of this kind can be canceled by including the diagrams of the real photon emission.

The infrared divergence associated with the real photon emission can be readily seen from the electron propagator contained in the emission vertex:

$$\begin{array}{c} \xrightarrow{q} \quad \xrightarrow{p} \\ \quad \quad \quad \ell \end{array} \sim \frac{1}{(p+\ell)^2 - m^2} = \frac{1}{\ell^2 + 2(p \cdot \ell)} \rightarrow \frac{1}{0}$$

for $\ell_\mu \rightarrow 0$. This type of the divergence was first recognized in the inelastic scattering of electrons with the emission of photons (36). The problem was so confusing to the researchers of quantum theory of radiation in early 1930's that it was termed as the "infrared catastrophe". In 1937, Block and Nordsiek showed that the infrared divergence disappears if an exact solution of the field equation is employed for that part of the Hamiltonian which couples the low frequency electromagnetic field to the electron (37). In the following year, Braunbeck and Weinmann made an observation that the infrared divergence due to the emission of one real photon and the infrared divergence which is contained in the lowest order virtual photon radiative correction exactly cancel (38). This point was later expounded by Bethe and Oppenheimer (39). Jauch and Rohrlich further gave a complete solution of the problem by showing that the infrared divergences contained in the real and virtual photon processes cancel to all orders in the fine structure constant α and for all types of processes (40). Thus the infrared divergence is a spurious phenomenon which only appears for the reason that the real and virtual photon processes are artificially separated in the perturbation expansion. In other words, the origin of the infrared divergence is the fact that in any scattering experiment the electrons can radiate photons whose energies are too small to be detected by the apparatus. Since any apparatus can have only finite energy resolution, it cannot make the distinction between soft photon processes and radiationless ones. For this reason, the infrared divergences of the individual processes discussed above are not physical.

We shall describe in detail the elimination of the infrared divergences from the radiative amplitude for our particular case. At the end of this section, we give a rough estimate of the radiative cross section.

A. Virtual Photon Radiative Corrections

The Feynmann diagrams for virtual photon radiative corrections are given by Fig. 6.

The classifications of these diagrams are as follows.

- a. Diagrams 6a through 6d; vertex corrections.
- b. Diagrams 6e and 6f; electron propagator corrections.
- c. Diagrams 6g through 6j; vacuum polarizations.
- d. Diagrams 6k and 6l; these diagrams will be considered in the discussion of the infrared divergence.

The T-matrix element for the above twelve diagrams can be expressed in the form

$$T_R = i \frac{Ze^4}{k_1^2} P_\alpha Q_\mu^\alpha u \frac{F(\vec{q})}{q^2} \quad (4.1)$$

where

$$P_\alpha = (p_1 + p_2)_\alpha \quad (4.2)$$

$$Q_\mu^\alpha = Q_{1\mu}^\alpha + Q_{2\mu}^\alpha + Q_{3\mu}^\alpha + Q_{4\mu}^\alpha \quad (4.3)$$

and Q_1 , Q_2 and Q_3 are given by

$$Q_{1\mu}^\alpha = \bar{u}(p_-) \left[\gamma_\mu \frac{\not{p}_- - \not{q} + m}{D_-} (p_- - q, -p_+) + \Lambda^\alpha(p_-, q - p_+) \frac{\not{q} - \not{p}_+ + m}{D_+} \gamma_\mu \right]$$

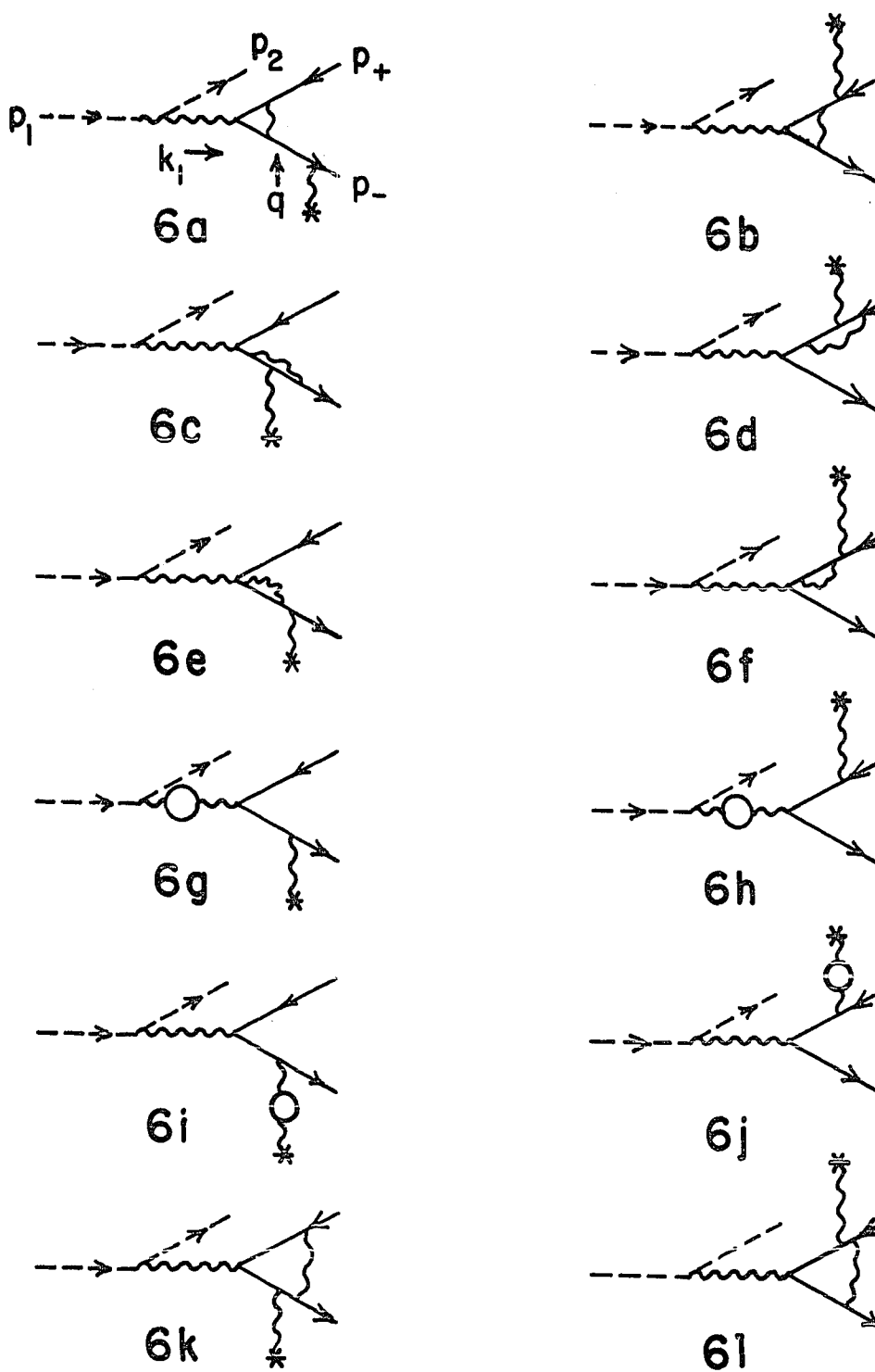


Figure 6. Feynman diagrams for virtual photon radiative corrections

$$+ \Lambda_{\mu}(p_-, p_- - q) \frac{\not{p}_- - \not{q} + m}{D_-} \gamma^{\alpha} + \gamma^{\alpha} \frac{\not{q} - \not{p}_+ + m}{D_+} \Lambda_{\mu}(q - p_+, -p_+) \Big] v(p_+) \quad (4.4)$$

$$Q_{2\mu}^{\alpha} = -\bar{u}(p_-) \left[\gamma_{\mu} \Sigma(p_- - q) \gamma^{\alpha} + \gamma^{\alpha} \Sigma(q - p_+) \gamma_{\mu} \right] v(p_+) \quad (4.5)$$

$$Q_{3\mu}^{\alpha} = -e^2 [\pi(k_1^2) + \pi(q^2)]$$

$$\times \bar{u}(p_-) \left[\gamma_{\mu} \frac{\not{p}_- - \not{q} + m}{D_-} \gamma^{\alpha} + \gamma^{\alpha} \frac{\not{q} - \not{p}_+ + m}{D_+} \gamma_{\mu} \right] v(p_+) \quad (4.6)$$

The expression of Q_4 will be given in the sub-section C. Q_1 corresponds to diagrams 6a through 6d, Q_2 to diagrams 6e and 6f and Q_3 to diagrams 6g through 6j. The symbols e and m here denote the physical charge and mass of the electron. The expressions of the regularized photon self-energy part $\Pi(p^2)$, the electron self-energy part $\Sigma(p)$ and the vertex part of $\Lambda_{\mu}(p, p)$ are given in App. E (41).

First we show that vacuum polarizations give negligible contributions to the radiative cross section. To see this, let us evaluate the integral in Eq. (E.1). Introducing a new variable $x = (1 + \eta)/2$, we rewrite $\Pi(p^2)$ in the form

$$\begin{aligned} -e^2 \Pi(p^2) &= \frac{\alpha}{4\pi} \int_{-1}^1 d\eta (1-\eta^2) \ln \left[1 - \frac{p^2}{4m^2} (1-\eta^2) \right] \\ &= \frac{\alpha}{3\pi} \left[\frac{1}{3} - \left(2 + \frac{1}{\beta^2} \right) \left(1 - \frac{1}{\beta} \sqrt{1-\beta^2} \sin^{-1} \beta \right) \right] \end{aligned} \quad (4.7)$$

where $\beta = p/2m$. For $|p^2| \ll m^2$, the above expression reduces to

$$-e^2 \Pi(p^2) = -\frac{\alpha}{15\pi} \frac{p^2}{m^2} . \quad (4.8)$$

For the case under consideration

$$-e^2 [\Pi(k_1^2) + \Pi(q^2)] = \frac{\alpha}{15\pi m^2} (\Delta^2 - k_1^2) . \quad (4.9)$$

The dominant contribution to the cross section comes from the minima of Δ^2 and $-k_1^2$. At these minima

$$\frac{1}{m^2} (\Delta^2 - k_1^2) \sim \frac{m^2}{\omega^2} \quad (4.10)$$

provided $E_1 \gg \omega$. (See Eqs. (2.59) and (2.69)) Thus we may neglect Q_3 in this approximation. When the pair energy ω becomes comparable to the incident energy E_1 , the photon self-energy part may not be negligible.

B. Real Photon Radiative Corrections

Before examining the vertex and the electron propagator part in detail, we consider the real photon radiative corrections. The main purpose of this consideration is to cancel the infrared divergences inherent in $\Sigma(p)$ and $\Lambda_\mu(p', p)$. As we shall see below, in order for this cancellation to occur, the energy of the emitted photon is required to be small (soft photon). The Feynman diagrams for real photon radiative corrections are given by Fig. 7.

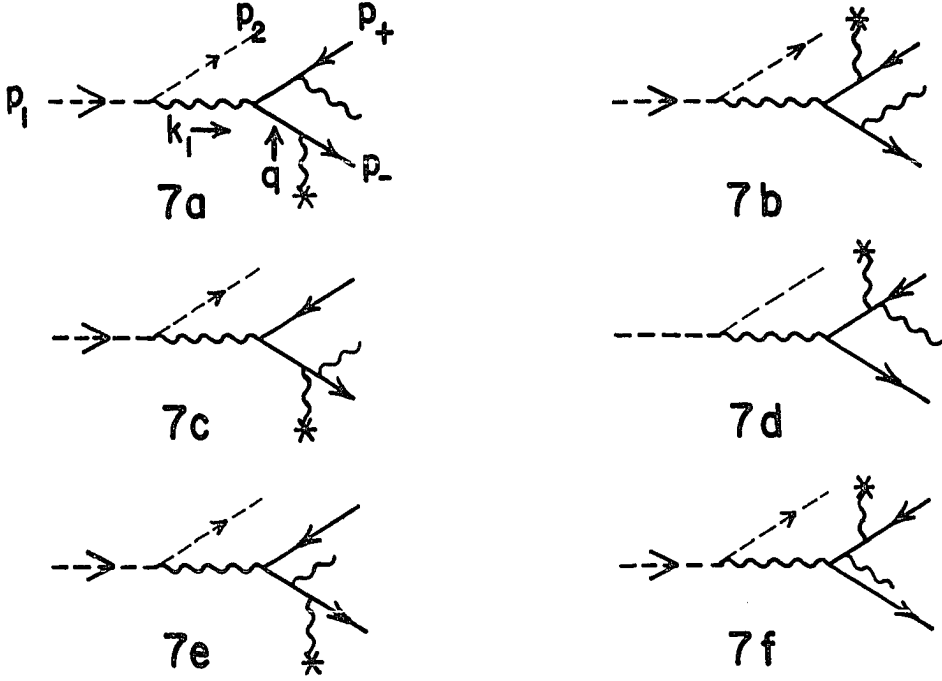


Figure 7. Feynman diagrams for real photon radiative corrections

The T-matrix element for the above six diagrams can be written in the form

$$T_R^\alpha = i \frac{Ze^4}{k_1^2} P_\alpha R_{\mu}^{\alpha\mu} \frac{F(\vec{q})}{q^2} \quad (4.11)$$

where P_α is previously defined by Eq. (4.2) and

$$R_\mu^\alpha = R_{1\mu}^\alpha + R_{2\mu}^\alpha \quad (4.12)$$

Here R_1 corresponds to diagrams 7a through 7d and R_2 to diagrams 7e and 7f. As we shall see below R_1 is infrared divergent, whereas R_2 is not.

To find an expression of R_1 for soft photons, we first consider diagram 7a only. The contribution of this diagram to R_1 is

$$\bar{u}(p_-) \gamma_\mu \frac{\not{p}_- - \not{q} + m}{D_-} \gamma^\alpha \frac{\not{\ell} + \not{p}_+ - m}{(\ell + p_+)^2 - m^2} \gamma_\sigma \varepsilon^\sigma v(p_+) \quad (4.13)$$

where ε denotes the photon polarization vector and ℓ the four-momentum of the emitted photon. Using the relation

$$(\ell + p_+ - m) \gamma_\sigma = 2(\ell + p_+)_\sigma - \gamma_\sigma (\ell + p_+ + m) \quad (4.14)$$

and the Dirac equation

$$(\not{p}_+ + m) v(p_+) = 0 \quad ,$$

we rewrite for small ℓ

$$\frac{\not{\ell} - \not{p}_+ - m}{(\ell + p_+)^2 - m^2} \gamma_\sigma \varepsilon^\sigma = \frac{2\varepsilon \cdot (\ell + p_+) - \not{\ell} \not{\ell}}{(\ell + p_+)^2 - m^2} v(p_+) \simeq \frac{(\varepsilon \cdot p_+)}{(\ell \cdot p_+)} v(p_+) \quad . \quad (4.15)$$

Hence Eq. (4.13) becomes

$$e \frac{(\varepsilon \cdot p_+)}{(\ell \cdot p_+)} \bar{u}(p_-) \gamma_\mu \frac{\not{p}_- - \not{q} + m}{D_-} \gamma^\alpha v(p_+) \quad . \quad (4.16)$$

Applying the same procedure for diagrams 7b through 7d we obtain the full

R_1

$$R_{1\mu}^\alpha = e \left[\frac{(\varepsilon \cdot p_+)}{(\ell \cdot p_+)} - \frac{(\varepsilon \cdot p_-)}{(\ell \cdot p_-)} \right] B_\mu^\alpha \quad (4.17)$$

where

$$B_\mu^\alpha = \bar{u}(p_-) \left[\gamma^\alpha \frac{\not{q} - \not{p}_+ + m}{D_+} \gamma_\mu + \gamma_\mu \frac{\not{p}_- - \not{q} + m}{D_-} \gamma^\alpha \right] v(p_+) \quad . \quad (4.18)$$

Note that the factor in front of B_μ^α is divergent for $\ell \rightarrow 0$.

For diagrams 7e and 7f, we have

$$R_{2\mu}^\alpha = -e \bar{u}(p_-) \left[\gamma_\mu \frac{\not{p}_- - \not{q} + m}{D_-} \not{\epsilon} \frac{\not{k}_1 - \not{p}_+ + m}{(k_1 - p_+)^2 - m^2} \gamma^\alpha \right]$$

$$+ \gamma^\alpha \frac{\not{p}_- - \not{k}_1 + m}{(p_- - k_1)^2 - m^2} \not{\epsilon} \frac{\not{q} - \not{p}_+ + m}{D_+} \gamma_\mu \Big] v(p_+) \quad . \quad (4.19)$$

From this expression it is apparent that R_2 does not give rise to the infrared divergence.

Let us note that B_μ^α is a part of the T-matrix element for the second order process. (See Eq. (2.1)) Taking the square of R_1 , we expect that real photon emissions described by diagrams 7a through 7d modify the cross section by the factor

$$\rho = e^2 \int \frac{d^3 \ell}{(2\pi)^3 2\ell_0} \sum_{\text{pol}} \left[\frac{(\epsilon \cdot p_+)}{(\ell \cdot p_+)} - \frac{(\epsilon \cdot p_-)}{(\ell \cdot p_-)} \right]^2 \quad (4.20)$$

where the summation \sum_{pol} runs over the unobserved polarization states of emitted photons, let μ be the "mass" of soft photons and $\ell^2 = \mu^2$. For vector bosons, we have

$$\sum_{\text{pol}} \epsilon_\mu \epsilon_\nu = -q_{\mu\nu} + \frac{\ell_\mu \ell_\nu}{\mu^2} \quad . \quad (4.21)$$

So that

$$\begin{aligned} \rho &= -\frac{\alpha}{4\pi} \int \frac{d^3 \ell}{\ell_0} \left[\frac{\mu^2}{(\ell \cdot p_+)^2} + \frac{\mu^2}{(\ell \cdot p_-)^2} - \frac{2(p_+ \cdot p_-)}{(\ell \cdot p_+)(\ell \cdot p_-)} \right] \\ &= \rho^{\text{ir}} + \frac{\alpha}{\pi} \left[\frac{1}{2} \frac{\epsilon_+}{\bar{p}_+} \ln \left(\frac{\epsilon_+ + \bar{p}_+}{\epsilon_+ - \bar{p}_+} \right) + \frac{1}{2} \frac{\epsilon_-}{p_-} \ln \left(\frac{\epsilon_- + \bar{p}_-}{\epsilon_- - \bar{p}_-} \right) \right. \\ &\quad \left. - (p_+ \cdot p_-) \int_0^1 \frac{dx}{\epsilon_x^2 - \bar{p}_x^2} \frac{\epsilon_x}{\bar{p}_x} \ln \left(\frac{\epsilon_x + \bar{p}_x}{\epsilon_x - \bar{p}_x} \right) \right] \quad (4.22) \end{aligned}$$

where the infrared divergent part is given by

$$\rho^{1r} = \frac{2\alpha}{\pi} \left[(p_+ \cdot p_-) \int \frac{dx}{\epsilon_x^2 - p_x^2} - 1 \right] \ln \left(\frac{2\Delta\epsilon}{\mu} \right) \quad (4.23)$$

and

$$\begin{cases} \epsilon_x = x \epsilon_+ + (1-x) \epsilon_- \\ \bar{p}_x = x \bar{p}_+ + (1-x) \bar{p}_- \end{cases} \quad (4.24)$$

The symbol $\Delta\epsilon$ denotes the maximum energy of emitted photons. The details of the calculation of ρ are given in App. F (42).

C. Cancellation of Infrared Divergences

Consider the virtual photon radiative corrections given by diagrams 6k and 6l. For these diagrams, Q_4 is written as

$$\begin{aligned} Q_{4\mu}^\alpha = & -i \frac{e^2}{16\pi^4} \int \frac{d^4 \ell}{\ell^2} \\ & \times \bar{u}(p_-) \left\{ \frac{\gamma^\sigma (\not{p}_- - \not{\ell} + m) \gamma^\alpha (\not{q} - \not{p}_+ - \not{\ell} + m) \gamma_\mu (\not{p}_+ + \not{\ell} - m) \gamma_\sigma}{[(p_+ + \ell)^2 - m^2][(p_- - \ell)^2 - m^2][q - p_+ - \ell]^2 - m^2]} \right. \\ & \left. + \frac{\gamma^\sigma (\not{p}_- + \not{\ell} + m) \gamma_\mu (\not{p}_- - \not{q} + \not{\ell} + m) \gamma^\alpha (\not{p}_+ - \not{\ell} - m) \gamma_\sigma}{[(\ell - p_+)^2 - m^2][(\ell + p_-)^2 - m^2][(\ell + p_- - q)^2 - m^2]} \right\} v(p_+) \quad (4.25) \end{aligned}$$

Due to the $1/\ell^2$ dependence we expect that the dominant contribution comes from small ℓ . Neglecting ℓ compared with p_+ and p_- , we write Q_4 in the form

$$\begin{aligned} Q_{4\mu}^\alpha & \approx -i \frac{\alpha}{4\pi^3} (p_+ \cdot p_-) \int \frac{d^4 \ell}{\ell^2} \frac{1}{(\ell \cdot p_+)(\ell \cdot p_-)} B_\mu^\alpha \\ & = -\frac{\alpha}{\pi} (p_+ \cdot p_-) \int_0^1 \frac{dx}{\epsilon_x^2 - p_x^2} \int \frac{d\bar{\ell}}{\ell} B_\mu^\alpha \quad (4.26) \end{aligned}$$

The calculation leading to the last line of the above equation is given in App. G. The contribution of radiative corrections to the cross section is proportional to the interference term between the leading amplitude and the radiative amplitude:

$$d\sigma_R \sim 2B_\mu^\alpha Q_{4\nu}^\beta = \rho' B_{\mu\nu}^{\alpha\beta} \quad (4.27)$$

where

$$\rho' = -\frac{2\alpha}{\pi} (p_+ \cdot p_-) \int_0^1 \frac{dx}{\epsilon_x^2 - p_x^2} \int \frac{d\bar{\ell}}{\bar{\ell}} \quad (4.28)$$

and $B_{\mu\nu}^{\alpha\beta}$ is given by Eq. (2.4). Comparing Eqs. (4.23) and (4.27), we see that ρ' cancels the first term of ρ^{ir} .

We next show that the remaining second term of ρ^{ir} cancel with the infrared divergent contributions from the vertex and electron propagator part. These infrared divergences are contained in the third terms of Eqs. (E.2) and (E.4). Performing the integrations, we obtain the infrared divergent part of Q_1 and Q_2 .

$$\begin{cases} (Q_1^{ir})_\mu^\alpha = \frac{2\alpha}{\pi} \ln\left(\frac{m}{\mu}\right) B_\mu^\alpha \\ (Q_2^{ir})_\mu^\alpha = -\frac{\alpha}{\pi} \ln\left(\frac{m}{\mu}\right) B_\mu^\alpha \end{cases} \quad (4.29)$$

Thus for diagrams 6a through 6f

$$(Q^{ir})_\mu^\alpha = \frac{\alpha}{\pi} \ln\left(\frac{m}{\mu}\right) B_\mu^\alpha \quad (4.30)$$

The infrared radiative cross section is proportional to

$$d\sigma_R \sim 2 B_\mu^\alpha (Q^{ir})_\nu^\beta = \rho'' B_{\mu\nu}^{\alpha\beta} \quad (4.31)$$

where

$$\rho'' = \frac{2\alpha}{\pi} \ln \left(\frac{m}{\mu} \right). \quad (4.32)$$

This cancels with the second term of ρ^{ir} in Eq. (4.23) provided we give the maximum energy $\Delta\varepsilon = m/2$ to emitted photons.

D. Matrix Elements for Radiative Corrections

We have seen above that the infrared divergences in $\Sigma(p)$ and $\Lambda_\mu(p', p)$ are eliminated completely if real photon emissions are taken into consideration. Henceforth, we may set $\mu = 0$ in the expressions of $\Sigma(p)$ and $\Lambda_\mu(p', p)$. For $\omega \ll E_1$

$$-\frac{k_1^2}{m^2} \sim \xi, \quad \frac{\Delta_{\text{min}}^2}{m^2} \sim \frac{m^2}{\omega^2} \quad (4.33)$$

and k_1^2 and q^2 may be neglected compared with m^2 . (See Eqs. (2.59) and (2.69)) With these approximations the integrals in $\Sigma(p)$ and $\Lambda_\mu(p', p)$ are readily evaluated. The electron propagator part is then expressed in the form

$$\begin{aligned} Q_{2\mu}^\alpha = & \frac{\alpha}{2\pi} \bar{u}(p_-) \left[a_+ \gamma^\alpha \frac{q' - \not{p}_+ + m}{D_+} \gamma_\mu + a_- \gamma_\mu \frac{\not{p}' - q' + m}{D_-} \gamma^\alpha \right. \\ & + 2m (q \cdot p_+) b_+ \gamma^\alpha \frac{q' - \not{p}_+ + m}{D_+^2} \gamma_\mu + 2m (q \cdot p_-) b_- \gamma_\mu \frac{\not{p}' - q' + m}{D_-^2} \gamma^\alpha \\ & \left. + (q \cdot p_+) b_+ \gamma^\alpha \frac{1}{D_+} \gamma_\mu + (q \cdot p_-) b_- \gamma_\mu \frac{1}{D_-} \gamma^\alpha \right] u(p_+) \end{aligned} \quad (4.34)$$

where

$$a_\pm = -\frac{3}{2} - \frac{m^2}{2[2(q \cdot p_\pm) - m^2]} - \left\{ \frac{(q \cdot p_\pm)}{2(q \cdot p_\pm) - m^2} - \frac{m^2(q \cdot p_\pm)}{[2(q \cdot p_\pm) - m^2]^2} \right\} \ln \left[\frac{2(q \cdot p_\pm)}{m^2} \right]$$

$$b_{\pm} = -\frac{m}{2(q \cdot p_{\pm}) - m^2} + \left\{ \frac{2m}{[2(q \cdot p_{\pm}) - m^2]^2} + \frac{2m(q \cdot p_{\pm})}{[2(q \cdot p_{\pm}) - m^2]^2} \right\} \ln \frac{2(q \cdot p_{\pm})}{m^2} . \quad (4.35)$$

The vertex parts are given by

$$\left\{ \begin{aligned} \Lambda_{\mu}(p_-, p_- - q) &= \frac{\alpha}{2\pi} (a_- \gamma_{\mu} - b_- p_{-\mu}) \\ \Lambda_{\mu}(q - p_+, -p_+) &= \frac{\alpha}{2\pi} (a_+ \gamma_{\mu} + b_+ p_{+\mu}) \\ \Lambda^{\alpha}(p_-, q - p_+) &= \frac{\alpha}{2\pi} (-b_+ p_-^{\alpha} + c_+ \gamma^{\alpha} - d_+ \not{p}_+^{\alpha} + e_+ \gamma^{\alpha} \not{p}_+) \\ \Lambda^{\alpha}(p_- - q, -p_+) &= \frac{\alpha}{2\pi} (b_- p_+^{\alpha} + c_- \gamma^{\alpha} - d_- \not{p}_-^{\alpha} - e_- \gamma^{\alpha} \not{p}_-) \end{aligned} \right. \quad (4.36)$$

where a_{\pm} and b_{\pm} are already given above and

$$\left\{ \begin{aligned} c_{\pm} &= -2 + \left[1 - \frac{(q \cdot p_{\pm})}{2(q \cdot p_{\pm}) - m^2} \right] \ln \left[\frac{2(q \cdot p_{\pm})}{m^2} \right] - \frac{m^2}{2(q \cdot p_{\pm})} \int_{1-2(q \cdot p_{\pm})/m^2}^1 dx \frac{\ln(1-x)}{x} \\ d_{\pm} &= -\frac{1}{(q \cdot p_{\pm})} + \frac{1}{2(q \cdot p_{\pm}) - m^2} + \left\{ \frac{1}{(q \cdot p_{\pm})} - \frac{m^2}{[2(q \cdot p_{\pm}) - m^2]^2} \right\} \ln \left[\frac{2(q \cdot p_{\pm})}{m^2} \right] \\ &\quad - \frac{m^2}{2(q \cdot p_{\pm})^2} \int_{1-2(q \cdot p_{\pm})/m^2}^1 dx \frac{\ln(1-x)}{x} \\ e_{\pm} &= \frac{m}{2(q \cdot p_{\pm}) - m^2} \ln \left[\frac{2(q \cdot p_{\pm})}{m^2} \right] . \end{aligned} \right. \quad (4.37)$$

The integral

$$f(z) = - \int_0^z dx \frac{\ln|1-x|}{x} \quad (4.38)$$

is known as the Spence function and cannot be expressed as a finite combination of elementary functions.

Various calculations of radiative cross sections are known in the literature (43). In these analyses the workers assume a set of appropriate approximations and evaluate only the leading terms. From the form of Eqs. (4.34) through (4.37), it is evident that we need further approximations to continue calculations of the radiative cross section. Unfortunately, the kinematic analysis does not yield a definite relative magnitude between $(q \cdot p_{\pm})$ and m^2 . Furthermore, it is not clear which terms give the dominant contributions. The present author did try to carry on calculations using the entire expressions of the matrix element. However, the task had to be terminated due to complexities of the expressions obtained in the process. Whatever the form of the amplitude may be, we expect that the contribution of the radiative corrections to the cross section is of the order $\alpha = 1/137$ down compared with the leading term.

V. NUMERICAL COMPUTATION OF CROSS SECTIONS

In this section, we present some examples of numerical cross sections for the π^- primary particle case. In particular, for the incident energy $E_1 = 360$ GeV, we compare our theoretical predictions with the data taken at the Fermi National Laboratory by the high energy experimental group of Iowa State University and collaborators (University of Maryland, Michigan State University, and Notre Dame University.)(32).

A. Formulae for the Pair Energy Distribution and the Pair Energy Partition Distribution

For the π^- case, we rewrite the cross section formulae given in Sec. II and III to obtain the pair energy distribution $d\sigma/d\omega$ and the pair energy partition distribution $d\sigma/d\lambda$. The final formulae are expressed in terms of three dimensional integrals which can be carried out numerically on a computer.

i) The pair energy distribution

We write

$$d\varepsilon_+ d\varepsilon_- = \omega dX_+ d\omega \quad . \quad (5.1)$$

Then for the second-order process

$$\frac{d\sigma_{II}}{d\omega} = \frac{2Z^2\alpha^4}{\pi} \frac{1}{\omega} \frac{E_2}{E_1} \int_{X_1}^{X_2} dX_+ \int_{S_1}^{S_2} \frac{dS}{S^2} F_{II} \quad (5.2)$$

and for the first-order process

$$\frac{d\sigma_I}{d\omega} = \frac{Z^2\alpha^4}{2\pi} \frac{1}{E_1\beta_1^2} \int_{X_1}^{X_2} dX_+ \int_{S_1}^{S_2} \frac{dS}{S^2} F_I \quad (5.3)$$

where

$$X_1 = \frac{m_e}{\omega}, \quad X_2 = 1 - \frac{m_e}{\omega} . \quad (5.4)$$

For the second-order (first-order) process, F_{II} (F_I) is defined by Eq. (2.65) (Eq. (3.67)) and the S-integration limits, S_1 and S_2 , are given in Eq. (2.69) (Eq. (3.70)).

ii) The pair energy partition distribution

For the high energy direct pair production, the second-order process dominates as we shall see in our theoretical predictions of the pair energy distributions. For this reason we consider the pair energy partition distribution only of the second-order process.

Let

$$\lambda = \left| \frac{\epsilon_+ - \epsilon_-}{\omega} \right| = |X_+ - X_-| . \quad (5.5)$$

We can obtain the pair energy partition distribution from Eq. (5.2) by a change of variables

$$dX_+ d\omega = \frac{1}{2} d\lambda d\omega . \quad (5.6)$$

Then

$$\frac{d\sigma_{II}}{d\lambda} = \frac{Z^2 \alpha^4}{\pi} \frac{E_2}{E_1} \int_{\omega_1}^{\omega_2} \frac{d\omega}{\omega} \int_{S_1}^{S_2} \frac{dS}{S^2} F_{II} \quad (5.7)$$

where ω_2 is the maximum pair energy of a set of data and

$$\omega_1 = \frac{2m_e}{1-\lambda} . \quad (5.8)$$

In F_{II} , X_+ and X_- can be expressed in terms of λ :

$$X_+ = \frac{1}{2} (1 + \lambda) , \quad X_- = \frac{1}{2} (1 - \lambda) . \quad (5.9)$$

In practice, a cut-off in ω_1 is probably necessary to be consistent with the data to be compared.

B. Atomic Form Factors

As mentioned in Sec. I, the presence of the atomic electrons give rise to the form factors of the atom. In general we can write

$$F(y) = F^{\text{el}}(y) + F^{\text{inel}}(y) \quad (5.10)$$

where F^{el} and F^{inel} are the elastic and inelastic contributions given by

$$F^{\text{el}}(y) = Z^2 [1 - G_Z(y)/Z]^2 \quad (5.11)$$

and

$$F^{\text{inel}}(y) = Z \{1 - [G_Z(y)/Z]^2\} \quad (5.12)$$

For hydrogen and helium atoms, G_Z can be calculated using the appropriate atomic wavefunctions (17):

$$\text{Hydrogen } Z = 1 \quad G_1(y) = \left(1 + \frac{\gamma_1 y}{4\alpha}\right)^{-2} \quad (5.13)$$

$$\text{Helium } Z = 2 \quad G_2(y) = \left(1 + \frac{\gamma_1 y}{16\alpha \eta}\right)^{-2} \quad (5.14)$$

where $\eta = 1.6875$.

In the following examples of numerical distributions, where the target is assumed to be hydrogen, we will set $F(y) = 1$. For the kinematics under consideration, the numerical analyses show that the use of Eq. (5.13) in the cross section formula changes the distributions less than 5%.

C. Examples

The pair energy distributions given by Eqs. (5.2) and (5.3) can be calculated with a computer. We present the results of the computation for the incident energies $E_1 = 200, 360, \text{ and } 600 \text{ GeV}$ in Fig. 8. As seen in this figure, the second-order processes are dominant for most of the range of ω not too close to the kinematic boundaries. In particular,

$$\frac{d\sigma_I/d\omega}{d\sigma_{II}/d\omega} \sim 10^{-5} \sim \left(\frac{m_e}{m_\pi}\right)^2$$

at $\omega \approx 1 \text{ GeV}$. This ratio can be understood qualitatively from the consideration of classical radiation by accelerating charged particles; the radiation amplitude is inversely proportional to the mass of the charged particle. At large values of ω , close to the upper limits of the kinematic boundaries, the first-order processes become comparable to the second-order ones. Here, however, the cross sections are only 10^{-6} of the peak values. Note that the second-order (the first-order) energy distributions increase (decrease) as the incident energy E_1 increases.

Finally we compare the theoretical predictions with the experimental data at $E_1 = 360 \text{ GeV}$ (32). The pair energy distribution is displayed in Fig. 9 with the solid curve indicating the theoretical prediction. (The second-order process only). The theory and the data are in excellent agreement. In Fig. 10, we show the pair energy partition distributions for three different ranges of ω . The energy ranges were chosen to yield approximately equal statistics while still showing the changing shape as a function of the pair energy. The agreement is again excellent. Fig. 11 presents the theoretical calculation of the pair

invariant mass distribution, in which $M^2 = (p_+ + p_-)^2$ (14). The present statistics and experimental energy resolution are still too crude to make a comparison with the data.

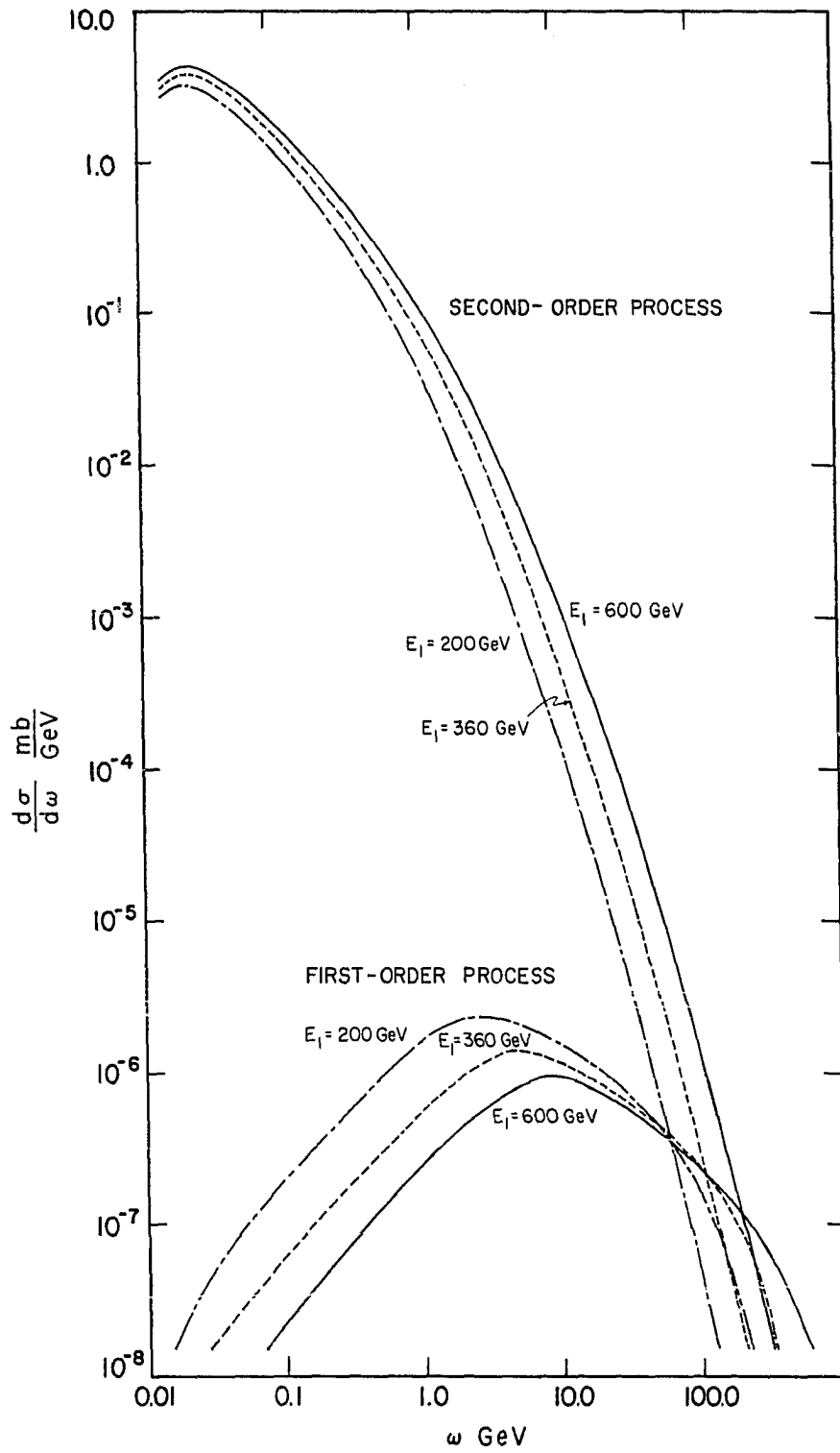


Figure 8. Pair energy distributions

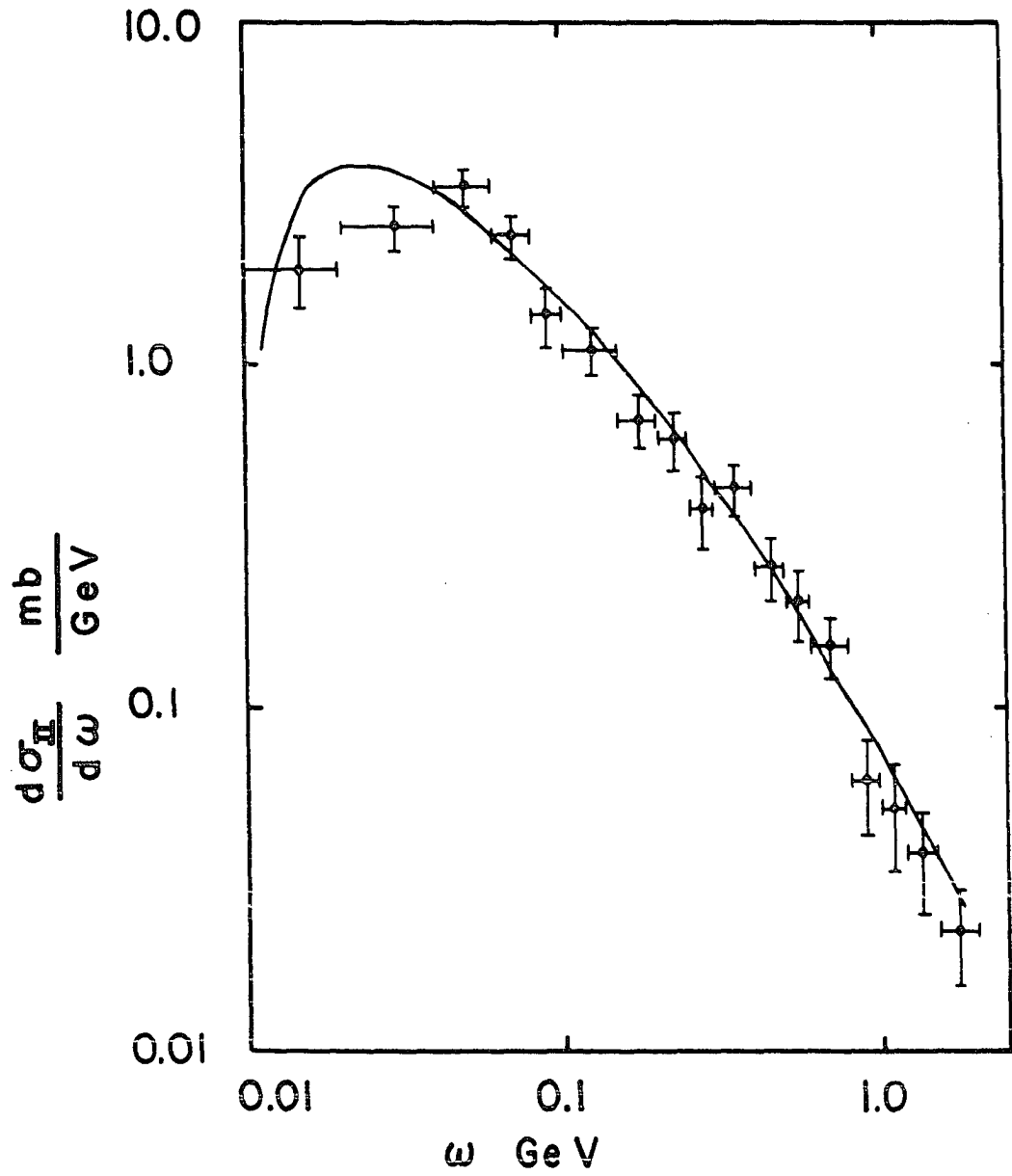


Figure 9. Pair energy distribution at $E_1 = 360 \text{ GeV}$

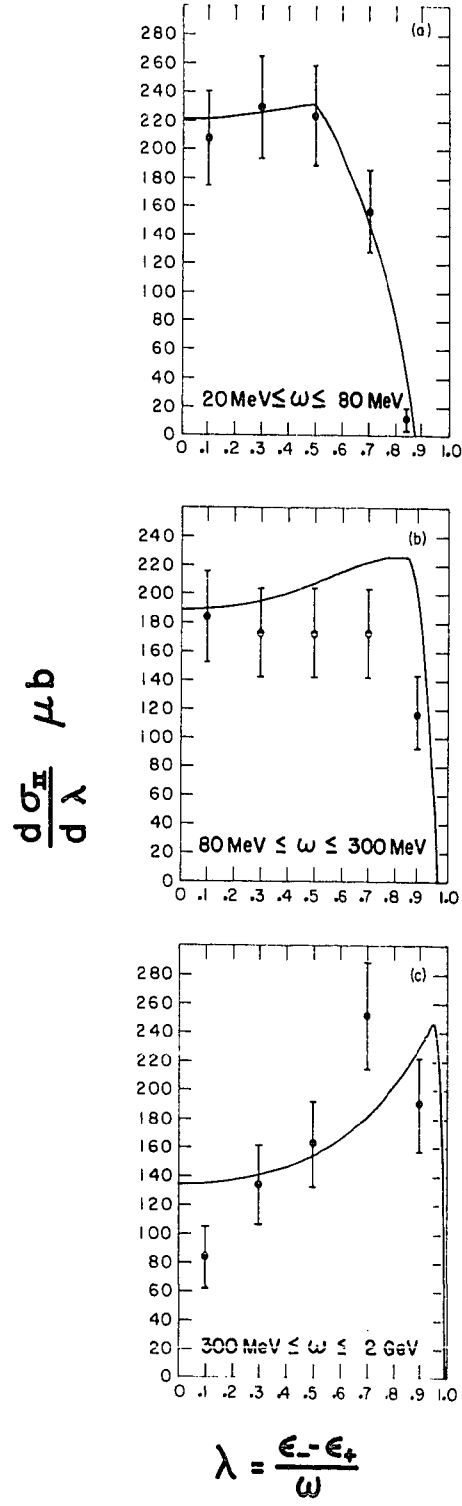


Figure 10. Pair energy partition distribution at $E_1 = 360$ GeV

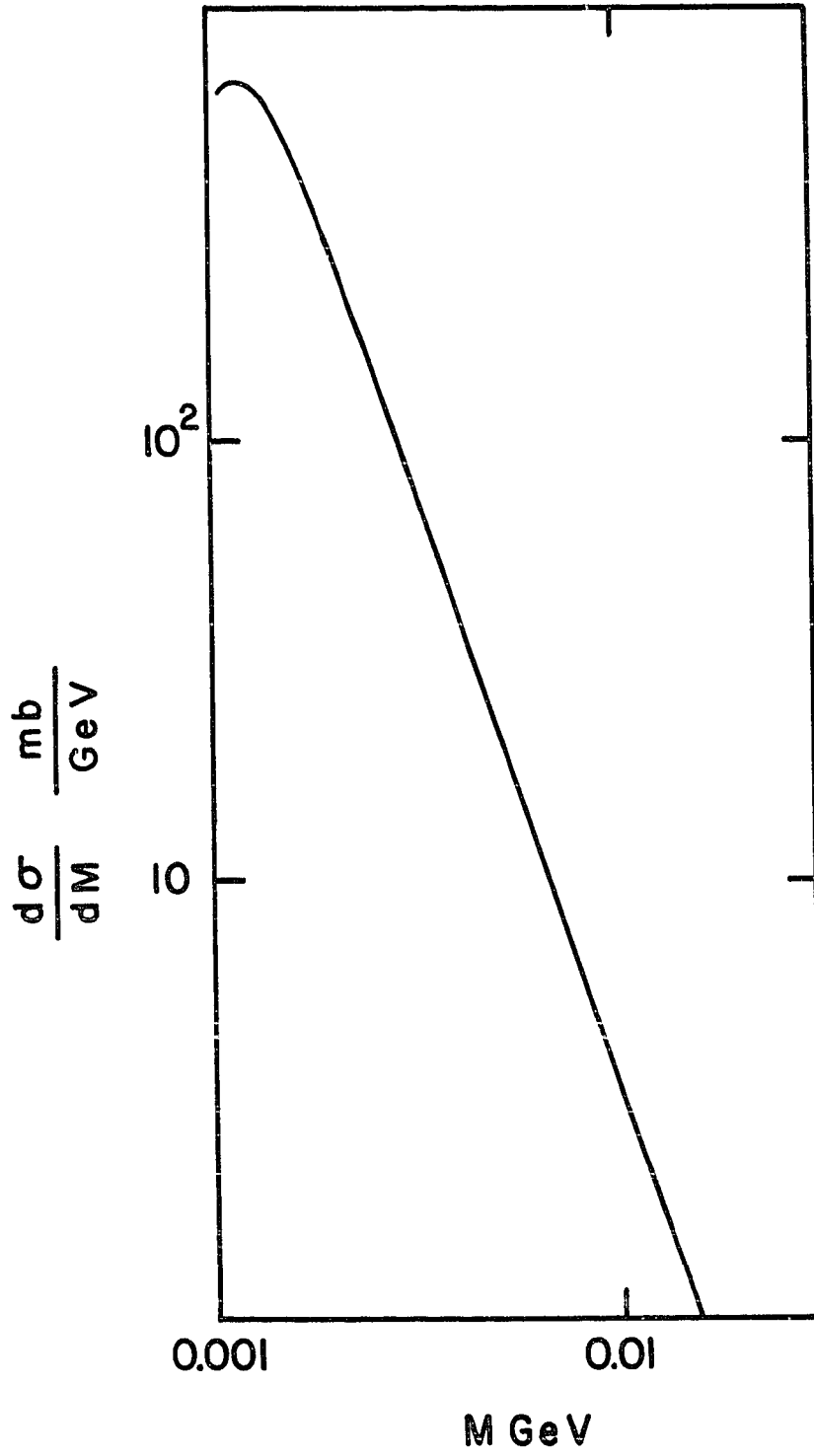


Figure 11. Invariant mass distribution at $E_1 = 360 \text{ GeV}$

VI. CONCLUSION

In this work we have considered the trident processes by high energy charged particles. The cross section formulae obtained are applicable to spin 0 boson and spin 1/2 fermion primaries. The calculations are carried out in the framework of the covariant perturbation theory of quantum electrodynamics. We present the detailed calculations of the differential cross sections to the lowest order in the fine structure constant. Some considerations of the radiative corrections are also given.

Of the two kinds of lowest order processes, the second-order process dominates over the first-order process for the most of pair energy regions except for $\omega \sim E_1$. When the pair energy approaches to the incident energy, the contribution of the first-order process becomes larger than that of the second-order process. The interference term between the first and the second-order processes is shown to vanish.

Our theoretical calculations of the pair energy distribution and the pair energy partition distributions for the π^- primary are in excellent agreement with the experimental data at $E_1 = 360$ GeV. It should be emphasized that our theoretical results do not contain any free parameter to be determined phenomenologically.

A brief comment on the role the present work plays in testing QED is in order. We have considered a kinematic configuration which involves virtual photons of small four-momentum, even though the primary charged particles are very energetic. We have seen that, on the level of a few percent which is the accuracy dictated by experimental

statistics, QED is valid. A more meaningful test of QED would involve wide-angle lepton pairs, i.e. high mass virtual photons connecting the produced lepton pair and the primaries. If the primaries are hadron, the effects of their em form factors will become important. In such a case, preliminary knowledge of the form factors would be necessary.

VII. BIBLIOGRAPHY

1. W. H. Furry and J. F. Carlson, Phys. Rev. 44, 237 (1933).
2. D. Skobel'tzyn, Nature 133, 23 (1934).
3. J. R. Oppenheimer and M. S. Plesset, Phys. Rev. 44, 53 (1933).
4. I. Curie and F. Joliot, J. Phys. 4, 429 (1933).
5. P. A. M. Dirac, Proc. Roy. Soc. (London) A126, 360 (1930).
6. K. F. Weizsäcker, Z. F. Physik 88, 612 (1934); E. J. Williams, Kgl. Danske Videnskab. Selskab, Mat-fys. Medd. 13, No. 4 (1935).
7. H. Bhabha, Proc. Roy. Soc. A152, 559 (1935); Proc. Cambr. Phil. Soc. 31, 394 (1935).
8. L. Landau and E. Lifschitz, Physik Zeits Soujetunion 6, 244 (1933); W. Heitler and L. Nordheim, J. De Phys. et Rad. 5, 449 (1934); E. J. Williams, Nature 135, 66 (1935); E. C. G. Stueckelberg, Helv. Phys. Acta. 8, 325 (1935); L. Nordheim, J. De Phys. et Rad. 6, 135 (1935); Y. Nishina, S. Tomonaga, and M. Kobayashi, Sci. Pap. Inst. Phys. Chem. Research, Japan 27, 137 (1935); G. Racah, Nuovo Cimento 14, 93 (1935).
9. T. Murota, A. Ueda, and H. Tanaka, Prog. Theor. Phys. 16, 482 (1956).
10. F. F. Ternovskii, Sov. Phys. JETP 10, 565 (1960) [Zh. eksp. teor. Fiz. 37, 793 (1959)].
11. S. R. Kelner, Sov. J. Nucl. Phys. 5, 778 (1967) [Jadern Fiz. 5, 1092 (1967)].
12. H. S. Zapoisky, Phy. D. Thesis, Cornell University, 1962 (unpublished); R. P. Kokoulin and A. A. Petrukhin, Proc. 11th Int. Conf. on Cosmic Rays, Budapest, (1969); Acta Phys. Acad. Scien. Hung. 29, Suppl. 4, 277 (1970); Proc. 12th Int. Conf. on Cosmic Rays, Hobart 6, 2436 (1971) (Hobart: Univ. of Tasmania).
13. A. Wright, J. Phys. A Math. Nucl. Gen. 6, 79 (1973).
14. B. L. Young, H. B. Crawley, and K. Mita, internal report, Phys. Dept. of Iowa State Univ., 1977 (unpublished).
15. S. D. Drell, Ann. of Phys. 4, 75 (1958); J. D. Bjorken, S. D. Drell, and S. Frautschi, Phys. Rev. 112, 1409 (1958); J. D. Bjorken and S. D. Drell, Phys. Rev. 114, 1368 (1959); S. J. Brodsky and S. C. C. Ting, Phys. Rev. 145, 1018 (1966); J. D. Bjorken and M. C. Chen, Phys. Rev. 154, 1335 (1967).

16. F. Perrin, *Comptes Rendus* 197, 1100 (1933); J. A. Wheeler and W. E. Lamb Jr., *Phys. Rev.* 55, 858 (1939).
17. Y. S. Tsai, *Rev. Mod. Phys.* 46, 815 (1974).
18. H. R. Crane and J. Halpern, *Phys. Rev.* 55, 838 (1939).
19. J. R. Feldmeier and G. B. Collins, *Phys. Rev.* 58, 200 (1940).
20. G. P. S. Occhialini, *Nuovo Cimento Suppl.* 6, 413 (1949); H. L. Bradt, M. F. Kaplon, and B. Peters, *Helv. Phys. Acta.* 23, 24 (1950).
21. M. M. Block, D. T. King, and W. W. Wada, *Phys. Rev.* 96, 1627 (1954).
22. W. H. Barkas, R. W. Deutsch, F. C. Gilbert, and C. E. Violet, *Phys. Rev.* 86, 59 (1952).
23. M. Camac, *Phys. Rev.* 88, 745 (1952); N. S. Shiren and R. F. Post, *Phys. Rev.* 86, 617 (1952).
24. S. Mora, *Comptes Rendus* 256, 4650 (1963).
25. R. Weil, *Helv. Phys. Acta.* 31, 641 (1958); L. Criegee, *Z. Phys.* 158, 433 (1960); J. Böhm, A. Matlova, J. Zacek, and V. G. Grishim, *Nucl. Phys.* B32, 632 (1971); A. S. Cary, W. H. Barkas and E. L. Hart, *Phys. Rev.* D4, 27 (1971); P. L. Jain, M. Kazuno, and B. Girard, *Phys. Rev. Lett.* 32, 1460 (1974); S. L. Leonard, *Bull. Am. Phys. Soc.* 1, 167 (1956); F. I. Loeffler, *Phys. Rev.* 108, 1058 (1957).
26. See Perrin in Ref. 15.
27. See Böhm, Matlova, Zacek, and Grishim in Ref. 25.
28. See Cary, Barkas, and Hart in Ref. 25.
29. B. Grossetete, R. Tchapoutain, D. J. Drickey, and D. Yount, *Phys. Rev.* 168, 1475 (1968).
30. R. L. Kinzer and R. Burwell, *Phys. Rev. Lett.* 20, 1050 (1968); J. E. Butt and D. T. King, *Phys. Rev. Lett.* 31, 904 (1973); P. L. Jain, M. Kazuno, B. Girard, and Z. Ahmad, *Phys. Rev. Lett.* 32, 797 (1974).
31. L. R. Fortney, A. T. Goshaw, J. W. Lamsa, J. S. Loos, D. A. Niemi, W. J. Robertson, and W. D. Walker, *Phys. Rev. Lett.* 34, 907 (1975); E. W. Anderson *et al.*, *Phys. Rev. Lett.* 37, 1593 (1976).

32. The present work started as a theoretical analysis for the data obtained by the high energy experimental groups at Iowa State University, University of Maryland, Michigan State University, and Notre Dame University. See Anderson et al. in Ref. 31.
33. J. D. Bjorken and S. D. Drell, "Relativistic Quantum Mechanics", McGraw-Hill, New York, 1964.
34. There are misprints in Kelner's expressions of S_{\pm} and Q_{\pm} (Ref. 11). They are corrected here.
35. V. N. Baier and V. A. Khoze, Sov. Phys. JETP 21, 629 (1965).
36. N. F. Mott, Proc. Camb. Phil. Soc. 27, 255 (1931).
37. F. Bloch and A. Nordsieck, Phys. Rev. 52, 54 (1937).
38. W. Braunbeck and E. Weinmann, Z. F. Physik 110, 360 (1938).
39. H. A. Bethe and J. R. Oppenheimer, Phys. Rev. 70, 451 (1946).
40. J. M. Jauch and F. Rohrlich, Helv. Phys. Acta. 13, 613 (1954).
41. B. L. Young, Associate Professor of Physics at Iowa State University, lecture note, 1975.
42. A. I. Akhiezer and V. B. Berestetskii, "Quantum Electrodynamics," Interscience Publication, New York, 1965, p. 425.
43. References for radiative corrections to various electromagnetic processes are given as follows.
 - (i) Electron magnetic moment: J. Schwinger, Phys. Rev. 75, 1912 (1949); R. Karplus and N. Kroll, Phys. Rev. 77, 536 (1950); C. M. Sommerfield, Phys. Rev. 107, 328 (1957).
 - (ii) Electron scattering; L. Elton and H. Robertson, Proc. Phys. Soc. (London) A65, 145 (1952); A. I. Akhiezer and R. Polovin, Doklady Akad. Naak USSR 90, 55 (1953); M. Redhead, Proc. Roy. Soc. (London) A220, 219 (1953); R. Polovin, JETP 31, 449 (1956); Sov. Phys. JETP 4, 385 (1957).
 - (iii) Compton effect: L. Brown and R. P. Feynman, Phys. Rev. 85, 231 (1952).
 - (iv) Two-photon pair annihilation: I. Harris and M. Brown, Phys. Rev. 105, 1656 (1957).
 - (v) Bremsstrahlung: P. I. Fomin, JETP 35, 707 (1958).
 - (vi) Photoproduction: J. Bjorken, S. Drell and S. Frautschi, Phys. Rev. 112, 1409 (1958); S. Guezenko and P. Fomin, JETP 38, 513 (1960); E. A. Vinokurov, E. A. Kuraev, and N. P. Merenkov, Sov. Phys. JETP 39, 942 (1974).
44. R. P. Feynman, Phys. Rev. 76, 679 (1949).

VIII. ACKNOWLEDGEMENT

I would like to thank Professor Bing-Lin Young for suggesting the present problem and also for many helpful discussions. I am grateful to Professor Bert Crawley for his help in computer programming.

IX. APPENDIX A. LIST OF PAIR PRODUCTION EXPERIMENTS

Electron Beam

Energy	Target and Detection scheme	Number of events and/or cross section	Comparison with Theory	Reference
230±20 MeV/c	thin Copper target		agree with theory (in the virtual photon approximation)	Camac, 23
25 MeV/c	counter		upper bound of σ agrees with theoretical pre- diction	Shiren and Post, 23
400 MeV/c	Ilford G-5 nuclear emulsion	42 events	-----	Leonard, 25
550 MeV/c	Ilford G-5 nuclear emulsion		good agreement with theory	Loeffler, 25
31.5 MeV/c	thin Copper foil as target		$\sigma_{\text{exp}} \sim \frac{1}{3}\sigma_{\text{theory}}$ (Bhabha)	Criegee, 25
500 MeV/c	Be, Al Pt target spectrometer		agree with theory	Grossetete <u>et al.</u> , 29
4 GeV/c	Propane bubble chamber		agree with theory with- in 30% (pair energy <810 MeV)	Böhm <u>et al.</u> , 25
13.75 GeV/c	Ilford G-5 nuclear emulsion	$\sigma_{\text{exp}} \sim$ (4.03 0.36) x 10 ⁻²⁵ cm ²	agree with theory ($\sigma_{\text{theory}} \sim 4.11 \times 10^{-25} \text{ cm}^2$)	Cary, Barkas, and Hart, 25

Muon Beam

Energy	Target and Detection scheme	Number of events and/or cross section	Comparison with Theory	Reference
4 GeV/c	Propane bubble chamber		agree with theory (pair energy <810 MeV)	Böhm <u>et al.</u> , 25
15.8 GeV/c	nuclear emulsion ($\bar{Z} \simeq 21.4$)	20 events	do not agree with theoretical prediction	Jain, Kazuno, and Girard, 25

Hadron Beam

Energy	Target and Detection scheme	Number of events and/or cross section	Comparison with Theory	Reference
π^- , 16 GeV/c		23 events		Mora, 24
π^- , 16.2 GeV/c	Ilford K-5 nuclear emulsion		$\sigma_{\text{theory}} < \sigma_{\text{exp}} < 2\sigma_{\text{theory}}$, marked disagreement with theory for high energy pairs	Kinzer and Burwell, 30
π^- , 4 GeV/c	Propane bubble Chamber		agree with theory within 30%(pair energy < 810 MeV)	Böhm <u>et al.</u> , 25
p, 200 GeV/c	nuclear emulsion $\bar{Z} \simeq 21.4$	8 events	$\sigma_{\text{theory}} \simeq 7 - 16 \sigma_{\text{exp}}$	Butt and King, 30
p, 200 GeV/c	nuclear emulsion $\bar{Z} \simeq 21.4$	40 events	$\sigma_{\text{theory}} > 5 \sigma_{\text{exp}}$	Jain <u>et al.</u> , 30
π^- , 200 GeV/c	neon chamber (Z = 10)	652 ± 31 events	good agreement with theory	Fortney <u>et al.</u> , 31
π^- , 360 GeV/c	Hydrogen bubble Chamber	493 events	good agreement with theory	Anderson <u>et al.</u> , 31

X. APPENDIX B

A. Evaluation of $g_{\alpha\beta}^{B\mu\nu}$

From Eq. (2.4)

$$g_{\alpha\beta}^{B\mu\nu} = \frac{1}{D_+^2} \text{Tr}(1) + \frac{1}{D_-^2} \text{Tr}(2) + \frac{1}{D_+ D_-} [\text{Tr}(3) + \text{Tr}(4)] \quad (\text{B.1})$$

where the traces are given by

$$\left\{ \begin{aligned} \text{Tr}(1) &= \frac{1}{8} \text{Tr}[\gamma^\alpha (\not{q} - \not{p}_+ + m_e) \not{p}_+ \not{p}_- \gamma_\alpha (\not{p}_- - m_e)] \\ \text{Tr}(2) &= \frac{1}{8} \text{Tr}[\not{p}_- \gamma^\alpha (\not{p}_+ - m_e) \gamma_\alpha (\not{p}_- - \not{q} + m_e) \not{p}_+] \\ \text{Tr}(3) &= \frac{1}{8} \text{Tr}[\gamma^\alpha (\not{q} - \not{p}_+ + m_e) \not{p}_+ \gamma_\alpha (\not{p}_- - \not{q} + m_e) \not{p}_-] \\ \text{Tr}(4) &= \frac{1}{8} \text{Tr}[\not{p}_- \gamma^\alpha (\not{p}_+ - m_e) \not{q} \gamma_\alpha (\not{p}_- + m_e)] \end{aligned} \right. \quad (\text{B.2})$$

To simplify the calculation let us note the trace identity

$$\text{Tr}A = \text{Tr}A^T \quad (\text{B.3})$$

and the charge conjugation property of the γ -matrices

$$C^{-1} \gamma^\mu C = -(\gamma^\mu)^T \quad (\text{B.4})$$

where C is the charge conjugation operator $C^{-1}C = 1$.

With these relations it is trivial to show that

$$\left\{ \begin{aligned} \text{Tr}(2) &= \text{Tr}(1; p_+ \text{ and } p_- \text{ interchanged}) \\ \text{Tr}(4) &= \text{Tr}(3) \end{aligned} \right. \quad (\text{B.5})$$

Thus we need to evaluate only $\text{Tr}(1)$ and $\text{Tr}(3)$. These traces can be obtained using the standard trace identities for γ -matrices (33).

$$\begin{aligned} \text{Tr}(1) &= -4 \epsilon_+^2 [(p_+ \cdot p_-) + 2m_e^2] + 4\epsilon_+ [\epsilon_+ (q \cdot p_-) - \epsilon_- (q \cdot p_+)] \\ &\quad + 2 \{ (q \cdot p_+) (q \cdot p_-) - \Delta^2 \epsilon_+ \epsilon_- + \frac{1}{2} \Delta^2 [(p_+ \cdot p_-) + 2m_e^2] \} \end{aligned} \quad (\text{B.6})$$

and

$$\begin{aligned} \text{Tr}(3) = & 2[\varepsilon_+^2(q \cdot p_-) + \varepsilon_-^2(q \cdot p_+) + 4\varepsilon_+\varepsilon_-m_e^2] \\ & + 2\varepsilon_+\varepsilon_-[2(p_+ \cdot p_-) - (q \cdot p_+) - (q \cdot p_-)] - \Delta^2(p_+ \cdot p_-) \end{aligned} \quad (\text{B.7})$$

Eqs. (B.1), (B.5), (B.6) and (B.7) give the desired expression Eq. (2.15).

B. Evaluation of $u_\alpha u_\beta B_{\mu\nu}^{\alpha\beta} u^\mu u^\nu$

$$u_\alpha u_\beta B_{\mu\nu}^{\alpha\beta} u^\mu u^\nu = \frac{1}{D_+^2} \text{Tr}(5) + \frac{1}{D_-^2} \text{Tr}(6) + \frac{1}{D_+ D_-} [\text{Tr}(7) + \text{Tr}(8)] \quad (\text{B.8})$$

where

$$\left\{ \begin{aligned} \text{Tr}(5) &= \frac{1}{8} \text{Tr}[\not{u}(\not{q}-\not{p}_++m_e)\not{p}_+(\not{p}_+-m_e)\not{p}_-(\not{q}-\not{p}_++m_e)\not{p}_-(\not{p}_++m_e)] \\ \text{Tr}(6) &= \frac{1}{8} \text{Tr}[\not{p}_-(\not{p}_--\not{q}+m_e)\not{p}_+(\not{p}_+-m_e)\not{p}_-(\not{p}_--\not{q}+m_e)\not{p}_-(\not{p}_++m_e)] \\ \text{Tr}(7) &= \frac{1}{8} \text{Tr}[\not{p}_-(\not{q}-\not{p}_++m_e)\not{p}_+(\not{p}_+-m_e)\not{p}_-(\not{p}_--\not{q}+m_e)\not{p}_-(\not{p}_++m_e)] \\ \text{Tr}(8) &= \frac{1}{8} \text{Tr}[\not{p}_-(\not{p}_--\not{q}+m_e)\not{p}_+(\not{p}_+-m_e)\not{p}_-(\not{q}-\not{p}_++m_e)\not{p}_-(\not{p}_++m_e)] \end{aligned} \right. \quad (\text{B.9})$$

As in the case of I,

$$\left\{ \begin{aligned} \text{Tr}(6) &= \text{Tr}(5; p_+ \text{ and } p_- \text{ interchanged}) \\ \text{Tr}(8) &= \text{Tr}(7) \end{aligned} \right. \quad (\text{B.10})$$

$\text{Tr}(5)$ and $\text{Tr}(7)$ are given by

$$\begin{aligned} \text{Tr}(5) = & 2\varepsilon_+^2[2\varepsilon_+\varepsilon_-(p_+ \cdot p_-) - m_e^2] + \frac{1}{2} \left\{ 2(q \cdot p_+)(q \cdot p_-) + \Delta^2(p_+ \cdot p_-) + m_e^2 \right\} \\ & + 2\varepsilon_+[\varepsilon_+(q \cdot p_-) + \varepsilon_-(q \cdot p_+)] \end{aligned} \quad (\text{B.11})$$

$$\begin{aligned}
\text{Tr}(7) = & -4\varepsilon_+\varepsilon_- [2\varepsilon_+\varepsilon_- (p_+\cdot p_-) - m_e^2] - \left\{ 2(q\cdot p_+)(q\cdot p_-) + \Delta^2 [(p_+\cdot p_-) + m_e^2] \right\} \\
& - 2(\varepsilon_+\varepsilon_-) [\varepsilon_+(q\cdot p_-) + \varepsilon_-(q\cdot p_+)]
\end{aligned} \tag{B.12}$$

Eqs. (B.8), (B.10), (B.11), and (B.12) lead to Eq. (2.16).

XI. APPENDIX C

The integrals I_1 and I_2 after the t -integration are given by

$$I_1 = \frac{1}{2} \int_{y_1}^{y_2} \frac{dy}{y} |F(y)|^2 \left[y(H_+(t,y) + H_-(t,y)) - \frac{\gamma_1 t}{\omega^2 X_+ X_-} \right]_{t_1}^{t_2} \quad (C.1)$$

and

$$I_2 = \frac{1}{2} \int_{y_1}^{y_2} \frac{dy}{y} |F(y)|^2 \left[G_+(t,y) + G_-(t,y) - 4X_+ X_- (H_+(t,y) + H_-(t,y)) - \frac{\gamma_1}{\omega^2} \left(\frac{1}{X_+^2 X_-^2 t} + \frac{2}{X_+ X_-} \ln t \right) \right]_{t_1}^{t_2} \quad (C.2)$$

where

$$G_{\pm}(t,y) = \int_0^t \frac{X_{\pm}^2 \sigma_{\pm}}{\sqrt{q_{\pm}^3}} dt = \frac{X_{\pm}}{\sqrt{q_{\pm}}} [X_{\mp} (2X_{\pm} t - y) - 2] \quad (C.3)$$

$$H_{\pm}(t,y) = \int_0^t \frac{dt}{t\sqrt{q_{\pm}}} = -\frac{2}{\sqrt{y(y+4)}} \ln \left(\frac{y(4+y - 2X_{\pm} t) + 2\sqrt{y(y+4)}q_{\pm}}{2t} \right) \quad (C.4)$$

The integration limits of t and y are given by Eqs. (2.57) and (2.59).

XII. APPENDIX D

The integrals J_1 and J_2 after the t -integration are given by

$$J_1 = \int_{y_1}^{y_2} \frac{dy}{y} |F(y)|^2 [N(t,y)]_{t_1}^{t_2} \quad (D.1)$$

and

$$J_2 = \int_{y_1}^{y_2} \frac{dy}{y^2} |F(y)|^2 \left[-\frac{2}{\eta} - 4\beta_2 N(t,y) + \frac{1}{2} \beta_2^2 M(t,y) \right]_{t_1}^{t_2} \quad (D.2)$$

where

$$M(t,y) = \int dt \frac{\lambda}{\sqrt{\mu^3}} = \frac{-1}{\beta_1 \beta_2 m_\pi^2 \sqrt{\mu}} (y - 2\beta_2 t + 2\beta_1 m_\pi^2) \quad (D.3)$$

and

$$N(t,y) = \int \frac{dt}{\eta \sqrt{\mu}} = -\frac{1}{\beta_1 \sqrt{y(y+4m_\pi^2)}} \ln \left[\frac{\beta_1 y(y-2\beta_2 t + 4\beta_1 m_\pi^2) + 2\beta_1 \sqrt{y(y+4m_\pi^2)} \mu}{2\eta} \right] \quad (D.4)$$

The integration limits of t and y are given by Eqs. (3.64) and (3.65).

XIII. APPENDIX E

The expressions of the regularized photon self-energy part $\Pi(p^2)$, the electron self-energy part $\Sigma(p)$ and the vertex part $\Lambda_\mu(p', p)$ are given as follows (41).

$$\left\{ \begin{aligned} -e^2 \Pi(p^2) &= \frac{2\alpha}{\pi} \int_0^1 dx \, x(1-x) \ln \left[1 - \frac{p^2}{m^2} x(1-x) \right] \end{aligned} \right. \quad (E.1)$$

$$\left\{ \begin{aligned} -\Sigma(p) (\not{p}-m)^2 &= \frac{\alpha}{2\pi} \int_0^1 dx \left[(\not{p}-m)(1-x) \ln \left(\frac{N}{D_x} \right) \right. \\ &\quad \left. - m(1+x) \ln \left(\frac{N}{D_x} \right) - 2m^2 (\not{p}-m) \frac{x(1-x)^2}{D_x} \right] \end{aligned} \right. \quad (E.2)$$

where

$$\begin{aligned} D_x &= m^2 x^2 + \mu^2 (1-x) \\ N &= m^2 x^2 + \mu^2 (1-x) - (p^2 - m^2) x(1-x) \end{aligned} \quad (E.3)$$

$$\begin{aligned} \Lambda_\mu(p', p) &= \frac{\alpha}{2\pi} \int_0^1 dx \int_0^1 dy \left[-\gamma_\mu \ln \left(\frac{F}{D_y} \right) \right. \\ &\quad \left. + \left(\frac{M_\mu}{F} \right) - m^2 \gamma_\mu \frac{y^2 - 2(1-y)}{D_y} \right] \end{aligned} \quad (E.4)$$

where

$$\left\{ \begin{aligned} D_y &= m^2 y^2 + \mu^2 (1-y) \\ F &= m^2 y + \mu^2 (1-y) - p'^2 xy(1-y) - p^2 (1-x)y(1-y) \\ &\quad - (p' - p)^2 x(1-x)y^2 \\ M_\mu &= (\not{p}_y + \not{p}) \gamma_\mu (\not{p}_y + \not{p}') - 2m(p_\mu + p'_\mu + 2p_{y\mu}) + m^2 \gamma_\mu \\ p_y &= -p' xy - p(1-x)y \end{aligned} \right. \quad (E.5)$$

XIV. APPENDIX F

In this appendix we give the calculation of $\rho(42)$.

$$\rho = -\frac{\alpha}{4\pi^2} \int \frac{\bar{\ell}^2 d\bar{\ell} d\Omega_{\bar{\ell}}}{\sqrt{\ell^2 + \mu^2}} \left[\frac{\mu^2}{(\ell_0 \epsilon_+ - \vec{\ell} \cdot \vec{p}_+)^2} + \frac{\mu^2}{(\ell_0 \epsilon_- - \vec{\ell} \cdot \vec{p}_-)^2} - \frac{2(\vec{p}_+ \cdot \vec{p}_-)}{(\ell_0 \epsilon_+ - \vec{\ell} \cdot \vec{p}_+)(\ell_0 \epsilon_- - \vec{\ell} \cdot \vec{p}_-)} \right] \quad (F.1)$$

The denominator of the last term in the above equation can be rewritten in the form

$$\frac{1}{(\ell_0 \epsilon_+ - \vec{\ell} \cdot \vec{p}_+)(\ell_0 \epsilon_- - \vec{\ell} \cdot \vec{p}_-)} = \int_0^1 \frac{dx}{(\ell_0 \epsilon_x - \vec{\ell} \cdot \vec{p}_x)^2} \quad (F.2)$$

where ϵ_x and \vec{p}_x are defined by Eq. (4.24). The angular integration is not difficult to carry out and given by

$$\int \frac{d\Omega_{\bar{\ell}}}{(\ell_0 \epsilon - \vec{\ell} \cdot \vec{p})^2} = \frac{4\pi}{\bar{\ell}^2 (\epsilon^2 - \vec{p}^2) + \epsilon^2 \mu^2} \quad (F.3)$$

So that

$$\rho = -\frac{\alpha}{\pi} \int \frac{\bar{\ell}^2 d\bar{\ell}}{\sqrt{\ell^2 + \mu^2}} \left[\frac{\mu^2}{\bar{\ell}^2 (\epsilon_+^2 - \vec{p}_+^2) + \epsilon_+^2 \mu^2} + \frac{\mu^2}{\bar{\ell}^2 (\epsilon_-^2 - \vec{p}_-^2) + \epsilon_-^2 \mu^2} - 2(\vec{p}_+ \cdot \vec{p}_-) \int_0^1 \frac{dx}{\bar{\ell}^2 (\epsilon_x^2 - \vec{p}_x^2) + \epsilon_x^2 \mu^2} \right] \quad (F.4)$$

Next consider the following $\bar{\ell}$ -integration

$$I = \int \frac{\bar{\ell}^2 d\bar{\ell}}{\sqrt{\ell^2 + \mu^2} [\bar{\ell}^2 (\epsilon^2 - \vec{p}^2) + \epsilon^2 \mu^2]} = \int_{\mu}^{\Delta \epsilon} \frac{\sqrt{\ell_0^2 - \mu^2}}{\ell_0^2 (\epsilon^2 - \vec{p}^2) + \mu^2 \vec{p}^2} d\ell_0 \quad (F.5)$$

Introducing the new variable $t^2 = (1 - \mu^2/\ell_0^2)$, rewrite I in the form

$$\begin{aligned} I &= \frac{1}{\varepsilon^2 - p^2} \int_0^X \left(\frac{1}{1-t^2} - \frac{2}{\varepsilon^2 - p^2 t^2} \right) dt \\ &= \frac{1}{2(\varepsilon^2 - p^2)} \left[\ln \left(\frac{1+X}{1-X} \right) - \frac{\varepsilon}{\bar{p}} \ln \left(\frac{\varepsilon + \bar{p}X}{\varepsilon - \bar{p}X} \right) \right] \end{aligned} \quad (\text{F.6})$$

where $X = \sqrt{1 - (\mu/\Delta\varepsilon)^2}$. We now take the limit as $\mu \rightarrow 0$ and obtain

$$I = \frac{1}{\varepsilon^2 - p^2} \left[\ln \left(\frac{2\Delta\varepsilon}{\mu} \right) - \frac{\varepsilon}{2\bar{p}} \ln \left(\frac{\varepsilon + \bar{p}}{\varepsilon - \bar{p}} \right) \right] \quad (\text{F.7})$$

The use of this expression in Eq. (F.4) yields Eq. (4.22).

XV. APPENDIX G

To find an expression of Q_4 , we need to evaluate the integral

$$\begin{aligned}
 J &= \int \frac{d^4 \ell}{\ell^2} \frac{1}{(\ell \cdot p_+)(\ell \cdot p_-)} \\
 &= \int \frac{d^3 \ell}{\epsilon_- (\vec{\ell} \cdot \vec{p}_+) - \epsilon_+ (\vec{\ell} \cdot \vec{p}_-)} \left[\epsilon_+ \int_{-\infty}^{\infty} \frac{d\ell_0}{(\ell_0^2 - \vec{\ell}^2)(\ell_0 \epsilon_+ - \vec{\ell} \cdot \vec{p}_+)} \right. \\
 &\quad \left. - \epsilon_- \int_{-\infty}^{\infty} \frac{d\ell_0}{(\ell_0^2 - \vec{\ell}^2)(\ell_0 \epsilon_- - \vec{\ell} \cdot \vec{p}_-)} \right] \tag{G.1}
 \end{aligned}$$

The ℓ_0 -integration can be done performing the Feynman rotation in the integral of the form (44)

$$L = \int_{-\infty}^{\infty} \frac{d\ell_0}{(\ell_0^2 - \vec{\ell}^2)(\ell_0 \epsilon_- - \vec{\ell} \cdot \vec{p}_-)} \tag{G.2}$$

By the Cauchy integral theorem, the following contour integral vanishes.

$$\oint_C \frac{d\ell_0}{(\ell_0^2 - \vec{\ell}^2 + i\delta)(\ell_0 \epsilon_- - \vec{\ell} \cdot \vec{p}_- + i\delta)} = 0 \tag{G.3}$$

where δ is an arbitrary small real number and the contour C is described in Fig. 12.

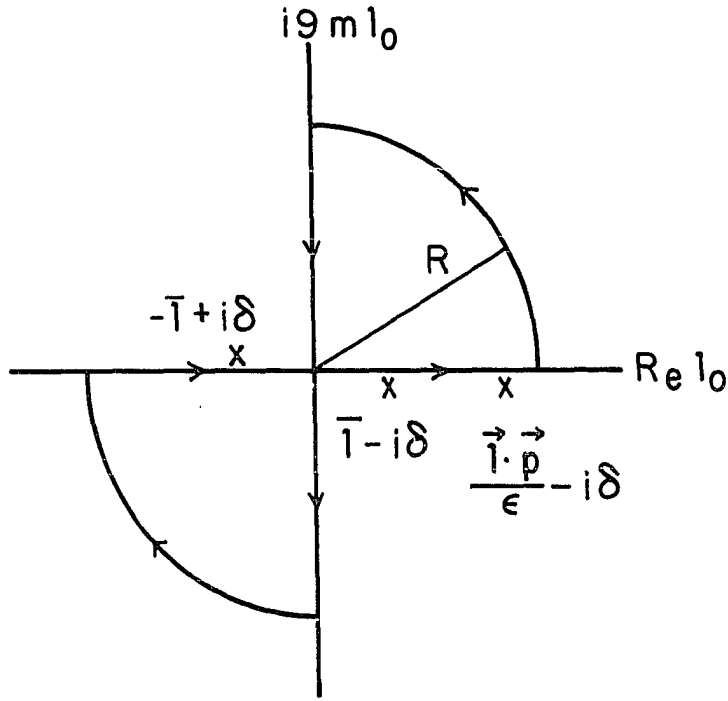


Figure 12. Contour C for the l_0 -integration

The above contour integral contains three line integrals. We may express these three parts in the abbreviated manner

$$\oint = \int_{-R}^R + \int_{iR}^{-iR} + \int_{\text{arcs}} = 0$$

Since the integral along the two arcs vanish as $R \rightarrow \infty$, Eq. (G.3) in this limit implies

$$\begin{aligned} L &= - \int_{i\infty}^{-i\infty} \frac{d l_0}{(\bar{l}_0^2 - \bar{l}^2)(\bar{l}_0 \epsilon - \vec{l} \cdot \vec{p})} \\ &= i \int_{-\infty}^{\infty} \frac{du}{(\bar{l}^2 + u^2)(\vec{l} \cdot \vec{p} - i \epsilon u)} = \frac{i\pi}{\bar{l}} \frac{1}{(\vec{l} \cdot \vec{p}) - \epsilon \bar{l}} \end{aligned} \quad (G.4)$$

where the change of variable $\ell_0 = iu$ is made. Using the expression of L in (G.1), we obtain

$$\begin{aligned}
 J &= -i\pi \int \frac{d^3\ell}{\bar{\ell}} \frac{1}{(\bar{\ell}\epsilon - \vec{\ell} \cdot \vec{p}_+) (\bar{\ell}\epsilon_- - \vec{\ell} \cdot \vec{p}_-)} \\
 &= -i\pi \int_0^1 dx \int \frac{\bar{\ell}^2 d\bar{\ell}}{\bar{\ell}} \int \frac{d\Omega_{\bar{\ell}}}{(\bar{\ell}\epsilon_x - \vec{\ell} \cdot \vec{p}_x)} = -i4\pi^2 \int_0^1 \frac{dx}{\epsilon_x^2 - p_x^2} \int \frac{d\bar{\ell}}{\bar{\ell}} \quad (G.5)
 \end{aligned}$$

where ϵ_x and \vec{p}_x are defined by Eq. (4.24).